



The age of the bone marrow microenvironment influences B-cell acute lymphoblastic leukaemia progression via CXCR5-CXCL13

Dissertation

zur Erlangung des Doktorgrades

der Naturwissenschaften

vorgelegt beim Fachbereich Biowissenschaften der Johann
Wolfgang Goethe-Universität in Frankfurt am Main

von

Costanza Zanetti

aus

Colleferro (Rome, Italy)

Frankfurt am Main, **2021**

Vom Fachbereich Biochem, Chemie und Pharmazie (FB14) der Johann Wolfgang Goethe-Universität als Dissertation angenommen.

Dekan: Prof. Dr. Clemens Glaubitz

Gutachter: Prof. Dr. Rolf Maschalek
Prof. Dr. Daniela S. Krause

Datum der Disputation:

Die Ergebnisse dieser Arbeit wurden bereits teilweise in folgenden Publikationen veröffentlicht:

Zanetti C., Kumar K., Ender J., Godavarthy P.S., Hartmann M., Hey J., Breuer K., Weissenberger E.S., Minciocchi V.R., Karantanou C., Gu Z., Roberts K.G., Metzler M., Stock W., Mullighan C.G., Bloomfield C.D., Filmann N., Bankov K., Hartmann S., Hasserjian R.P., Cousins A.F., Halsey C., Plass C., Lipka D.B., Krause D.S.

The age of the bone marrow microenvironment influences B-cell acute lymphoblastic leukemia progression via CXCR5-CXCL13. *Blood* 2021. PMID: 34424946 DOI: 10.1182/blood.2021011557

Declaration

I herewith declare that I have not previously participated in any doctoral examination procedure in a mathematics or natural science discipline.

Frankfurt am Main,(Date),(Signature).

Authours' declaration

I herewith declare that I have produced my doctoral dissertation on the topic of

“The age of the bone marrow microenvironment influences B-cell acute lymphoblastic leukaemia progression via CXCR5-CXCL13”.

Independently and using only the tools indicated therein. In particular, all references borrowed from external sources are clearly acknowledged and identified.

I confirm that I have respected the principles of good scientific practice ad have not made use of services o any commercial agency in respect of my doctorate.

Frankfurt am Main,.....

.....

(Signature)

Table of Contents



	1
1 Zusammenfassung	9
2 Summary	15
3 Introduction	17
3.1 Haematopoiesis	17
3.1.1 The Haematopoietic hierarchy	17
3.2 Leukaemia	19
3.2.1 CML	21
3.2.2 B-ALL	22
3.2.3 BCR-ABL signalling pathway	23
3.3 Bone marrow microenvironment	24
3.3.1 Endothelial cells	26
3.3.2 Osteoblasts and osteoclasts	26
3.3.3 Mesenchymal stromal cells	27
3.3.4 Macrophages	27
3.4 Ageing	28
3.4.1 Ageing and haematopoiesis	31
3.5 Chemokines/Chemokine receptors	33
3.5.1 CXCL13-CXCR5	34
3.6 Targeting the BMM	36
4 Hypothesis:	38
5 Materials and Methods	39
5.1 Ethical approval	39
5.2 Mice	39
5.3 Drug treatment	39
5.4 BM transduction and transplantation	40
5.4.1 Virus production	40
5.4.2 CML	41
5.4.3 B-ALL in syngeneic mouse model	42
5.4.4 B-ALL in patient derived xenograft	43
5.4.5 Homing	44
5.4.6 Analysis of diseased mice and tumour burden	45
5.5 Southern Blotting	45
5.6 Methylcellulose assay	45

5.7	Culture of primary cells and cell lines.....	46
5.8	Isolation of bone marrow derived macrophages (MΦ)	46
5.9	Measurement of p-γ-H2AX and ROS	48
5.10	Quantification of CXCL13	48
5.10.1	RNA isolation and quantitative polymerase chain reaction.....	48
5.10.2	Cytokine flow cytometry.....	49
5.10.3	ELISA.....	49
5.10.4	Western blot	50
5.11	Proliferation analysis	51
5.12	Migration and adhesion assays.....	51
5.13	Immunofluorescence	52
5.15	Immunoblotting	53
5.14	In vivo microscopy.....	53
5.15	Human patients.....	54
5.16	Immunohistochemistry.....	55
5.17	RNA-sequencing (RNA-seq).....	56
5.18	ATAC-seq.....	56
5.18.1	ATAC-seq data processing.....	58
5.18.2	ATAC-seq - Differential accessibility analysis	58
5.18.3	ATAC-seq - Transcription factor activity analysis	59
5.18.4	ATAC-seq - Genomic overlap enrichment analysis	59
5.18.5	ATAC-seq - Motif analysis	59
5.18.6	ATAC-seq - Code availability	60
5.19	Statistical methods	60
6	<i>Results</i>	<i>61</i>
6.1	Differential efficiency of CML induction in a young versus aged BMM	61
6.2	Differential efficiency of B-ALL induction in a young versus aged BMM in sublethally irradiated mice.	63
6.3	B-ALL can be induced without pre-conditioning irradiation.....	64
6.4	The contribution of an ageing BMM to B-ALL development	66
6.5	B-ALL is more aggressive in young unirradiated mice	68
6.6	The engraftment of human primary B-ALL cells is higher in young versus old NOD/SCID IL-2receptor gamma KO mice	71
6.7	The location and characteristics of B-ALL-initiating cells differ in a young versus an old BMM	73
6.8	BCR-ABL1+ cells proliferate more on young BM derived macrophages compared to old counterparts.	76
6.9	Leukaemia cells migrate faster towards young BM derived macrophages.....	78
6.10	Released factors from young macrophages may be responsible for the proliferation of leukaemia cells.	79

6.11	Age-related differences between macrophages from the BMM of young versus old mice	80
6.12	Young BM-derived macrophages produce higher levels of CXCL13.....	83
6.12.1	CXCL13 level is higher in young unirradiated leukaemic mice.....	85
6.13	CXCL13 supports the proliferation of B-ALL cells in vitro	86
6.14	CXCL13 increases the migration of leukaemia cells	88
6.15	CXCL13 induces pAKT upregulation in B-ALL cells.....	89
6.16	Young BM derived macrophages and CXCL13 are supportive factors in B-ALL in vivo ...	90
6.17	CXCL13 expression is higher in human macrophages and in non-classical human monocytes	92
6.18	CXCR5 expression is higher on leukaemia cells from a young BMM.....	94
6.18.1	CXCR5 impacts survival in murine B-ALL.....	94
6.18.2	CXCR5 expression may predict outcome in the human setting	96
6.18.1	CXCR5 expression may predict central nervous system relapse of B-ALL.....	97
7	Discussion	98
7.1	Differential progression of CML and B-ALL in young and aged mice	98
7.2	Macrophages as a supportive niche for leukaemia.....	102
7.3	CXCL13 levels are higher in a young BMM.....	104
7.1	CXCR5.....	106
8	Conclusion.....	109
9	References	110

LIST OF FIGURES.

FIGURE 1 CLASSICAL OVERVIEW OF HAEMATOPOIESIS.	18
FIGURE 2 THE DISCRETE/STEPWISE VERSUS CONTINUOUS HAEMATOPOIETIC DIFFERENTIATION MODEL.	19
FIGURE 3 CHRONIC MYELOID LEUKAEMIA INCIDENCE RELATED TO AGE.	21
FIGURE 4 ACUTE LYMPHOBLASTIC LEUKAEMIA INCIDENCE RELATED TO AGE.	22
FIGURE 5 THE NORMAL BONE MARROW MICROENVIRONMENT.	25
FIGURE 6 THE HALLMARKS OF AGEING.	29
FIGURE 7 MODEL OF AGEING IN HAEMATOPOIESIS	32
FIGURE 8 CXCR5-CXCL13 PATHWAY	35
FIGURE 9 CHRONIC MYELOID LEUKAEMIA (CML) INDUCED IN YOUNG AND AGED MICE.	62
FIGURE 10 B-CELL ACUTE LYMPHOBLASTIC LEUKAEMIA (B-ALL) INDUCED IN YOUNG AND AGED IRRADIATED MICE.	63
FIGURE 11 INDUCTION OF CML AND B-ALL IN IRRADIATED AND NON-IRRADIATED MICE.	65
FIGURE 12 B-CELL ACUTE LYMPHOBLASTIC LEUKAEMIA (B-ALL) IS INFLUENCED BY LIC-INTRINSIC	67
FIGURE 13 THE EFFICIENCY OF INDUCTION OF B-ALL IN A YOUNG VERSUS OLD BMM DIFFERS.	69
FIGURE 14 B-ALL CELLS INFILTRATE IN DIFFERENT ORGANS.	70
FIGURE 15 A YOUNG MICROENVIRONMENT SUPPORTS THE ENGRAFTMENT AND MAINTENANCE OF B-ALL CELLS.	72
FIGURE 16 THE LOCATION AND BEHAVIOUR OF B-ALL CELLS DIFFER IN A YOUNG VERSUS AND OLD BMM.	74
FIGURE 17 THE MOVEMENT OF B-ALL CELLS IS LESS RANDOM IN YOUNG MICE.	75
FIGURE 18 LEUKAEMIA CELLS PROLIFERATE MORE ON YOUNG MACROPHAGES	77
FIGURE 19 MIGRATION OF LEUKAEMIA CELLS TOWARDS YOUNG VERSUS OLD MACROPHAGES DIFFERS	79
FIGURE 20 CONDITIONED MEDIUM FROM YOUNG MACROPHAGES INFLUENCE THE PROLIFERATION OF LEUKAEMIA CELLS.	80
FIGURE 21 AGEING EFFECTS IN BM MACROPHAGES FROM OLD MICE.	81
FIGURE 22 YOUNG AND OLD MACROPHAGES DIFFER WITH REGARDS TO THEIR TRANSCRIPTOME AND EPIGENETIC SIGNATURE	82
FIGURE 23 CXCL13 IS HIGHER IN MACROPHAGES AND THE BONE MARROW OF YOUNG MICE	84
FIGURE 24 CXCL13 LEVELS DO NOT CHANGE WITH IRRADIATION.	85
FIGURE 25 CXCL13 LEVEL DOES NOT CHANGE UPON IRRADIATION	85
FIGURE 26 CXCL13 SUPPORTS THE PROLIFERATION OF B-ALL CELLS.	87
FIGURE 27 CXCL13 REGULATES MIGRATION OF LEUKAEMIA CELLS	88
FIGURE 28 CXCL13 INDUCES PAKT UPREGULATION.	89
FIGURE 29 YOUNG MACROPHAGES AND CXCL13 ARE SUPPORTIVE FACTORS IN B-ALL.	91
FIGURE 30 INCREASED STAINING FOR MACROPHAGES AND CXCL13 IN BONE SECTIONS FROM PAEDIATRIC VERSUS ADULT PATIENTS WITH B-ALL	93
FIGURE 31: EXPRESSION OF CXCR5 ON LEUKAEMIA CELLS	94
FIGURE 32: CXCR5 EXPRESSION ON B-ALL CELLS IMPACTS OUTCOME IN THE MURINE MODEL	95
FIGURE 33: CXCR5 EXPRESSION MAY PREDICT OUTCOME IN THE HUMAN SETTING.	96
FIGURE 34: CXCR5 EXPRESSION ON B-ALL BLASTS MAY PREDICT CNS RELAPSE OF HUMAN B-ALL.	97

1 Zusammenfassung

Leukämie ist eine hämatologische Erkrankung, die durch eine Funktionsstörung normaler hämatopoetischer Stammzellen (HSC) und/oder stärker differenzierter Vorläuferzellen verursacht wird und zu einer unkontrollierten Vermehrung und Anhäufung nicht funktionsfähiger Leukozyten führt. Die B-Zell akute lymphoblastische Leukämie (B-ALL) ist durch eine Überproduktion von Lymphoblasten im Knochenmark gekennzeichnet und ist die häufigste Krebserkrankung bei Kindern, während sie bei Erwachsenen vergleichsweise selten vorkommt. Von allen Patienten mit chronisch myeloische Leukämie (CML) sind 70% über 50 Jahre alt, während Kindern eher selten betroffen sind. Sowohl bei der CML als auch bei bis zu 3 % der pädiatrischen B-ALL-Fälle wird das Fusionsgen BCR-ABL1 diagnostiziert, das durch eine reziproke Translokation zwischen den Chromosomen 9 und 22 das zytoplasmatische, konstitutiv aktive Onkoprotein, die Tyrosinkinase BCR-ABL1, hervorbringt. Die konstitutiv aktive BCR-ABL-Tyrosinkinase führt zur Deregulierung verschiedener Signaltransduktionswege wie Zellwachstum, Proliferation und Zellüberleben. Die Rolle des Knochenmarksmikromilieu (KMM) als extrinsischer Faktor, der die Krankheitsentstehung bei den Leukämien, das Fortschreiten, die Therapieresistenz und den Rückfall beeinflussen kann, wurde in den letzten zwei Jahrzehnten zunehmend anerkannt. Im Allgemeinen ist das KMM ein sehr komplexes Gefüge aus verschiedenen Zelltypen wie Osteoblasten, Osteoklasten, Endothelzellen, Adipozyten, mesenchymalen Stromazellen, Makrophagen und einigen anderen. Darüber hinaus besteht das KMM aus einer Vielzahl chemischer und mechanischer Faktoren und EZM (extrazelluläre Matrix) Proteinen, die zu den Eigenschaften des KMM beitragen und das Verhalten von HSC und Leukämie beeinflussen. In Anbetracht der bereits beschriebenen Häufigkeit von B-ALL und CML bei Kindern bzw. Erwachsenen stellen wir die Hypothese auf, dass das junge und/oder alte KMM eine bisher unerkannte Rolle für die Aggressivität von B-ALL und CML spielen könnte. Wir vermuteten,

dass junges KM, also KM von 6 Wochen alten Mäusen, transduziert mit BCR-ABL1-exprimierendem Retrovirus im murinen Transduktions-/Transplantationsmodell der B-ALL, transplantiert in junge gegenüber alten, unbestrahlten Empfängermäusen, zu einer aggressiveren Erkrankung in jungen Mäusen führen würde, und dass in ähnlicher Weise die CML in alten Empfängermäusen aggressiver sein würde. In der Tat führte die Induktion von CML in alten Empfängermäusen (BALB/c) zu einer signifikanten Verkürzung der Überlebenszeit, was dem Verhalten dieser Erkrankung beim Menschen sehr nahekommt. Andererseits zeigte sich bei der Induktion von B-ALL eine signifikant höhere Anzahl von Leukozyten und eine höhere Tumorlast im peripheren Blut sowie eine Verkürzung der Überlebenszeit bei jungen im Vergleich zu alten (BALB/c und C57/BL6) Empfängermäusen. In Übereinstimmung mit dem syngenem Modell führte die Transplantation menschlicher B-ALL-Zellen in NOD-SCID-Mäuse mit Interleukin-2-Rezeptor- γ -Immundefizienz zu einer verkürzten Überlebenszeit bei jungen Mäusen. Da die Lokalisierung von Leukämiezellen im KMM mit der Aggressivität und dem Fortschreiten der Krankheit korreliert sein könnte, stellten wir mit Hilfe des 2-Photonen-Mikroskops fest, dass Leukämiezellen bei jungen Mäusen näher am Endosteum lokalisiert waren und eine höhere Geschwindigkeit mit einem stärker gerichteten Wanderungsverhalten zeigten als bei alten Mäusen. Dies veranlasste uns zu der Annahme, dass spezifische Reaktionen auf Faktoren in der jungen und nicht im alten KMM die Aufrechterhaltung von Leukämiezellen unterstützen könnten. Wie bereits erwähnt, untersuchten wir im Rahmen der sehr heterogenen Zusammensetzung des KMM, die den beobachteten Phänotyp beeinflusst haben könnte, die Rolle von jungen und alten Makrophagen *in vitro*. Die Bedeutung von Monozyten/Makrophagen wurde teilweise bei B-ALL, T-ALL und chronischer lymphatischer Leukämie (CLL) durch andere Gruppen, sowie bei der normalen Hämatopoese in unseren früheren Arbeiten im Labor beobachtet. In mehreren *in-vitro*-Experimenten haben wir eine unterschiedliche Interaktion von B-ALL-Zellen mit

Makrophagen aus jungem und altem KMM beobachtet. Die Ergebnisse zeigten, dass Leukämiezellen einen Proliferationsvorteil haben, wenn sie jungen Makrophagen ausgesetzt sind, insbesondere sinkt die Wachstumskurve disproportional, wenn die Leukämiezellen gemeinsam mit Makrophagen zunehmenden Alters kultiviert werden. In Bezug auf die Stärke der Adhärenz gab es keine signifikanten Unterschiede, während die Migration der Leukämiezellen zu jungen Makrophagen im Vergleich zu alten Makrophagen verstärkt war. In Anbetracht der Tatsache, dass unterschiedliche Faktoren unterschiedlich sezerniert werden könnten, zeigte die Exposition von Leukämiezellen gegenüber konditioniertem Medium von jungen Makrophagen eine erhöhte Proliferation. Aufgrund der in unseren Experimenten beobachteten Unterschiede zwischen jungen und alten Makrophagen analysierten wir die Alterungsmerkmale in jungen und alten Makrophagen. Alte Makrophagen zeigten im Vergleich zu jungen Makrophagen einen seneszenzähnlichen Phänotyp mit einem veränderten Transkriptom und einer veränderten epigenetischen Signatur. Insbesondere wurde eine globale und auffällige epigenetische Veränderung festgestellt, die bei jungen Makrophagen funktionelle Eigenschaften im Zusammenhang mit Entzündungen und Immunreaktionen erkennen ließ.

Die Auswirkungen der konditionierten Medien auf die Proliferation, die Migration und die potenzielle Entzündungsreaktion veranlassten uns, Zytokine und/oder Chemokine zu identifizieren, die für die beobachteten Unterschiede verantwortlich sein könnten. Da das Chemokin CXCL13 nachweislich eine Rolle bei der Migration von B-Zellen spielt und als diagnostischer Marker in der Zerebrospinalflüssigkeit von Patienten mit Neuroborreliose fungiert, stellten wir die Hypothese auf, dass ein solches Chemokin für das verstärkte Wachstum von Leukämiezellen in einem jungen KMM verantwortlich sein könnte. Auf transkriptioneller Ebene wurden keine signifikanten Unterschiede in der CXCL13-Expression zwischen jungen und alten Makrophagen festgestellt. Allerdings wiesen gespültes

Knochenmark junger Mäuse und konditionierte Medien junger Makrophagen eine höhere Konzentration von CXCL13 auf als die entsprechenden alten Kontrollen, sowohl im gesunden als auch im B-ALL-Modell. Da wir wissen, dass CXCL13 über seinen Rezeptor CXCR5 die Migration von B-Zellen fördert, haben wir die Expression von CXCR5 auf B-ALL-Zellen untersucht. In der Tat fanden wir eine höhere Expression von CXCR5 auf B-ALL-Zellen im peripheren Blut und in der Milz junger Mäuse im Vergleich zu alten Mäusen. Daher untersuchten wir die potenzielle Funktion der CXCR5-CXCL13-Achse im jungen und alten KMM im Zusammenhang mit Leukämiezellen genauer. Die Hemmung von CXCL13 reduzierte signifikant die Proliferation und Migration von Zellen, wenn sie jungen Makrophagen ausgesetzt waren, und der Phänotyp wurde durch die Verwendung von rekombinantem CXCL13 umgekehrt. Zur Bestätigung der pro-proliferativen Rolle von CXCL13 beschleunigte die *In-vitro*-Vorbehandlung von B-ALL mit rekombinantem CXCL13 vor der Transplantation die Leukämieentwicklung in Empfängermäusen erheblich. In Anbetracht der Beteiligung junger Makrophagen wollten wir diese Ergebnisse *in vivo* validieren. Zu diesem Zweck verabreichten wir Clodronat-Liposomen in leukämischen Mäusen, einem gut etablierten Modell, um Makrophagen zu entfernen. Die Entfernung von Makrophagen führte zu einer signifikanten Verringerung der Tumorlast sowie zu einer Verlängerung der Überlebenszeit bei jungen Mäusen. Die weitere Quantifizierung von CXCL13 im Knochenmark und im Plasma bestätigte, dass der Phänotyp teilweise auf eine Verringerung der CXCL13-Menge zurückzuführen ist. Diese Daten deuten daher darauf hin, dass CXCL13, das zumindest teilweise von Makrophagen sezerniert wird, die Migration und Proliferation von B-ALL-Zellen fördert und damit das Überleben bei B-ALL beeinflusst. Um die Beteiligung der CXCL13-CXCR5-Achse *in vivo* weiter zu validieren, wurde ein weiteres Mausmodell (CXCR5-defiziente Mäuse) verwendet. In Übereinstimmung mit unseren früheren Ergebnissen führten Leukämiezellen mit CXCR5-Mangel zu einer signifikanten

Verlängerung des Überlebens junger Empfängermäuse. Neben der Beobachtung verschiedener Mäusestämme und Mausmodelle, um den Beitrag von Makrophagen und CXCL13 in der jungen Mikroumgebung zu bestätigen, untersuchten wir diese Proteine auch in Proben erkrankter Menschen. Zu diesem Zweck führten wir immunhistochemische Untersuchungen an menschlichen KM-Schnitten durch. In Übereinstimmung mit unseren Daten aus Mäusen konnten wir zeigen, dass CD68⁺ Makrophagen und CXCL13 in Knochenschnitten von pädiatrischen Patienten im Vergleich zu erwachsenen Patienten mit B-ALL häufiger vorkommen. In Anbetracht der neuartigen Rolle einer Untergruppe von Monozyten, die als nicht-klassische Monozyten bezeichnet werden und deren Häufigkeit prädiktiv für B-ALL ist, untersuchten wir außerdem, ob es einen unterschiedlichen Beitrag dieser Zelltypen in der Mikroumgebung von jungen und alten Patienten gibt. Tatsächlich fanden wir in Knochenschnitten von Patienten mit pädiatrischer B-ALL eine erhöhte Anzahl dieser Zellen, die auch CXCL13 produzierten. In Anbetracht unserer Daten aus Mäusen war die Expression von CXCR5 bei B-ALL-Patienten ebenfalls stratifizierbar, was darauf hindeutet, dass dies als prognostischer Marker sowie als prädiktiver Marker für einen Rückfall im zentralen Nervensystem bei menschlicher B-ALL fungieren könnte. Insgesamt zeigen die Ergebnisse, dass junges KMM und insbesondere Makrophagen das Fortschreiten der B-ALL beeinflussen. Wir zeigen deutliche Unterschiede in der Interaktion von jungem und altem KMM mit Leukämiezellen. Vor allem sezernierte Faktoren beeinflussen die Proliferation, den Zellzyklus und die Migration von Leukämiezellen, obwohl ein Einfluss des Zell-Zell-Kontakts oder von Leukämiezell-immanenten Faktoren nicht ausgeschlossen werden kann. Wir konnten zeigen, dass CXCL13, das zum Teil von jungen Makrophagen sezerniert wird, die Migration und Proliferation von B-ALL-Zellen fördert und das Überleben bei B-ALL über seinen verwandten Rezeptor CXCR5 beeinflusst. Die CXCR5-CXCL13-Achse könnte bei menschlicher B-ALL

von Bedeutung sein, und eine höhere CXCR5-Expression bei menschlicher B-ALL könnte als prädiktiver Marker dienen.

Schlüsselwörter: Akute lymphoblastische Leukämie; Knochenmarksmikromilieu; Alterung; Makrophagen; CXCL13; CXCR5.

2 Summary

B-cell acute lymphoblastic leukaemia (B-ALL) is characterized by the overproduction of lymphoblasts in the bone marrow (BM), and it is the most common cancer in children while being comparatively uncommon in adults. On the other hand, in chronic myeloid leukaemia (CML), 70% of cases are found in patients older than 50 years, making it uncommon in children. All CML cases and up to 3% of paediatric B- ALL (and 25% of adult B-ALL) cases are due to fusion gene BCR-ABL1, which gives rise to the cytoplasmatic, constitutively active oncoprotein, tyrosine kinase BCR-ABL1 through a reciprocal translocation between chromosomes 9 and 22. The constitutively active BCR-ABL tyrosine kinase leads to deregulation of different signal transduction pathways such as cell growth, proliferation and cell survival. The role of the bone marrow microenvironment (BMM) can mediate disease initiation (only in mice), progression, therapy resistance, and relapse, as has been increasingly recognized over the last two decades. In general, the BMM is a very complex arrangement of various cell types such as osteoblasts, osteoclasts, endothelial cells, adipocytes, mesenchymal stromal cells, macrophages and several others. In addition, the BMM is composed of multiple chemical and mechanical factors and extra cellular matrix (ECM) proteins which contribute to the BMM's features influencing leukaemia behaviour. Considering the incidence of B-ALL and CML in children and in adults respectively, we hypothesized that the young and/or an aged BMM might also play a previously unrecognized role in the aggressiveness of B-ALL and CML. We proposed that BM, transduced with BCR-ABL1-expressing retrovirus in the murine transduction/transplantation model of B-ALL, transplanted into young versus old recipient mice would lead to a more aggressive disease in young mice, and similarly CML would be more aggressive in old recipient mice. In close recapitulation with the human incidence, induction of CML led to a significantly shortened survival in old recipient mice. On the other hand, induction of B-ALL showed a shortened survival in young compared to old syngeneic

mice, as well as in a xenotransplantation model. Among the highly heterogenous composition of the BMM, we implicate young BM macrophages as a supportive niche for B-ALL cells. The results were found to be mostly due to potential soluble factors differentially secreted from young and old macrophages. Therefore, we hypothesized that the chemokine CXCL13, which has been demonstrated to play a role in B cell migration and act as a diagnostic marker in the cerebrospinal fluid of patients with neuroborreliosis, might be responsible for the observed phenotype. CXCL13 was found to be more highly expressed in healthy and leukaemic young mice as well as in conditioned medium of young macrophages. Using a variety of *in vitro* experiments, CXCL13 showed to significantly increase the proliferation and the migration of leukaemia cells when exposed to young macrophages, and the phenotype was rescued while using a CXCL13 neutralizing antibody. The CXCL13 role was also confirmed *in vivo*, since macrophage ablation led to a prolongation of survival in young mice and a reduction of CXCL13 levels. The use of an additional mouse model, leukaemia cells with CXCR5 deficiency, led to a significant prolongation of survival of young mice, confirming the importance of the CXCL13-CXCR5 axis in B-ALL. In line with our murine results, we found that human macrophages and CXCL13 levels were higher in pediatric B-ALL patients than in adults. Consistent with our murine data, the expression level of CXCR5 may act as a prognostic marker in B-ALL, as well as a predictive marker for central nervous system relapse in human B-ALL. The overall findings show that a young BMM, and in particular macrophages, influences B-ALL progression. We specifically identified CXCL13, secreted by young macrophages, as a promoter of proliferation of B-ALL cells, influencing survival in B-ALL via CXCR5. The CXCR5-CXCL13 axis may be relevant in human B-ALL, and higher CXCR5 expression in human B-ALL may act as a predictive marker.

Key words: Acute lymphoblastic leukaemia; bone marrow microenvironment; ageing; macrophages; CXCL13; CXCR5.

3 Introduction

3.1 Haematopoiesis

The term haematopoiesis is derived from the Greek words *haima*, which means blood, and *poiesis*, which means production. Haematopoiesis is the process that generates the entire blood cell pool during the life span of the organism, and it is dependent on haematopoietic stem cells (HSCs). The growth and origin of HSCs have been investigated using a variety of model systems. Haematopoiesis in vertebrates occurs in two distinctive organs and temporal frames: the primitive wave and the definitive wave or haematopoiesis⁶. In mammals, haematopoiesis occurs sequentially in the yolk sac, the fetal liver and the bone marrow (BM). Primitive haematopoiesis in the yolk sac generates nucleated erythrocytes, macrophages and other myeloid cells⁷. The primitive haematopoiesis is transient, and in mammals it is promptly replaced by definitive haematopoiesis which takes place in the fetal liver, thymus, spleen and in the end in the BM⁸.

3.1.1 The Haematopoietic hierarchy

In the human and murine system, the origin of all blood is believed to lie in HSCs which are characterized by two essential properties, self-renewal capacity and multipotent differentiation via intermediate multipotent progenitor cells as multipotent progenitors (MPPs)⁹⁻¹⁴. The classical way of describing haematopoiesis is via a step-by-step model shown in figure 1¹. MPPs are further subdivided into common lymphoid progenitor (CLP)s and common myeloid progenitor (CMP)s; according to the classical view of haematopoiesis, CLPs represent the earliest lymphoid population which go on to form T-cells, B-cells, NK cells and dendritic cells. CMPs are in turns classified into granulocyte-macrophage progenitors (GMP)s and megakaryocyte-erythrocyte progenitors (MEP)s. GMPs are committed to

granulocyte/macrophage lineages¹⁵ and MEPs are principally erythroid precursors¹⁶. The classical model of haematopoiesis was extensively investigated by Weissman' group^{14,17,18}. The classical step-by-step model is simplified and based on surface markers and bulk of transplantation studies¹.

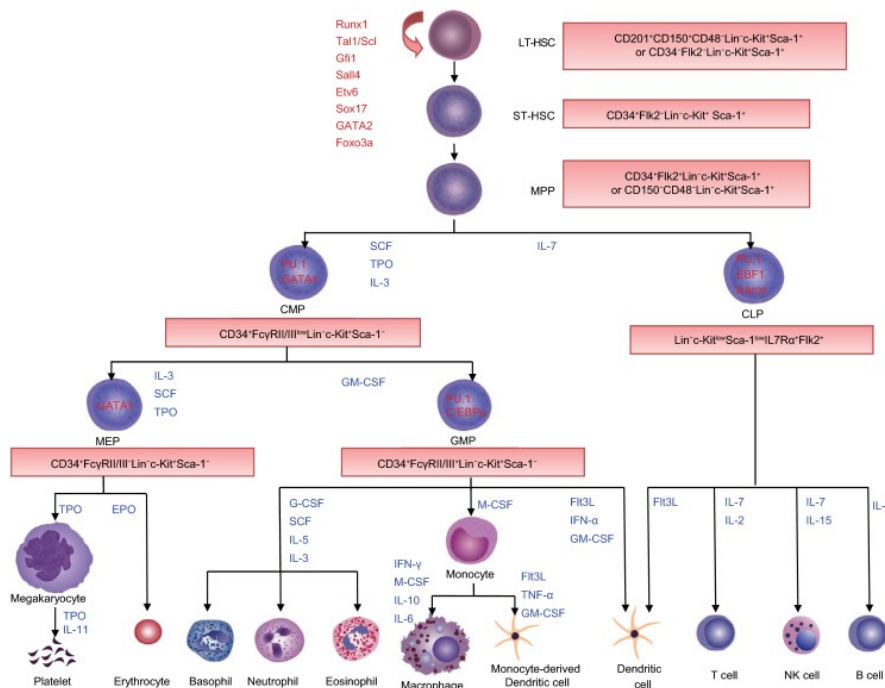


Figure 1 Classical overview of haematopoiesis.

LT-HSCs differentiate into ST-HSCs, and subsequently to MPPs. Downstream of MPPs, a strict separation between the myeloid (CMPs) and lymphoid (CLPs) branches. CMPs generate MEPs and GMPs. CLPs give rise to lymphocytes and dendritic cells. MEPs differentiate into megakaryocytes/platelets and erythrocytes. GMPs produce granulocytes, macrophages, and dendritic cells¹.

However, the conventional stepwise process has been challenged in recent decades by the development of various techniques capable of purifying, image^{19,20} and characterize^{14,21} the HSC heterogeneity. This demonstrates that haematopoiesis is a continuous process that lacks boundaries between cell populations previously assigned to a specific hierarchical level, and that the process is maintained by distinct stem/progenitor cell populations (figure 2¹).

The following reviews provide additional information on the new view of haematopoietic model^{1,22,23}.

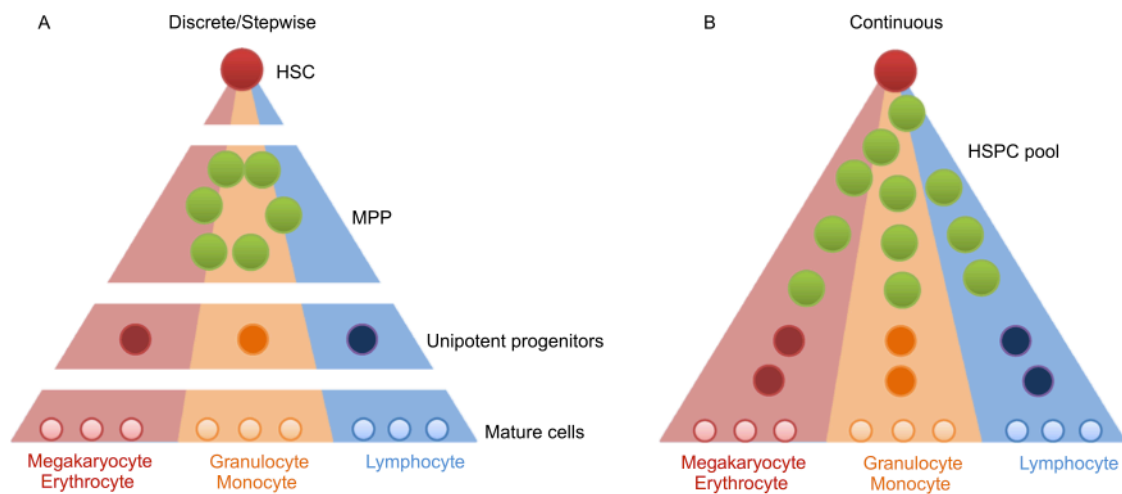


Figure 2 The discrete/stepwise versus continuous haematopoietic differentiation model.
 The discrete/stepwise model (A) and the continuous haematopoietic differentiation model (B)¹.

Even if, intrinsic gene expression profiles orchestrate and govern the HSC stemness, early lineage bias and differentiation^{24,25}, haematopoiesis is also regulated by stem cell niches in the bone marrow microenvironment (BMM)^{26,27}.

3.2 Leukaemia

Leukaemia is a hematological disease that is caused by mutagenesis or epigenetic changes in normal HSC or, depending on the type of leukaemia, in their respective progenitors leading to uncontrolled proliferation and accumulation of mature and or immature cancerous leukocytes. These leukaemia cells exhibit abnormal functions and eventually outnumber normal blood cells in blood, bone marrow and other organs. We can classify leukaemia into four major types based on the course of the disease and the affected lineage: acute lymphoblastic leukemia (ALL), chronic lymphocytic leukaemia (CLL), acute myeloid leukemia (AML), and chronic myeloid leukaemia (CML).

- **Acute myeloid leukaemia**

AML is a heterogeneous disease that is characterized by clonal expansion of myeloid progenitors (blasts) in the bone marrow, peripheral blood, and possibly other organs²⁸. According to recent reports, the disorder is caused by a series of recurrent changes in hematopoietic stem or progenitor cells that occur naturally as people age. The risk of disease evolution (the risk of developing a myeloid neoplasm as AML) varies according to the mutation type and other factors. Thus, clonal haematopoiesis (CH) and the mutations associated with it can be classified as CH with indeterminate potential (CHIP) or CH with oncogenic potential (CHOP). CHIP mutations provide the molecular basis for a neoplastic process, CHOP mutations are disease-associated or even disease-specific lesions that promote neoplastic cell differentiation and/or proliferation²⁹. Gene sequencing has identified frequent mutations in fms-like tyrosine kinase 3 (FLT3), nucleophosmin 1 (NPM1), tyrosine-protein kinase (KIT), CCAAT/enhancer-binding protein alpha (CEBPA), Tet methylcytosine dioxygenase 2 (TET2) and DNA methyltransferase (DNMT3)³⁰⁻³³. Considering the heterogeneity group of AML different selective therapies are required. Since 2017, nine agents have been approved such as venetoclax, FLT3 inhibitors, and others³⁴.

- **Chronic lymphoblastic leukaemia**

CLL is characterized by an accumulation of small mature B lymphocytes in the blood, bone marrow, and lymph nodes. CLL is more common in adults. Chemotherapy and anti-CD20 monoclonal antibodies are the standard of care for many patients with CLL. The remarkable efficacy of the kinase inhibitors ibrutinib and idelalisib, as well as venetoclax, has altered the standard of care for certain subgroups of patients³⁵.

3.2.1 CML

CML is a myeloproliferative neoplasm that originates in LT-HSC. The genetic basis of all CML patients relies on the Philadelphia (Ph) chromosome, which is the hallmark of the disease. The Ph chromosome is formed upon a reciprocal translocation of chromosomes 9 and 22, termed (9;22) (q34; q11)^{36,37} giving rise to the fusion gene *BCR-ABL1*, which is a constitutively active tyrosine kinase protein³⁸ (the activity of BCR-ABL1 is further discussed in paragraph 3.2.3). CML occurrence and diagnosis is associated with an aged population, with 70% of cases involving adults over 50, and an average age at diagnosis being between 65 and 69 years old, as shown in figure 3 (Cancer Research, UK). The presence of the Ph chromosome leads to an expansion of myeloid cells of varying maturation status. Depending on the number of blasts in the peripheral blood, CML can be categorized into three different phases. Chronic phase shows < 5% of blast in the peripheral blood, accelerated phase in which the number of blasts is 5-19%. Without treatment the disease will progress to blast crisis with >20% of blasts³⁹.

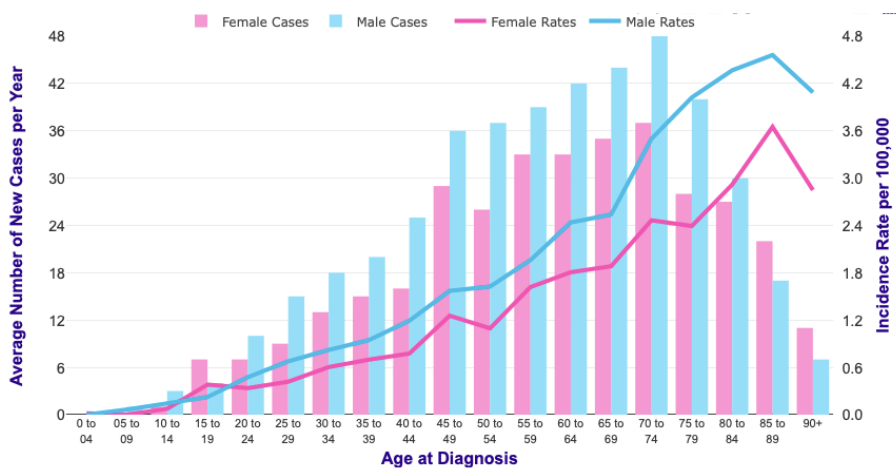


Figure 3 Chronic myeloid leukaemia incidence related to age.

Age-specific incidence rates rise gradually from birth and more steeply from around age 65-69.

3.2.2 B-ALL

B-ALL is the most common cancer in children and relatively rare in adults (figure 4, Cancer Research, UK). Specifically, the highest incidence of patients is between zero and four years old. The use of monoclonal antibodies helped to distinguish B-ALL from T-ALL, which is very rare. B-ALL is defined by the expression of B cells markers: CD19, CD79 or CD22,⁴⁰ while TALL is characterized by CD1a and CD3⁴¹.

Genetic diseases such as Down syndrome, Fanconi anemia, ataxia telangiectasia are predisposition syndromes in some cases of B-ALL cases⁴²⁻⁴⁴. However, in the majority of cases, the disease appears as *de novo*.

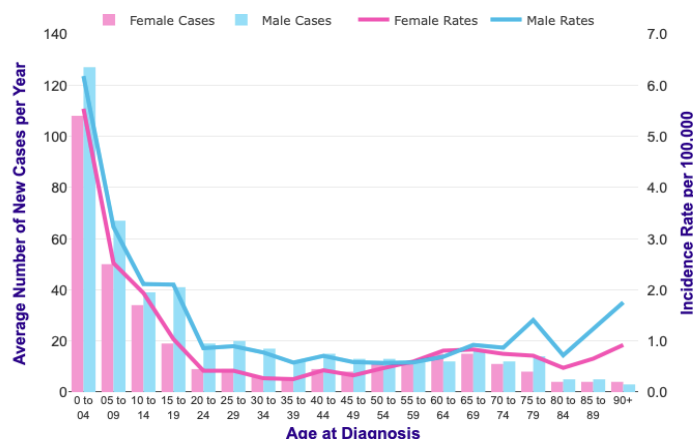


Figure 4 Acute lymphoblastic leukaemia incidence related to age.

The highest incidence rates being in the 0 to 04 age group (Cancer Research, UK).

B-ALL can be caused by multiple aberrations, such as: t(12;21) [ETS Variant Transcription Factor 6 (ETV6)- Runt-related transcription factor1 (RUNX1)], t(1;19) [Transcription Factor 3 (TCF3)- Pre-B-cell leukaemia homeobox (PBX) transcription factor (1) (PBX1)], t(9;22) [BCR-ABL1], Ph-like and rearrangement of mixed-lineage leukaemia (MLL)⁴⁵. Genetic alterations such as deletions, amplifications, point mutations and structural rearrangement in B-ALL, involve transcriptional alteration of normal B-cell development such as Paired Box 5

(*PAX5*), IKAROS Family Zinc Finger 1 (*IKZF1*), Early B-Cell Factor 1 (*EBF1*) and Lymphoid Enhancer Binding Factor 1 (*LEF1*)⁴⁶. Typically, ALL is treated with chemotherapy, which aims to eradicate the majority of the disease while restoring normal haematopoiesis in 80-90 percent of children⁴⁷. Imatinib (tyrosine kinase inhibitor) in combination with the standard intensive chemotherapy significantly improved 3-year event free survival (EFS) in children and adolescents with Ph+ ALL, with no significant increase in toxicity⁴⁸.

The majority of B-ALL patients achieve clinical and morphological remission following induction chemotherapy. However, the disease may relapse usually in the central nervous system (CNS), with survival rates of 10-20%. Consequently, addition of craniospinal or cranial irradiation and intrathecal chemotherapy prolongs complete remission⁴⁹.

3.2.3 BCR-ABL signalling pathway

The Ph chromosome was the first chromosomal abnormality detected in cancer biology. It develops by fusion of the *ABL1* and *BCR* genes. The *ABL* gene on chromosome 9 encodes a nonreceptor tyrosine kinase. Structural domains can be defined within the protein with different functions related to cell cycle and apoptosis^{50,51}. Among the three Proto-oncogene tyrosine-protein kinase (SRC) homology domains (SH1-SH3), SH1 carries the tyrosine kinase. The *BCR* gene on chromosome 22 is ubiquitously expressed⁵². The fusion gene is transcribed into BCR-ABL1 mRNA and then translated into the BCR-ABL1 protein. However, depending on the breakpoints the molecular weight of the protein can vary between 185 to 210 kDa. The classical Ph+ CML phenotype is derived from the p210 type of BCR-ABL1⁵³. The constitutively active BCR-ABL tyrosine kinase leads to deregulation of different signal transduction pathways such as those impacting cell growth, proliferation and survival^{51,52,54}. The affected pathways include the phosphatidylinositol-3-kinase (PI3K)/Akt and the mammalian target of rapamycin (mTOR), mitogen activated protein kinase (MAPK)/

extracellular-signal-regulated kinase (ERK), and Janus kinase (JAK)/ signal transducer and activator of transcription (STAT) pathways are explained elsewhere^{55,56}.

3.3 Bone marrow microenvironment

The term “stem cell niche” was coined in 1978 to refer to a niche with a specific location which prevents stem cell maturation⁵⁷. *Drosophila* has been an attractive animal model for studying the stem cell due to its basic anatomical structure^{58,59}. However, stem cell niches in mammals are highly specialized due to the organism's complexity, and the concept of the niche has been studied in a variety of direct and indirect systems. Recently, the BM has been the subject of intense research using a variety of transgenic mouse models⁶⁰⁻⁶², imaging technologies⁶³⁻⁶⁵, and multi-omics approaches^{66,67} which have helped identify multiple cellular and acellular components of the bone.

By and large, it is recognized that the BMM is a complex entity, as illustrated in figure 5⁵. It is composed of a variety of cellular and acellular components such as mesenchymal stromal cells (MSC), endothelial cells (EC)s, osteoblasts, osteoclasts, osteocytes, adipocytes, CXCL12-abundant reticular (CAR) cells, fibroblasts, sympathetic neurons, megakaryocytes, macrophages, as well as chemical and mechanical factors and extra cellular matrix (ECM) proteins⁶⁸. Additionally, pH, an oxygen gradient, cytokines and mechanical factors, all of which have been extensively reviewed elsewhere⁶⁹, contribute to the BMM's unique features influencing HSC and LSC behaviour⁵.

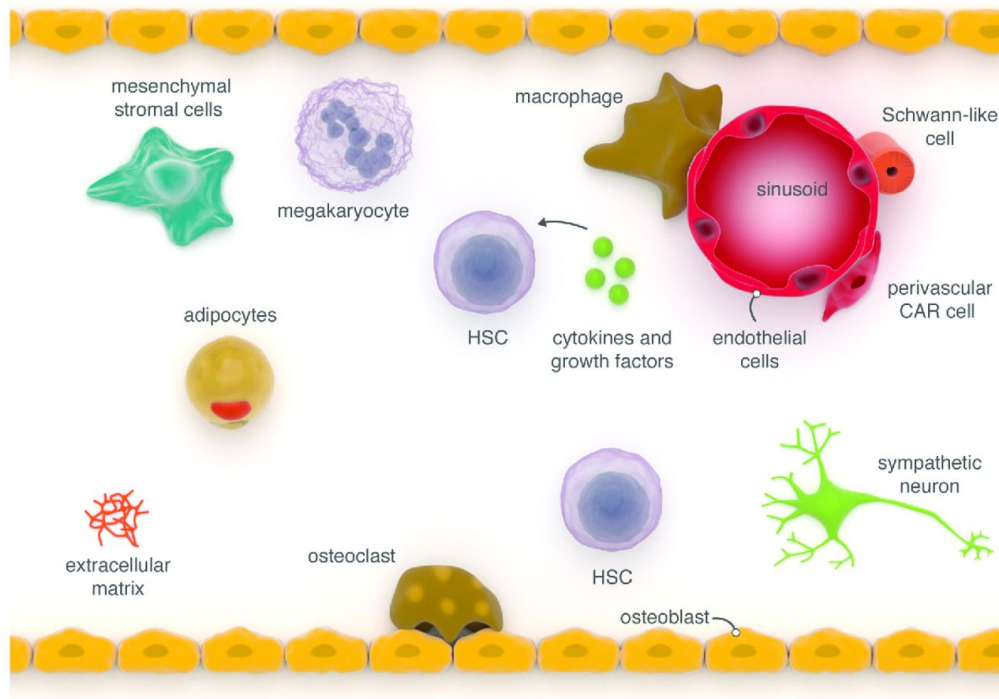


Figure 5 The normal bone marrow microenvironment.

The BM microenvironment is composed of different cell populations that regulate HSC fate. CAR cell: CXCL12-abundant reticular cell⁵.

This biological complexity motivated a large number of researchers to investigate the molecular mechanisms underlying the HSC-BM crosstalk. Despite the intrinsic properties of HSC discussed previously, many other characteristics such as mobilization, homing, and engraftment that are necessary for normal physiological function, rely on the BMM, for example through adhesion and/or migration to a specific niche^{70,71}. As previously stated, various factors influence HSCs, but anatomical differences within the same niche, have a differential effect on HSC behaviour. The precise anatomical relationship of HSCs in the BM was also examined using sophisticated live imaging techniques, such as confocal and two-photon microscopy. The usage of the two-photon microscopy allowed the visualization of HSCs in the BM with more mature cells being localized further away from the bone¹⁹. Phagocytotic cells as BM derived macrophages (MΦ) are also crucial for HSCs trafficking, since they contribute to the retention of HSC/progenitors^{72,73}. Further details on BM MΦ are

provided extensively below. The functional aspects of the interaction between the BMM and the HSC are discussed in greater detail elsewhere^{69,74}.

3.3.1 Endothelial cells

ECs are a diverse cell population that line the vasculature in the BMM which is composed of sinusoids, arterioles, and transition zones. ECs play a critical role in the function and maintenance of HSCs. Arterioles maintain HSCs in a quiescent stage⁷⁵ with low levels of Reactive Oxygen Species (ROS)⁷⁶. On the other hand, permeable sinusoids increase ROS levels of HSCs, triggering HSCs activation, migration and differentiation⁷⁶. In addition, ECs support HSC maintenance by providing factors such as C-X-C Motif Chemokine Ligand 12 (CXCL12), stem cell factor (SCF), angiopoietin, fibroblast growth factor (FGF) 2, and Delta-like 1 (DLL1)^{26,27}. Furthermore, E-selectin an adhesion molecule that it is exclusively expressed on ECs promotes HSC proliferation and is a critical component of the vascular niche⁷⁷.

3.3.2 Osteoblasts and osteoclasts

The endosteum lies between bone and BM which is composed of osteoblastic lineage cells such as osteoprogenitor cells, pre-osteoblasts, mature osteoblasts, and osteocytes, as well as osteoclasts. In mice osteoblasts ablation causes mobilization of HSCs to spleen and liver⁷⁸. In addition, osteoblasts also support the differentiation of murine B-cell commitment and maturation⁷⁹. Osteoblasts secrete cytokines and growth factors such as osteopontin (OPN), which limits the size of the stem cell pool⁸⁰. Osteoclasts induce HSC mobilization leading also to an increase of osteoclastogenesis⁸¹. Osteoclasts depletion leads to an increased proportion of mesenchymal progenitors while reduced osteoblastic differentiation and an impairment HSC homing to the bone⁸².

3.3.3 Mesenchymal stromal cells

MSCs are heterogenous population of cells, generally located closer to the perivascular areas⁷⁴ and they can give rise to osteoblasts, adipocytes or chondrocytes and tightly they regulate HSCs functions in mice and humans⁸³. Based on defined markers, MSCs characterized as Neural-glial antigen (NG)2+ cells, maintain LT-HSCs⁷⁵, while MSCs as leptin receptor (Lepr)+ cells are source of stem cell factor (Scf) a non-cell factor required for HSC maintenance⁸⁴.

3.3.4 Macrophages

Macrophages were first described as a type of cell capable of engulfing and eliminating foreign substances by Mechnikov in the nineteenth century. The term macrophages is derived from the Greek words *makros*, meaning ‘big’, and *phagein*, meaning to ‘eat’ or, here, to encapsulate external particles. In standard terms macrophages as myeloid immune cells engulf and digest debris generated during tissue remodelling, cancer cells, and microbes via a process called phagocytosis. For many years the development of macrophages from embryonic to adult stages, as well as their progenitors have been a difficult and contentious subject. Van Furth and Cohn proposed the first view, in which tissue-resident macrophages are derived primarily from circulating bone marrow-derived blood monocytes⁸⁵. Different genes regulate macrophage fate; for example, yolk sac macrophages are dependent on the transcription factor myeloblastosis (Myb)⁸⁶, whereas the TF PU.1, which is frequently required for macrophage development⁸⁷ is not required for yolk sac macrophage development⁸⁶. Yolk sac macrophages, also called primitive macrophages migrate to the fetal liver where they give rise to fetal liver monocytes. These enter the circulation and differentiate into macrophages in peripheral tissues. With the exception of microglia, Ginhoux and colleagues using colony stimulating factor(CSF)-1R and Runt-related transcription factor (Runx)1 Cre mouse models, strongly

suggest that yolk sac macrophages and microglia share a common origin⁸⁸. The origins and functions of macrophages vary significantly between tissues, and whether resident macrophages are derived from the yolk sac or monocytes is still being discussed^{89,90}. Additionally, tissue-resident macrophages perform specialized functions in accordance with their location. In the spleen, red pulp macrophages are primarily generated during embryogenesis and are maintained throughout adulthood. Their role is to phagocytose injured and senescent erythrocytes⁹¹. In the BM, other specialized macrophages, osteoclasts, considered bone-resident macrophages, are specialized in bone reabsorption⁹². BM derived macrophages, besides being phagocytic cells, increase the efficiency of HSC/progenitor mobilization in autologous transplantation⁷², as well as they maintain the HSC endosteal niche⁷³. Additionally, CD169⁺ macrophages have been shown to significantly impair the engraftment of phenotypic LT-HSC⁹³. It is also well known that administration of CSF1, a secreted cytokine that induces HSCs to differentiate into macrophages⁹⁴ can be used in bone marrow transplantation (BMT) to increase antibacterial and antifungal protection⁹⁵. The role of macrophages is also being investigated with regards to ageing, as the immune system deteriorates with age (additional information is provided in paragraph 3.4.1).

3.4 Ageing

Over the last century, a global trend towards increased life expectancy has been observed, but at the expense of a significant increase in the occurrence of diseases⁹⁶. In recent decades, numerous biologists have been interested in elucidating the mechanisms that limit lifespan. Using an elderly organism as a model to investigate the genetic processes underlying the ageing phenotype is by far the simplest approach. However, since 1959, unicellular organisms such as *Saccharomyces cerevisiae* have been extensively used as models for ageing research. At the time, it was discovered that the replicative life span of a cell is defined as the total number of

daughter cells produced⁹⁷, whereas the chronological life span is considered as the length of time in which a cell can survive in a nondividing state⁹⁸. Researchers gained a better understanding of the human ageing process through the use of complex mammalian and mouse models, as well as large-scale analysis⁹⁹. Ageing mouse models are outlined here⁹⁹. The identification and characterization of age-related characteristics results in a global view of primary, antagonistic, and integrative age-related characteristics, as illustrated in figure 6⁴.

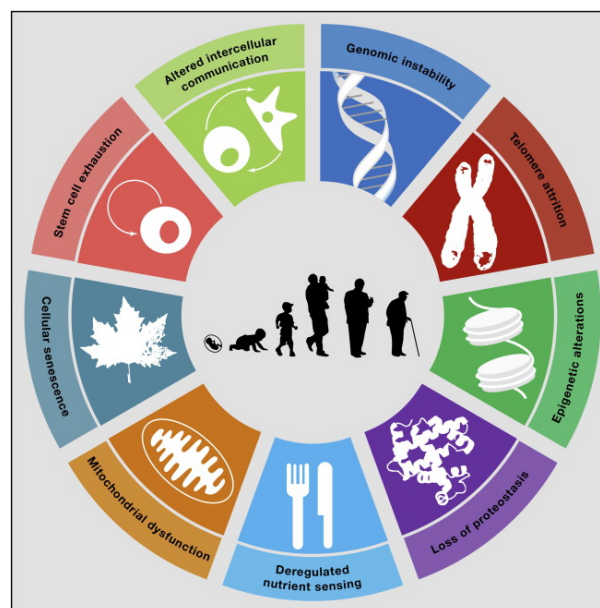


Figure 6 The hallmarks of ageing.

Genomic instability, telomere attrition, epigenetic alterations, deregulated nutrient sensing, loss of proteostasis, mitochondrial dysfunction, cellular senescence, stem cell exhaustion, and altered intercellular communication contribute to the ageing process⁴.

Genetic lesions accumulate over time as a result of intrinsic (ROS, point mutations, translocations, and telomerase shortening) and extrinsic (physical, chemical, and biological agents) damage and are strongly associated with ageing¹⁰⁰. Telomere length and integrity are regulated at different levels and telomere damage is one of the main causes of ageing¹⁰¹. In mice with dysfunctional telomeres, recovery of the premature phenotype was demonstrated following inducible telomerase activation¹⁰². The nuclear lamina¹⁰³ also regulates genome maintenance, as mutations in numerous genes encoding the nuclear lamina are responsible for

a variety of human diseases, including the well-known accelerated aging disease Hutchinson-Gilford progeria syndrome^{104,105}. Caloric restriction is a dietary regimen that, increases lifespan and retards age-related chronic diseases^{106,107}. This phenomenon was first observed in rodents in 1930¹⁰⁸. Numerous epigenetic modifications occur over time, and these modifications have an effect on lifespan extension. Epigenetic alterations, which accumulate over time, can influence gene expression by affecting gene expression and may be passed on to the next generation of cells. Significant loss of histone proteins is associated with ageing, whereas histone overexpression significantly prolongs life span in yeast¹⁰⁹. Another major target of ageing is the mitochondria. Specifically, mutations in the mitochondrial (mt)-DNA lead to mitochondrial disfunctions which correlate with an age-related decline^{110,111}. In addition, nucleotide mutations in mtDNA-encoded respiratory chain subunits, lead to respiratory chain deficiency, which in turn have ageing related consequences¹¹². Several lines of evidence allow the scientific community to propose the “mitochondria free radical theory of ageing”, focused on the excessive accumulation of ROS which leads to a chronic condition of oxidative stress¹¹³⁻¹¹⁵. Even though the theory has long been accepted, new data in recent years has cast doubt on the role of ROS in ageing¹¹⁶⁻¹¹⁸. Another attribute of ageing is cellular senescence, since by definition it is as an irreversible cell growth arrest¹¹⁹, and the number of senescent cells increases along with lifespan. However, because it is capable of responding positively to stress and illness, senescent cells can act as a rejuvenator¹²⁰. Thus, recent evidences suggest that senescent cells exhibit the “senescence-associated secretory phenotype” with expression of secreted factors, inflammatory proteins, mediators of ECM remodelling^{119,121,122}, which allows the communication among cells, leading a new concept: “senescence-messaging secretome”¹²³. The immune system undergoes significant changes as an organism ages, and high levels of inflammatory cytokines are linked to a phenomenon known as “inflamm-ageing” which

increases susceptibility to age-related diseases/disabilities¹²⁴. The paragraph below discusses ageing and the immune system in greater detail.

3.4.1 Ageing and haematopoiesis

There is now growing evidence that the immune system is affected by ageing¹²⁵. In mice, it was shown that HSCs have an age-related reduction in homing and engraftment capacities^{3,126-128}. However, the quantitative and qualitative alterations differ considerably between mouse strains, rendering it an important caveat to consider when analysing and comparing ageing research¹²⁹. Also in humans, changes in HSCs have been observed with ageing. This includes a substantial, significant increase in the frequency of CD34+ CD38- cells in elderly people, but no change over time in myeloid progenitors. A decrease was found in the frequency of early and committed B-lymphoid progenitor cells positive for CD34 and CD19^{130,131}. From a functional point of view, aged long term (LT)-HSCs display higher stem cell self-renewal capacity, lower cycling activity, and decreased lymphopoiesis with deficiencies in lymphoid precursors^{3,132,133}. As previously mentioned, studies have identified intrinsic defects in HSC function and epigenetic dysregulation as significant contributors to hematopoietic decline and malignancy during aging (figure 7)³. As HSCs are affected by ageing, also it has been reported that ageing impact many functions of macrophages^{134,135}. Old peritoneal macrophages secrete substantially less tumour necrosis factor (TNF)1- α and interleukin (IL)-6 with an impairment in Toll like receptor expression¹³⁶. The number of macrophages seems to be differed between old humans and old mice. A decrease in CD68+ macrophages is found in the BM of old humans¹³⁷, while a general marker for myeloid cells as Mac1+ shows to be expressed more on myeloid cells in the BM of old mice¹³⁸. A reduced clearance of parasitic and salmonella

infections has been reported in old mice^{139,140} and lower phagocytic activity was also observed in old mice¹⁴¹.

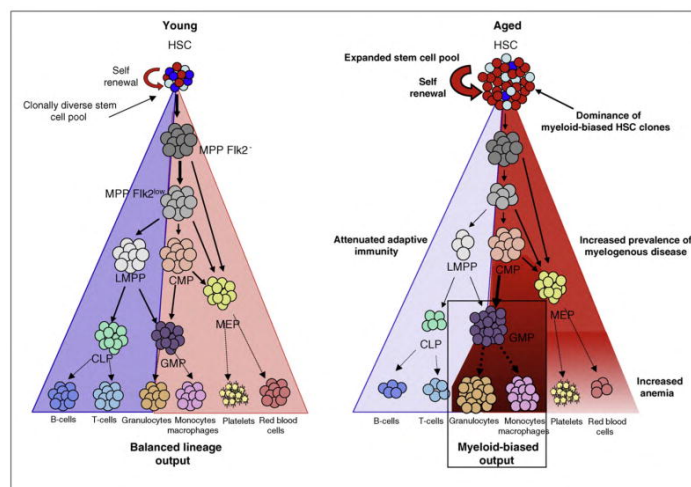


Figure 7 Model of ageing in haematopoiesis

Intrinsic alterations in HSC function and epigenetic changes contribute to haematopoietic decline and myeloid bias during ageing³.

The phagocytic activity of macrophages from aged mice decreases as macrophage-derived chemokines are produced. It was discovered that phagocytosis is impaired with ageing in tissue-resident peritoneal macrophages, but not in BM-derived macrophages/monocytes, implying that the microenvironment may influence phagocytic activity¹⁴².

The mechanism by which age affects the haematopoietic pool is still a matter of debate. However, a reversible phenotype may be achieved by targeting “rejuvenating” factors. Targeted pharmacological approaches such as inhibition of mTOR and cell division cycle 42 (CDC)42 were able to restore haematopoiesis^{143,144}. In addition, the age-associated myeloid skewing phenotype can be rescued by placing HSC in a young environment, implying that aged niches are subject to selection pressure, for example via the secretion of C-C Motif Chemokine Ligand 5 (CCL5)¹⁴⁵. Additionally, as humans aged, increased BM fat content was associated with decreased HSC numbers, which was correlated with changes in cytokine levels such as insuline-like growth factor-1 (IGF-1) and stromal cell-derived factor 1 (SDF-1)¹⁴⁶. The HSC ageing phenotype and the exponential increase in the prevalence of leukaemias in elderly

people are also caused by a reciprocal relationship between microenvironment and haematopoiesis.

3.5 Chemokines/Chemokine receptors

The word chemokine is derived from the Greek word *-chemo-kinein*, which means "to move." Its name refers to the ability of secreted proteins (ligands) to induce chemotaxis of cells by forming a chemokine gradient towards responsive cells¹⁴⁷. Chemokines are a class of small proteins (8-14 kDa) that share a common structure consisting of an N-terminal loop, a three-stranded beta-sheet, and a C-terminal alpha-helix. Chemokines contain cysteines, which are responsible for their integrity and binding to their cognate receptors via disulfide bonds.

Depending on the tissue's homeostasis or pathology, the expression of chemokines and their receptor counterparts on the surface of responsive cells is tightly controlled. The first biologically active chemokines were found in the 1980s and early 1990s, making them one of the most recent scientific discoveries. They were discovered in the culture supernatants of neutrophils and macrophages, and their chemo-attractive properties quickly identified them as part of the inflammatory response¹⁴⁸.

Chemokines can be classified according to their cysteine configuration and their functions. Chemokines are classified into four types based on their cysteine residues: CC, CXC, CX3C, and CX, whereby X represents an arbitrary AA between pairs of cysteines¹⁴⁹. In 2000, a new systematic nomenclature was updated, and each subfamily was followed by a representing letter L, for "ligand"^{150,151}. Chemokines are divided into two categories based on their functions: inflammatory and homeostatic. Inflammatory chemokines are produced in high amounts during inflammation, injury, and in tumours¹⁵². Certain pro-inflammatory cytokines are also activated rapidly following tissue irradiation and are involved in the recruitment of inflammatory cells^{153,154}. In contrast, homeostatic chemokines are continuously released under

normal conditions to maintain a pool of leukocytes. Additionally, certain chemokines, dubbed mixed-function chemokines, have the ability to perform multiple functions¹⁵⁵. Chemokines exert their biological effects through their binding to cell surface receptors; thus, the receptor nomenclature system is based on the chemokine subfamily names (CC, CXC, CX3C, and CX), which are suffixed with an "R" to denote the receptor, followed by a number. Chemokine receptors are members of the GPCR family. They typically contain 340–370 amino acids and are defined by a long N-terminal extracellular domain, seven parallel transmembrane helices, and a C-terminal cytoplasmic region containing an alpha-helix important for providing a lipid anchor. The first conformational change that occurs upon chemokine binding is an exchange of GDP/GTP and the dissociation of GTP-bound subunits, which activates a large number of downstream molecules¹⁵⁶. Signal cascades are then activated, resulting in a variety of biological effects such as cell migration and immune response.

3.5.1 CXCL13-CXCR5

Chemokine (C-X-C motif) ligand 13 (CXCL13), alternatively referred to as B lymphocyte chemoattractant (BLC) or B cell-attracting chemokine 1 (BCA-1), is a protein ligand encoded by the CXCL13 gene in humans^{157,158}. CXCL13 binds to its receptor C-X-C chemokine receptor type 5 (CXCR5) expressed in mature B-cells and Burkitt's lymphoma. In humans, the CXCR5 protein is encoded by the CXCR5 gene¹⁵⁹. In normal conditions, this axis contributes to the lymphoid tissue microarchitecture and shape of B-cell dynamics¹⁶⁰. CXCL13 has been implicated in the pathogenesis of a variety of autoimmune and inflammatory diseases, as well as lymphoproliferative disorders. The exact signal transduction mechanisms of CXCL13-CXCR5 still remain unclear. In addition, CXCR5 induces Ca²⁺ signalling and chemotaxis¹⁶¹. In cancer, CXCR5 seems to regulate the PI3K/Akt, MEK/ERK, and Rac pathways as shown in figure 8 ².

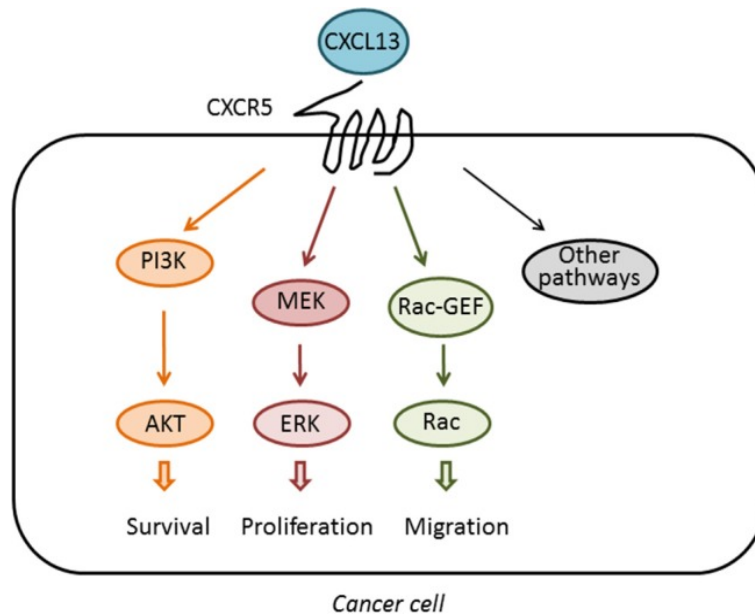


Figure 8 CXCR5-CXCL13 pathway

CXCL13 binds to the CXCR5 receptor. The activated signaling pathways activated are related to cell survival, proliferation, and migration².

In both haematological and solid tumours, CXCL13 appears to be an essential biomarker of cancer progression. CXCR5 expressed on B-CLL cells, for example, stimulates resident MSCs-CXCL13 secretion via lymphotoxin β receptor (LT β R)¹⁶². In addition, CXCL13 and CCL19 induced significant resistance to TNF-alpha-mediated apoptosis in B-ALL and B-CLL¹⁶³. The role of CXCL13-CXCR5 in solid tumours is well explained elsewhere¹⁶⁴. Interestingly, in addition to being involved in cancer, CXCL13 was reported to be higher expressed in children with neuroborreliosis (73%), and it is used as a biomarker for this specific cohort^{165,166}.

On the other hand, studies in mice shows that loss of *Cxcr5* leads to increased proliferation in aged neuroblasts¹⁶⁷. In another report, CXCL13 was discovered to promote the modulation of cellular response in aged osteoblastic cells¹⁶⁸, inverse response of osteoblasts from old and young donors. In addition, CXCL13 has been expressed in an age-dependent way in adult mice regulating the immune response against hepatitis B virus (HBV)¹⁶⁹. Even though more research is needed to characterize and elucidate the downstream pathway of this axis, our current

understanding indicates that CXCL13 and its receptor CXCR5 play critical roles in physiological as well as pathological conditions.

3.6 Targeting the BMM

Decades of research have been devoted to deciphering the leukaemia stem cells (LSC)-intrinsic pathways that underpin LSC biology. However, a paradigm shift in oncology has emphasized the BMM's role in the maintenance of LSC. Due to the fact that the BMM provides a protective environment for LSCs, resulting in disease persistence following therapy resistance, a number of studies have been conducted to investigate the interaction between LSCs and the BMM. The first strategy was demonstrated via the use of granulocyte-colony stimulating factor (G-CSF) in combination with chemotherapy, which resulted in an improved disease-free survival¹⁷⁰. Additionally, mice with AML, subjected to standard chemotherapy along with AMD3100 (a CXCR4 competitive antagonist), displayed a decreased tumour burden, accompanied by an increased overall survival compared to mice treated with chemotherapy only¹⁷¹. CXCR4 has also been studied in CLL and recently targeted with NOX-A12 (CXCL12 inhibitor), which effectively inhibits CLL cell migration¹⁷². Another strategy consists of treatment with parathyroid hormone, the most potent regulator of bone, which attenuated CML due to the release of Transforming growth factor beta 1 (TGF- β 1) from the remodeling of the BMM. In contrast, no effects were observed in a murine MLL-AF9-induced AML model. This highlighted the importance of the BMM in different types of leukaemia¹⁷³. Recently, in our laboratory we also identified the interaction of BCR-ABL1 cells with T315I mutation with ECM via the integrin β 3, integrin-linked kinase (β 3/ILK)-mediated signaling pathway, suggesting that modulation of the ECM may be a potential therapeutic approach^{68,174}. In addition, we found that B-ALL cells instruct the BMM via the secretion of TNF-alpha, resulting in increased MMP-9 production by MSC, ECM degradation, and leukaemia

invasiveness¹⁷⁵. In another study, we discovered that inhibition of E-selectin causes BCR-ABL1+ cells to dissociate from the endothelium, resulting in increased cell proliferation and a better response to imatinib treatment¹⁷⁶. Recent data also demonstrate that a dynamic shifts in the myeloid compartment over B-ALL progression, specifically, non-classical monocyte emergence at the time of diagnosis and relapse in the bone marrow¹⁷⁷. In addition, tumour-associated myeloid cells provide signals critical for T-ALL growth¹⁷⁸. Further knowledge on the BMM in acute leukaemias and the ongoing efforts to target the BMM are highlighted in this review¹⁷⁹. To summarize, a significant challenge is the inhibition of the development and maintenance of leukaemias while also preserving normal tissue function. A better understanding of the BMM would pave the way for the development of new drugs capable of eradicating LSCs more effectively.

4 Hypothesis:

Based on the discussed information, we hypothesized that a young BMM may specifically promote the development and progression of B-ALL, whereas old BMM supports the aggressiveness of CML. We focused the research on B-ALL, and we investigated the role of BM derived macrophages. We hypothesized that a soluble factor released by young macrophages, CXCL13, promotes the proliferation of B-ALL cells via its cognate receptor, CXCR5.

5 Materials and Methods

5.1 Ethical approval

All animal studies were conducted in accordance with the approval (F123/1035-45) by the local animal care committee (Regierungspräsidium Darmstadt). The use of bone sections from patients was approved by the Ethics Committee of the University Clinic of the Goethe University Frankfurt (Approval number 274/18 and SHN-5-2020) and by the other respective local ethics committees. All studies were carried out under Prof. Dr. D. S. Krause supervision.

5.2 Mice

Young (3-4 weeks), 6 weeks old (used as a donor) and old (>18 months) BALB/c, C57BL/6 mice or NOD scid gamma mouse (NSG) were purchased from Charles River Laboratories (Sulzfeld, Germany) and used for all experiments. Only in the CML and B-ALL induction (paragraphs 6.1 and 6.2) in which the recipient mice were sublethally irradiated, the aged mice were >16 weeks old, as 12 weeks is the timepoint when puberty and bone growth in mice is considered to have been completed¹⁸⁰. CXCR5 KO mice were purchased from The Jackson Laboratory (Bar Harbor, ME, USA). All mice colonies were bred in the Institute for Tumor Biology and Experimental Therapy. For all *in vivo* experiments, the mice were monitored daily and if abnormalities were observed, the mice were sacrificed accordingly to the animal approval.

5.3 Drug treatment

2.5 µg of an Ig2a-isotype control or an anti-CXCL13 antibody (R&D Systems, Minneapolis, MN, USA) were added to the *in vitro* assays. 100 ng of recombinant CXCL13 (Peprotech, Hamburg, Germany) were added to the proliferation and migration assays, while testing of the

dynamic range, recombinant CXCL13 was also performed with 1000 ng on 3×10^5 BCR-ABL1⁺ BA/F3 cells for 10 minutes at 37° C. Clodronate liposomes or control liposomes (Liposoma, Amsterdam, The Netherlands) were administered intravenously at 5 mg/10g of animal weight weekly starting from day 12 after transplantation.

5.4 BM transduction and transplantation

5.4.1 Virus production

MSCV empty vector-, MSCV-IRES GFP BCR-ABL expressing retroviruses (Thermo Fisher Scientific, Darmstadt, Germany), were produced by calcium phosphate transfection of 293T cells. The day prior to transfection, $3-4 \times 10^6$ 293T cells were plated, and 18 hours after the medium was replaced with fresh media containing chloroquine (25µM). The transfection mixture was prepared as shown below and mixed with 500 µl of 2X HBS, before the mixture was added dropwise (table 1). After 8 and 24 hours, the medium was replaced with fresh media. The virus was harvested 48 hours after transfection and filtered through a 0.2 µm filter and stored at -80 °C.

Reagent or constructs	Transfectio media
DNA (plasmid)	10 µg
Ecopak	5 µg
CaCl ₂	62 µl
H ₂ O	Up to 500 µl
VSV	
Delta 8.9	

Table 1: Mixture for retrovirus transfection

In order to titer the virus, 3×10^5 3T3 cells were plated the day before transduction. Cells were transduced with the virus in a 1:3 and 1:30 dilution supplemented with 8 $\mu\text{g}/\text{ml}$ of polybrene. After 3-5 hours, the media was replaced, and the transduction efficiency was determined by flow cytometry, considering the percentage of GFP+.

5.4.2 CML

For CML induction (paragraph 6.1), 6 weeks old BALB/c mice were injected with 200 mg/kg 5-fluorouracil (5-FU) by tail vein injection. On day 4 post 5-FU, mice were sacrificed by CO₂ asphyxiation. Bones were harvested and the BM was flushed with media (DMEM + 10% Fetal Calf Serum (FCS) + 1% penicillin streptomycin, 1% L-glutamine). The pellet was lysed with Ammonium-Chloride-Potassium (ACK) lysing buffer and the cells were resuspended in a pre-stimulation media (table 2) and incubated overnight in a 10 cm dish. The next day, cells were resuspended in 2 ml of spinfection media (table 2) in a 6 well plate and transduced with 2 ml cryopreserved retrovirus expressing MSCV IRES GFP BCRABL for 90 minutes at 32 °C at 2500 rpm. After centrifugation, cells were resuspended, placed in an incubator for 2-4 hours and later resuspended in incubation media (table 2). The next day, 2 ml virus was again added back to the well and the spinfection procedure was followed as described above^{181,182}. Cells were counted and 2.5×10^5 cells were intravenously transplanted into sublethally irradiated young and old recipient mice (750 cGy). CML was also induced with lower doses of irradiation (paragraph 6.3). whereby the protocol was followed as mentioned above. However, recipient BALB/c mice were sublethally irradiated with 50,100, 200, 450 cGy.

Reagent	Pre-stimulation media	Spinfection media	Incubation media
DMEM			
FCS	10 %	10 %	10 %
WEHI	5 %	5 %	5 %
P/S	1 µg/ml	1 µg/ml	1 µg/ml
L-Glutamine	2 nM	2 nM	2 nM
Ciprofloxacin	1 µg/ml	1 µg/ml	1 µg/ml
IL3	6 ng/ml	6 ng/ml	6 ng/ml
IL6	10 ng/ml	10 ng/ml	10 ng/ml
SCF	100 ng/ml	100 ng/ml	100 ng/ml
Polybrene		2 µg/ml	
Hepes		10 mM	

Table 2: Composition of the pre-stimulation, spinfection and incubation media for induction of CML.

5.4.3 B-ALL in syngeneic mouse model

For B-ALL induction (only paragraphs 6.3 and 6.18.1), tibias and femurs from 6 weeks old BALB/c or C57BL/6 mice were harvested and the BM was flushed with DMEM + 10% FCS + 1% P/S, 1% L-glutamine. The pellet was lysed with ACK lysing buffer and cells were transduced with 2 ml of cryopreserved retrovirus expressing MSCV-IRES-GFP and centrifuged for 90 minutes at 32 °C at 2500 rpm. After centrifugation, cells were resuspended in DMEM + 10% FBS + 1% P/S, 1% L-glutamine and placed in the incubator for 4 hours. Cells were counted, and 1×10^6 cells were intravenously transplanted into sublethally irradiated (750 cGy for BALB/c and 900 cGy for C57BL/6) young and aged recipient mice. Trial experiments to assess the induction efficiency of B-ALL in unirradiated and irradiated mice

were also performed. In this case, doses of 1×10^6 , 2×10^6 and 3×10^6 and 2×10^6 , 3×10^6 and 5×10^6 BCR-ABL1-transduced BM cells for the BALB/c and C57BL/6 mice strains, respectively, were transplanted into unirradiated and sublethally irradiated BALB/c and C57BL/6 (750 cGy for BALB/c and 900 cGy for C57BL/6) young recipient mice (paragraph 6.3). After that, the remaining B-ALL transplants followed the protocol previously mentioned, but 2×10^6 cells were intravenously transplanted into young and old BALB/c or C57BL/6. In another experiment, B-ALL initiating cells were pretreated *in vitro* with 1% BSA or 100 ng/ml recombinant CXCL13 for 18 hours prior to transplantation into unirradiated 6-week old BALB/c mice at a dose of 2×10^6 cells. To assess the role of ageing as a hematopoietic cell-intrinsic, as well as -extrinsic factor, 3, 6- and 78-week old BM cells transduced with BCR-ABL1 were transplanted into either young or old unirradiated recipient mice (paragraph 6.4).

5.4.4 B-ALL in patient derived xenograft

2×10^6 total BM cells from four individual adult human patients with B-ALL were each intravenously transplanted into sublethally irradiated (200 cGy) pairs of young (4 weeks old) versus old (>18 months) NSG mice. Human patients used in this study are listed in the table 3.

Name	Patient age (years)	Diagnosis	Used IHC / FACS / Xenotransplantation
1	Adult (21)	B-ALL	FACS / Xenotransplantation
2	Adult (53)	B-ALL	FACS / Xenotransplantation
3	Adult (23)	B-ALL	FACS / Xenotransplantation
4	Adult (56)	B-ALL	FACS / Xenotransplantation
5	6	B-ALL	FACS
6	14	B-ALL	FACS
7	6	B-ALL	FACS
8	2	B-ALL	FACS
9	8	B-ALL	FACS
10	3	B-ALL	FACS
11	13	B-ALL	IHC
12	6	B-ALL	IHC
13	11	B-ALL	IHC
14	5	B-ALL	IHC
15	8	B-ALL	IHC
16	Adult	B-ALL	IHC
17	Adult	B-ALL	IHC
18	Adult	B-ALL	IHC
19	4	T-ALL	IHC

Table 3: Human samples used for the patient derived xenograft (PDX) transplant, FACS and IHC.

5.4.5 Homing

In the homing assays, 2.5×10^6 5-FU-treated (in the CML model) or 5×10^6 BM cells (in the B-ALL model) transduced with BCR-ABL1 were intravenously injected into sublethally irradiated young and old recipient mice. 18 hours later, BM and spleen were harvested and analysed by flow cytometry for BCR-ABL1 (GFP+) Lin- c-Kit+ (CML) or BCR-ABL1 (GFP+) BP-1+ (B-ALL) cells.

5.4.6 Analysis of diseased mice and tumour burden

To assess the disease progression of the transplanted mice, blood samples were collected on day 15 for CML and day 12, 19, 21, 34 for B-ALL, using Scil Vet animal blood counter (Scil Animal Care Company, Viernheim, Germany). Cells were lysated with ACK lysis buffer followed staining with CD11b (CML) and BP-1 (B-ALL) and analysed for GFP+/CD11b+ or GFP+/BP-1+ by flow cytometry. In addition, antibody to human CD45 was used to monitor the NSG mice. At the time of dead spleen, bone, lung and liver were collected for further analysis and a pathological report was created. The antibodies used in this study are listed in table 4. Bone sections of deceased mice were decalcified in 0.5 M Ethylenediaminetetraacetic acid (EDTA), paraffin-embedded and stained with haematoxylin and eosin according to standard protocols.

5.5 Southern Blotting

Genomic DNA from spleen of young versus old recipient mice with CML was digested with the restriction enzyme BglII, run on an agarose gel and transferred onto a nylon membrane. The blot was then hybridized with a radioactively labeled probe targeting the GFP gene, in order to detect distinct proviral integration sites, as described^{173,183}.

5.6 Methylcellulose assay

2×10^5 of total BM or 2×10^4 spleen cells from CML recipient mice were plated in cytokine-free methylcellulose (M3231, Stem Cell Technologies, Vancouver, Canada) supplemented with 100 pg/ml IL-3 (Peprotech, Rocky Hill, NJ, USA). After 10 days colonies were scored.

5.7 Culture of primary cells and cell lines

The murine pro-B cell line BA/F3 was purchased from the DSMZ (German Collection of Microorganisms and Cell Cultures GmbH) and grown in RPMI, 10% FCS, 1% P/S and 1% L-glutamine supplemented with 5% (v/v) WEHI as a source of interleukin-3. Primary murine BCR-ABL1⁺ B-ALL cells were cultured in RPMI, 10% FBS, 1% P/S and 1% L-glutamine supplemented with IL-7 (10 ng/ml). Primary murine macrophages were grown in α -MEM, 20% FBS, 1% penicillin/streptomycin and 1% L-glutamine. Primocin (100 μ g/ml) (InvivoGen, Toulouse, France) was added to the culture medium. All cell lines were maintained in a 37 C, 5% CO₂ incubator.

5.8 Isolation of bone marrow derived macrophages (M Φ)

Young versus old BM marrow derived macrophages (M Φ) were obtained by crushing femora, tibiae, and humeri of young and old mice in Phosphate buffered saline (PBS) using mortar and pestle and then expanded and maintained in media, once non-adherent cells were removed. BM derived M Φ were used when they reached 70-80 % confluence. The immunophenotype was confirmed by staining for CD11b and F4/80 or CD169 by flow cytometry. The immunophenotype of the adherent cells was confirmed by use of the following markers: F4/80⁺ CD169⁺ for macrophages, F4/80⁺ CD169⁻ CX3CR1⁺ CD115⁺ CD11c⁻ for monocytes, F4/80⁺ CD169⁻ CX3CR1⁺ CD115⁻ CD11c⁺ for dendritic cells and F4/80⁺ CD169⁻ CD115⁻ Gr-1⁺ for neutrophils by flow cytometry (Cytek Aurora, Netherlands, Germany) (table 4).

Conditioned medium was harvested after 48 hours and stored at -80°C. For the coculture assays, primary cells and/or empty vector- or BCR-ABL1-transduced BA/F3 cells were used in order to assess the proliferation, adhesion and migration on young and old BM M Φ , respectively.

Antibody	Fluorochrome	Company
Anti - human CD45		Miltenyi Biotec, Germany
Anti - human CD19	FITC	BioLegend San Diego, CA
Anti - human CXCR5	APC	R & D Systems
Anti - human CD68	PB	Thermo Fisher Scientific
Anti - human CD14	BV-711	BioLegend San Diego, CA
Anti - human CD16	APC	BioLegend San Diego, CA
Anti - human CXCL13		BioLegend San Diego, CA
Anti - mouse F4/80 - biotin	APC	BioLegend San Diego, CA
Anti - mouse CXCR5	PE	BioLegend San Diego, CA
Anti - mouse Ki67	PE	BioLegend San Diego, CA
Anti - mouse CD11b	PE	BioLegend San Diego, CA
Anti - mouse BP-1	APC - Cy7	BioLegend San Diego, CA
Anti - mouse Gr-1	BV - 605	BioLegend San Diego, CA
Anti - mouse CD169	PE	BioLegend San Diego, CA
Anti - mouse CX3CR1	PerCP - Cy5.5	BioLegend San Diego, CA
Anti - mouse Ly-6G/Ly-6C	FITC	BioLegend San Diego, CA
Anti - mouse CD11b	APC	BioLegend San Diego, CA
Anti - mouse Ly6c	APC	BioLegend San Diego, CA
Anti - mouse MHC II	FITC	BioLegend San Diego, CA
Anti - mouse CXCL13	BV - 421	R & D Systems
Anti - mouse B220 - biotin	PE-Cy7	BioLegend San Diego, CA
Anti - mouse CD11c	FITC	BioLegend San Diego, CA

Table 4 Antibodies used in this study.

5.9 Measurement of p- γ -H2AX and ROS

Young versus old BM M Φ were fixed with the cytoperm/cytofix kit (BD Biosciences, San Jos., CA, USA) and stained overnight with an antibody to p- γ -H2AX (Cell Signalling, Danvers, MA, USA) at a 1:50 dilution. Cells were washed and incubated with the secondary antibody Alexa Fluor 647 (Invitrogen, Grand Island, NY) at a 1:400 dilution for one hour at room temperature. The amount of DNA damage was assessed by flow cytometry. ROS levels were determined using the CellROX Deep Red oxidative stress reagent (Thermo Fisher Scientific, Darmstadt, Germany). The CellROX[®] Reagent was added at a final concentration of 5 μ M to the BM M Φ and incubated for 30 minutes at 37°C. The media was removed, cells were washed 3 times with PBS, and the amount of ROS was analysed by flow cytometry.

5.10 Quantification of CXCL13

5.10.1 RNA isolation and quantitative polymerase chain reaction

4x10⁵ BM M Φ from young versus old mice were plated. 18 hours after they were collected and washed twice with PBS. The cell pellet was resuspended in TRIzol (Thermo Fisher Scientific, Darmstadt, Germany), and RNA extraction was performed using the Qiagen kit protocol (Cat. No. 74034, Qiagen, Germany) and stored at -80 °C. The RNA content was quantified after thawing using the NanoDrop spectrophotometer, and 300 ng of RNA was used for complementaryDNA(cDNA) synthesis as indicated in the procolol (New England Biolabs, USA). A mastermix was prepared with Power SyBR Green and using the *Cxcl13* primers 5'-CTCCAGGCCACGGTATTCTG-3' (forward) and 5'-CCAGGGGGCGTAACTTGAAT-3' (reverse) and *Gapdh* primers 5'-GGGGTCGTTGATGGCAACA-3' (forward) and 5'-AGGTCGGTGTGAACGGATTTG-3' (reverse) (Thermo Fisher Scientific, Darmstadt), as indicated in Table 5. The qPCR reaction was started on a StepOnePlus Real-Time PCR System, AB Applied Biosystem. The average of the triplicate Ct value was calculated and normalized

to the CT values of GAPDH. The $2^{-\Delta\Delta C_t}$ formula was used to calculate the fold change expression of *Cxcl13* in young and old BM MΦ.

Component	Volume or Concentration
cDNA	5 ng
SyBR Green	10 μl
Nuclease free H ₂ O	7 μl
<i>CxCl13</i> (forward)	10 μM
<i>CxCl13</i> (reverse)	10 μM
<i>Gapdh</i> (forward)	10 μM
<i>Gapdh</i> (reverse)	10 μM

Table 5: qPCR mix

5.10.2 Cytokine flow cytometry

Expression of CXCL13 in different cell populations such as macrophages, monocytes, dendritic cells and neutrophils from young versus old mice was tested by flow cytometry using the same gating strategy, as described above. CXCL13 expression was also assessed in classical (hCD45⁺ hCD14⁺ hCD16⁻) and non-classical monocytes (hCD45⁺ hCD14^{dim} CD16⁻) in human B-ALL samples by flow cytometry (Cytek Aurora, Netherlands), as described¹⁷⁷.

5.10.3 ELISA

Conditioned medium from young versus old BM macrophages was collected as described above. Macrophages from mice with established disease were isolated, and the conditioned medium was collected as above. The BM from young and old mice (healthy), as well as from mice with established disease was flushed with equal amounts of PBS. Plasma from PB (in

EDTA) was obtained by centrifugation for 10 min at 2000 x g at room temperature. The concentration of CXCL13 was determined using the mouse CXCL13 ELISA Kit (Biolegend, San Diego, CA, USA) according to the manufacturer's instructions.

5.10.4 Western blot

When the macrophages had reached confluence, the cells were pelleted and washed two times with cold PBS. The pellets were lysed in RIPA buffer (50 mM Tris HCl, pH 7.4, 150 mM NaCl, 1% Triton X-100, 1% sodium deoxycholate (NaDOC), 0.1% sodium dodecyl sulfate (SDS) and 1 mM EDTA, 50 mM sodium fluoride (NaF), 1 mM Na₃VO₄, aprotinin and phenylmethylsulfonyl fluoride (PMSF) and incubated on ice for 20 minutes, followed by centrifugation at 4°C at 14000 rpm for 20 minutes. The supernatant was collected, and the protein concentrations were measured using the Bradford protein assay (Bio-Rad, Hercules, CA, USA). The absorption was measured at 595 nm and equal concentrations of samples were mixed with SDS running buffer Roti-load 4x (Carl Roth, Karlsruhe, Germany), boiled at 95 °C for 5 minutes and loaded on 4-12% NuPAGE Bis Gel (Thermo Fisher Scientific, Darmstadt) and run for 120 minutes at 120 V. Proteins were blotted onto a polyvinylidene difluoride (PVDF) membrane (Thermo Fischer Scientific, Darmstadt, Germany) for 60 minutes at 200 V. In the macrophage experiment, membranes were blocked with 5% milk in TBST for 30 minutes. The membranes were probed with antibodies to CXCL13 (Biorbyt, Cambridge, United Kingdom) (1:500 dilution) and actin (Sigma-Aldrich, Munich, Germany) (1:1000 dilution) overnight at 4°C. The following day, the membranes were washed three times with TBST for 10 minutes. Consequently, the membranes were stained with the secondary antibodies anti-rabbit HRP (70748, Cell Signaling, Danvers, MA, USA) and anti-mouse enzyme horseradish peroxidase (HRP) (Cell Signaling, Danvers, MA, USA) for 1 hour at room temperature. Membranes were washed 3 times with TBST for 10 minutes and incubated with

luminol-enhancer and peroxide solution using the ECL Western Blotting Substrate mixture (Thermo Fisher Scientific, Darmstadt) for 1 minute, and the films were developed.

5.11 Proliferation analysis

The proliferative index, i.e. the total amount of divisions divided by the number of cells that went into division, of young versus old macrophages was determined using the CellTrace™ CFSE Cell Proliferation Kit (Thermo Fischer Scientific, Darmstadt, Germany) and FlowJo's Proliferation Tool. In the coculture experiment, 5×10^4 young or old macrophages were plated, before 1×10^5 sorted GFP⁺ (BCR-ABL1⁺) BP-1⁺ BM cells or 3×10^4 BCR-ABL1⁺ or empty vector⁺ BA/F3 cells were added to the culture and leukemia cells were enumerated for 48 hours or 5 continuous days. For the enumeration of primary B-ALL cells, mice with established B-ALL were euthanized, and their BM was flushed, and 1×10^5 total BM cells were plated on young versus old macrophages. Assessment of leukemia cell numbers started on day 8 post culturing.

5.12 Migration and adhesion assays

For the migration assay, 7×10^5 young versus old macrophages were plated into wells of a 24-well-plate and allowed to adhere overnight. $4 \mu\text{m}$ (for primary cells) or $8 \mu\text{m}$ (for BCR-ABL1⁺ BAF/3 cells) transwell polycarbonate membrane cell culture inserts (Corning, NY, USA) were inserted into the wells, and 1×10^5 sorted GFP⁺ (BCR-ABL1⁺) BP-1⁺ BM cells or BCR-ABL1⁻ or empty vector-transduced BA/F3 cells were added to the upper compartment. 1% of BSA or 100 ng/ml of recombinant CXCL13 (Peprotech, Hamburg, Germany) and 2.5 μg isotype control or anti-CXCL13 antibody (R&D Systems, Minneapolis, MN, USA) were added to the lower compartment. 8 hours (for BAF/3 cells) or 24 hours (for primary cells) after plating the migrated cells in the lower chamber were counted.

For the adhesion assay, 7×10^5 young versus old BM M Φ were plated into wells of a 48-well-plate and left to adhere overnight at 37° C. The next day, the media was removed and 1×10^5 primary B-ALL cells or BCR-ABL1+ or empty vector+ BAF/3 cells were plated. After 6 hours, non-adherent cells were removed and the adherent primary and/or BAF/3 were scored by analysing 3 images taken at random, non-overlapping locations.

5.13 Immunofluorescence

BCR-ABL1+ BA/F3 cells were cultured on young versus old BMM Φ in the presence of 2.5 μ g IgG2a control or anti-CXCL13 antibodies for 5 days. The BM M Φ from young or old mice had been cultured on poly-L-lysine coated cover slips. Subsequently, the BCR-ABL1+ BA/F3 cells were removed from the cocultures and cytopun at 500 rpm for 1 minute. The slides were air dried and the area of interest was encircled with a PAP pen. Cells were fixed with 4% paraformaldehyde for 10 minutes at room temperature and permeabilized with 0.25% Triton X-100 for 10 minutes. The cells were then blocked with 2% goat serum and incubated with a primary antibody to p-AKT (Cell Signalling, Danvers, MA, USA) at a 1:50 dilution overnight at 4 °C. In the other immunofluorescence experiment cultured BM M Φ from young or old mice were fixed, permeabilized and blocked as described above and, consequently, stained with an antibody to translocase of the outer membrane (TOM)20 (Santa Cruz Biotechnology, Dallas, TX, USA) at a 1:200 dilution overnight. Cells for both experiments were gently washed three times with PBS and incubated with the secondary antibodies Alexa Fluor 647 or 488 (Invitrogen, Grand Island, NY, USA) at a 1:400 dilution for one hour at room temperature and then washed twice with PBS. The nuclear staining was assessed by using 4',6-diamidino-2-phenylindole (DAPI) at a dilution of 1:2500 for 5 minutes. The slides were washed again twice with PBS and once with H₂O. The slides were then mounted using mounting media with DAPCO (Sigma-Aldrich, Munich, Germany), and images were taken using a confocal laser

scanning microscope (CSLM) (Leica, Wetzlar, Germany). Quantification of nuclear pAKT was performed using ImageJ. The pAKT signal was corrected by subtraction of background signal. The integrated density of nuclear pAKT was calculated with the formula: Corrected total cell fluorescence (CTCF) = Integrated Density – (Area of selected cell x mean fluorescence of background readings).

5.15 Immunoblotting

BCR-ABL1⁺ BA/F3 cells had been cultured in the presence of 100 and 1000 ng rCXCL13 for 10 minutes. The same procedure was followed, as described previously in paragraph 5.10.4. For this experiment, antibodies to phospho-Akt (Ser473) (Cat. no. 9271, Cell Signaling, Danvers, MA, USA) (1:500) and vinculin (MA5-11690, Invitrogen, Grand Island, NY, USA) (1:1000) were used and incubated overnight at 4°C.

5.14 In vivo microscopy

Unirradiated young versus old BALB/c mice were intravenously injected with 5×10^5 sorted GFP⁺ (BCR-ABL1⁺) BP-1⁺ BM cells from mice with established B-ALL (day 20 after transplantation) or 5×10^5 Lin⁻ cells from healthy mice. The cells were labelled with Cell Tracker orange 5-(and-6) - (((4-chloromethyl)benzoyl)amino) tetramethylrhodamine (CMTMR) dye (C2927, Thermo Fisher Scientific, Darmstadt, Germany) at a 1:1000 dilution for 30 minutes at 37° C in a water bath. To visualize vessels, 1mg of dextran FITC (Sigma-Aldrich, Munich, Germany) was intravenously injected per mouse. The mice were then anaesthetized and the scalp removed. The surface of the skull of the mouse was cleaned with PBS using a clean cotton ball and a drop of Methocell was applied to keep the skull moist. The imaging window was placed on the skull, while the mouse was fixated in a holder. The calvarium was visualized under a 2-photon microscope (LaVision Biotech, Bielefeld,

Germany) using a 20x objective in a 37° C chamber. Using the XYZ-axis controller a well-defined area and the central sinus were identified. Z stacks of 2µm distance and movies at 1 frame/second were acquired using the Inspector Pro software. The representative pictures in paragraph 6.7 represent leukaemia cells labelled with the dye CMTMR (red), vessels labelled with dextran (green). Bone is label-free (blue) due to second and third harmonic generation (SHG-THG)¹⁸⁴.

The total travelled path length and the distances of CMTMR-labelled cells to bone and vessels were measured by ImageJ analysis. The velocity was calculated in µm/s^{19,185}. The distances in µm were normalized for each mouse by dividing by the area of the skull.

5.15 Human patients

The clinical and RNA-sequencing data on *CXCR5* expression in human B-ALL were taken from the study¹⁸⁶. They include childhood, adolescents and young adults (AYA) and adults with B-ALL treated on the Eastern Cooperative Oncology Group (ECOG), Cancer and Leukaemia Group B (CALGB) and MD Anderson Cancer Center (MDACC) trials. Childhood was defined as up to the age of 16, while AYA were defined as ages 16-39 and adults as > 40 years. Childhood NCI standard-risk includes children aged 1 to < 10 with a white blood cell count (WBC) < 50K. The childhood NCI high-risk category includes children of the age 10-16 or WBC > 50K. Associations between *CXCR5* expression and treatment outcomes event-free survival (EFS) and overall survival (OS) from diagnosis samples were calculated using the Kaplan-Meier method and log-rank test. An event was defined as a failure to achieve remission, a relapse after remission, death from any cause, or the development of a second malignancy. CNS relapse of B-ALL in relation to *CXCR5* expression was analysed using the van der Velden dataset¹⁸⁷. This dataset contains microarray gene expression data from B-ALL cells retrieved from the cerebrospinal fluid of 8 children with a CNS relapse of B-ALL, compared with cells

from the BM of 22 patients at diagnosis and cells from the BM of 20 patients with BM relapse. BM samples were purified and analysed using Affymetrix U133 Plus 2.0 Array. The data was deposited on the NCBI GEOData Sets as GSE60926. In healthy human individuals, hCD45⁺ hCD19⁺ CXCR5⁺ leukocytes were detected in the peripheral blood by flow cytometry (Cytex Aurora, Netherlands) after red blood cell lysis. The human samples used for flow cytometry analysis are listed above. The antibodies used are listed in Table 4.

5.16 Immunohistochemistry

Immunohistochemistry was performed using the DAKO FLEX-Envision Kit (Agilent, Santa Clara, CA, US) and the fully automated DAKO Omnis staining system (Agilent) according to the manufacturer's instructions. DAKO CD68 primary antibody (GA609, ready to use dilution, Agilent, Santa Clara, CA) was used for immunohistochemical epitope staining, applied for 30 min after heat-induced epitope retrieval in pH 9 at 97°C. CXCL13 primary antibody (AF801, diluted 1:200, R&D Systems, Minneapolis, MN, US) was used for immunohistochemical epitope staining. The antibody was applied for 1 hour after heat-induced epitope retrieval in pH 9 at 97°C. Epitope visualization was done by DAKO EnVision™ FLEX DAB⁺ Substrate Chromogen System (Agilent, Santa Clara, CA) resulting in a brown cytoplasmic, membranous signal. Co-staining of CD14 and CD16 was performed by a manual procedure using the DAKO FLEX-Envision Kit according to the manufacturer's instructions. CD14 primary antibody (clone 1H5D8, ab181470, diluted 1:100, abcam, Cambridge, UK) was used for immunohistochemical epitope staining, applied for 30 min after heat-induced epitope retrieval in pH 9 at 97°C. CD16 primary antibody (EPR22409-124, ab246222, diluted 1:100, abcam, Cambridge, UK) was used for immunohistochemical epitope staining, applied for 30 min after heat-induced epitope retrieval in pH 9 at 97°C. CD16 epitope visualization was done by DAKO EnVision™ FLEX DAB⁺ Substrate Chromogen System resulting in a brown cytoplasmic,

membranous signal. CD14 epitope visualization was done by DAKO EnVision™ FLEX Magenta Chromogen HRP System (Agilent, Santa Clara, CA) resulting in a pink cytoplasmic, membranous signal. Nuclear counterstaining was performed using DAKO hematoxylin solution (Agilent, Santa Clara, CA). The human samples are listed above (Table 3).

5.17 RNA-sequencing (RNA-seq)

The RNA of 10,000 cells per replicate was isolated using the RNeasy Plus Micro Kit (Qiagen) following the standard protocol. Library preparation was performed by the Genomics & Proteomics Core Facility of the German Cancer Research Center (DKFZ) conducting the standard Ultra Low RNA-Seq protocol. Sequencing was performed on the Illumina HiSeq 4000 in paired-end 100 bp mode. Data processing was done by applying the nf-core/rnaseq pipeline (<https://github.com/nf-core/rnaseq>).

5.18 ATAC-seq

Bone marrow-derived macrophages were obtained as described above. ATAC-seq libraries from young and old BM macrophages were prepared according to the Omni-ATAC protocol¹⁸⁸. 50,000 viable cells in suspension (α -MEM, 1 % penicillin/streptomycin, 20% FBS, 1% L-glutamine) were processed per replicate. The cells were washed in PBS and, subsequently, nuclei were isolated using cold lysis buffer (0.01% digitonin (Sigma-Aldrich, Munich, Germany), 1% NP40 (Genaxxon Bioscience, Ulm, Germany) and 0.1% Tween-20 (Sigma-Aldrich, Munich, Germany)). Nuclei were washed and resuspended in ATAC resuspension buffer (10 mM Tris-HCl pH 7.4 [Sigma-Aldrich, Munich, Germany], 10 mM NaCl [Sigma-Aldrich, Munich, Germany], 3 mM MgCl₂ [Sigma-Aldrich, Munich, Germany]). Pelleted nuclei were then resuspended in 2x transposition buffer (20 mM Tris-HCl pH 7.6 [Sigma-Aldrich, Munich, Germany], 3 mM MgCl₂ [Sigma-Aldrich, Munich, Germany], 20% dimethyl

formamide [Sigma-Aldrich, Munich, Germany]). The tagmentation reaction was performed by adding 2.5 µl of tagment DNA Enzyme 1 (Illumina, San Diego, CA, USA) and rotating the mixture at 1000 rpm for 30 minutes at 37°C. Transposed chromatin was then purified using 30 µl of AMPure XP beads (Beckman Coulter, Brea, CA, USA), 20 µl of 5 M Guanidinium thiocyanate (Sigma-Aldrich, Munich, Germany), and 110 µl of PEG buffer (2.5 M NaCl [Sigma-Aldrich, Munich, Germany], 20% PEG 8000 [Sigma-Aldrich, Munich, Germany]). Library amplification was performed in two steps by adding 25 µl of NEBNext High Fidelity 2x Master Mix (NEB, Ipswich, MA, USA), 0.8 µl of 10 µM Custom Nextera PCR Primer 1, and 0.8 µl of 10 µM Custom Nextera PCR Barcode to 25 µl of the transposed DNA. The first amplification was performed using the following program: 5 minutes at 72°C, 30 seconds at 98°C, 5 cycles of 10 seconds at 98°C, 30 seconds at 63°C, and 1 minute at 72°C, and finally 1 minute at 72°C. To determine how many additional cycles were needed to reach sufficient amplification, 5 µl of the pre-amplified PCR mixture were analyzed using Sybr Green I nucleic acid gel stain (Thermo Fisher Scientific, Waltham, MA, USA) and a light cycler instrument (Roche, Basel, Switzerland) by applying the following program: 30 seconds at 98°C, 20 cycles of 10 seconds at 98°C, 30 seconds at 63°C, 1 minute at 72°C, and, finally, 1 minute at 72°C. In a second round, based on the quantitative PCR results, n additional cycles were applied to the remaining pre-amplified mixture. The resulting library was purified with a 2-sided size selection applying 0.5x and 1.4x of AMPure XP beads (Beckman Coulter, Brea, CA, USA) and finally resuspended in 1X EB buffer (Qiagen, Hilden, Germany). Concentration of the library was measured using the Qubit dsDNA HS Assay Kit (Thermo Fisher Scientific, Waltham, MA, USA). Quality control was performed on a Bioanalyzer station using the Agilent High Sensitivity DNA Kit (Santa Clara, CA, USA). Sequencing was performed at the DKFZ Genomics and Proteomics Core Facility using the High Seq 2000 v4 Paired-End 125 bp platform.

5.18.1 ATAC-seq data processing

Sequencing reads were quality- and adapter-trimmed using Trim Galore v. 0.4.4 ¹⁸⁹ in combination with Cutadapt v. 1.14 ¹⁹⁰ by deploying the parameters “--paired”, “--nextera”, “--length_1 35”, “--length_2 35”. Sequencing reads were aligned against the reference genome GRCm38 using Bowtie2 v. 2.2.6 ¹⁹¹ with the “--very-sensitive” flag enabled and the maximal insertion length set to 2500 bp. Aligned reads of the same library preparation sequenced on multiple lanes were combined using SAMtools merge v. 1.5 ¹⁹². Picard MarkDuplicates v. 2.17.4 ¹⁹³ was applied to remove PCR duplicates. Reads that did not map as proper pairs or that exhibited a mapping quality below 20 on the Phred scale were filtered out by means of SAMtools view. Adey et al. ¹⁹⁴ previously showed that each Tn5 transposase homodimer binds a stretch of 29 bp, consisting of a 9 bp central region which is subject to the transposition event and two 10 bp flanking regions. Thus, the minimal fragment size resulting from tagmentation of two neighbouring Tn5 transposase homodimers is 38 bp (9 bp +10 bp +10 bp +9 bp). All read pairs showing a smaller size were removed. To reconstruct the 29 bp transposase binding regions, the 5' end of each read was extended by 19 bp into 5' direction and 10 bp into 3' direction. All downstream analyses were based on these adjusted read coordinates. Peak calling was performed using MACS2 callpeak v. 2.1.0.20140616 ¹⁹⁵ with a q-value cutoff of 0.05 and the arguments “--broad”, “--nomodel”, “--keep-dup”, and “--gsize mm”. The analysis workflow was described using the Common Workflow Language v. 1.0 ¹⁹⁶.

5.18.2 ATAC-seq - Differential accessibility analysis

Differential accessibility analysis, as well as related plots were performed using the DiffBind R package (R package version 2.12.0) ¹⁹⁷. In short, a common peak set was identified by the presence of a peak in at least two samples. Differential analysis was performed using edgeR ¹⁹⁸. Regions with a false discovery rate (FDR) <0.05 and an absolute log₂ fold change > 1 were

considered as significantly differentially accessible. Further annotation of all differentially accessible regions was performed with the R package ChIPseeker (R package version 1.20.0)¹⁹⁹.

5.18.3 ATAC-seq - Transcription factor activity analysis

To assess differential transcription factor activity, diffTF was applied to the ATAC-seq data set ²⁰⁰. diffTF (version 1.3.3) was used with default parameters comparing young versus old BM macrophages. As a reference 442 mouse transcription factors with *in silico* predicted transcription factor binding sites, based on the HOCOMOCO 10 database, were used ²⁰¹. For analysis of enriched DNA motifs, the command line tool Homer was used ²⁰². Significantly differentially accessible regions were stratified by increased or decreased accessibility in young versus old BM macrophages, and enrichment was performed against the common peak set identified with DiffBind.

5.18.4 ATAC-seq - Genomic overlap enrichment analysis

The R package LOLA was used for testing overlap and enrichment of differentially accessible peaks with MSigDB Hallmarks gene sets ²⁰³ (R package version 1.14.0) ²⁰⁴. Differentially accessible regions with an FDR < 0.05 were stratified by increased or decreased accessibility in young versus old macrophages, and enrichment was performed against the common peak set identified with DiffBind.

5.18.5 ATAC-seq - Motif analysis

For analysis of enriched DNA motifs, the command line tool Homer was used ²⁰². Significantly differentially accessible regions were stratified by increased or decreased accessibility in young

versus old macrophages, and enrichment was performed against the common peak set identified with DiffBind.

5.18.6 ATAC-seq - Code availability

Publicly available software tools were used and are listed in the methods section. The custom scripts used for the analyses described in the manuscript are available upon request.

5.19 Statistical methods

If normality could be assumed, a student's *t*-test was used to compare the mean of two groups of samples. Otherwise a Mann-Whitney-U-test was employed. Differences in survival were assessed by Kaplan-Meier non-parametric estimates (log-rank test). When multiple hypotheses were tested, one-way ANOVA or, if the groups were not normally distributed, a Kruskal-Wallis test was performed. For normal distribution a Tukey test was used as post-hoc test. All data were presented as mean \pm s.d.. GraphPad Prism (Version 7.0b) was used for performing group comparisons. For definition of the optimal cut-off point for CXCR5 levels, we used time-dependent receiver operating characteristic (ROC) analysis²⁰⁵. For this we applied R (packages: survival, timeROC). Statistical analyses for the ATAC-seq experiment were performed using R version 3.6²⁰⁶ (URL <https://www.R-project.org>). *P* values ≤ 0.05 were accepted as significant.

6 Results

6.1 Differential efficiency of CML induction in a young versus aged BMM

Recent reports have emphasized the significance of the BMM in leukaemias¹⁷⁴⁻¹⁷⁶. Given that adults have the highest incidence of CML, (details in paragraph 3.2.1), we hypothesized that an aged BMM favors CML, while a young BMM favors B-ALL. To test our hypothesis, we transplanted BM from 6-week old mice, transduced with BCR-ABL1- into either young (3-4-week-old) or aged (>16-week-old) sub-lethally irradiated mice. We observed a trend towards an increase of tumour burden in the PB of aged mice (figure 9 A), which may reflect a higher aggressiveness of CML in aged mice (figure 9 B). Hematoxylin and eosin (H&E) examination of bone sections from aged mice with CML revealed an increased overall cellularity with an increased myeloid to erythroid ratio, consistent with efficient CML induction^{173,183}, while the BM of young mice was hypocellular with accumulation of an eosinophilic mass, indicative of inefficient induction of CML in this model (figure 9 C). There were no significant differences in the homing of BCR-ABL1+ Lin- c-Kit+ or BCR-ABL1+ Lin- cells to an aged versus a young BMM (Figure 9D, left and right). Southern blotting of spleen tissue showed a significant increase in clonality with an increased engraftment of proviral clones compared to a young BMM in aged mice (figure 9 E-F). The function of CML cells was assessed via a colony-forming unit (CFU) assay in methylcellulose. The number of colonies was higher when the plated BM cells were derived from aged mice with CML (figure 9 G), suggesting that the number and/or function of myeloid progenitors in young mice with CML is decreased and/or impaired.

In summary, these findings indicate that an aged BMM is more supportive of CML progenitors and leukemia-initiating cells (LIC) maintenance than a young BMM.

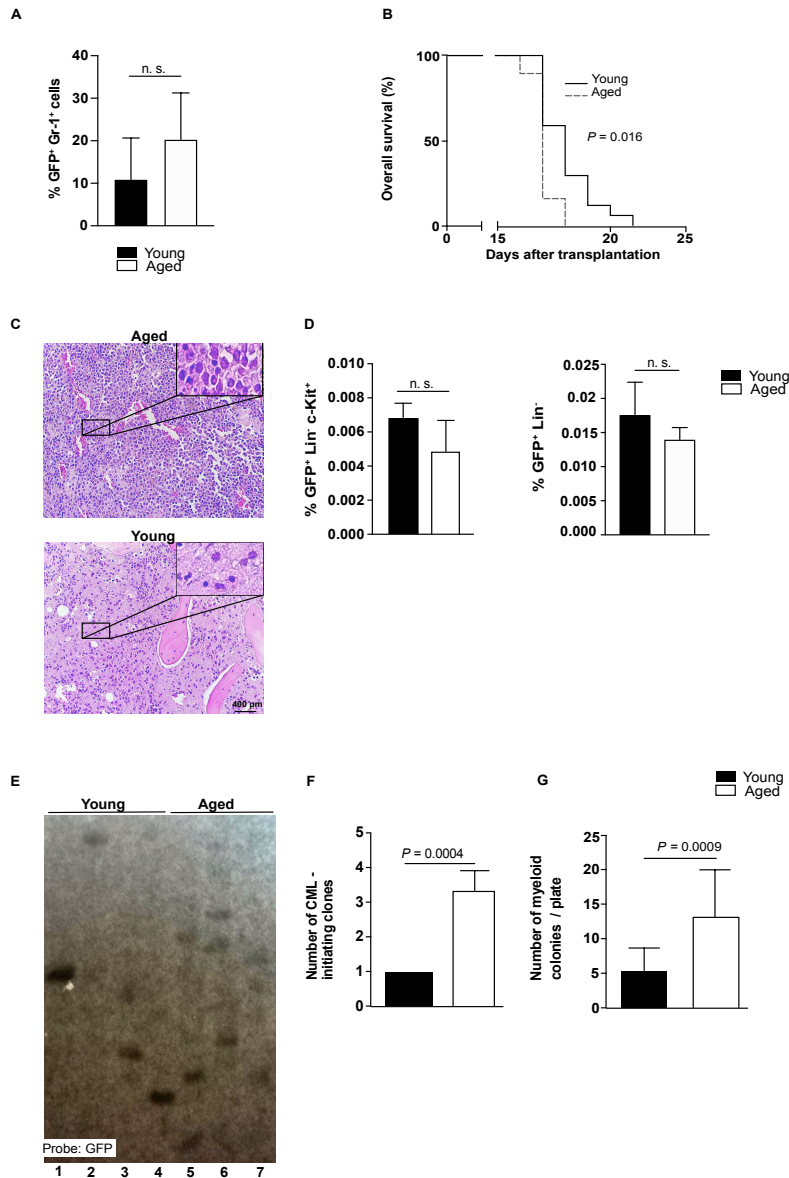


Figure 9 Chronic myeloid leukaemia (CML) induced in young and aged mice.

A) Percentage of GFP⁺ (BCR-ABL1⁺) Gr-1⁺ cells in peripheral blood (PB) of young (black) or aged (white) BALB/c recipient mice on day 15 of transplantation in the CML model. **B)** Kaplan-Meier-style survival curve for young (solid line) or aged (dashed line) irradiated (750 cGy) BALB/c recipients of 2.5×10^5 5-fluorouracil-pretreated BCR-ABL1-transduced BM cells. **C)** Hematoxylin and eosin stain of the femora of representative young versus aged recipient of BCR-ABL1-transduced BM in the CML model as in (B). **D)** Percentage of GFP⁺ (BCR-ABL1⁺) Lin⁻ c-Kit⁺ cells (left) and percentage of GFP⁺ (BCR-ABL1⁺) Lin⁻ cells (right) of total leukocytes which homed to the bone marrow (BM) of young (black) versus aged (white) mice. **E and F)** Southern blot showing disease clonality in spleens of young (lanes 1-4) versus aged (lanes 5-7) BALB/c recipients of BCR-ABL1-transduced BM (E) and disease clonality (F) in the CML model. **G)** Number of myeloid colonies per plate from the BM of young (black) versus aged (white) mice with CML. (*P* values are as indicated).

6.2 Differential efficiency of B-ALL induction in a young versus aged BMM in sublethally irradiated mice.

Given our findings on the role of an aged microenvironment for the aggressiveness of CML, as well as the highest incidence of human B-ALL in children (paragraph 3.2.2), we hypothesized that a young environment may contribute to the phenotype of (BCR-ABL1+) paediatric B-ALL. BM transduced with BCR-ABL1 in the retroviral transduction/transplantation model of B-ALL was transplanted into young and aged mice. This revealed a significant prolongation of survival in aged sub-lethally irradiated recipient mice (figure 10). This data suggests that in B-ALL the young BMM accelerates the B-ALL progression.

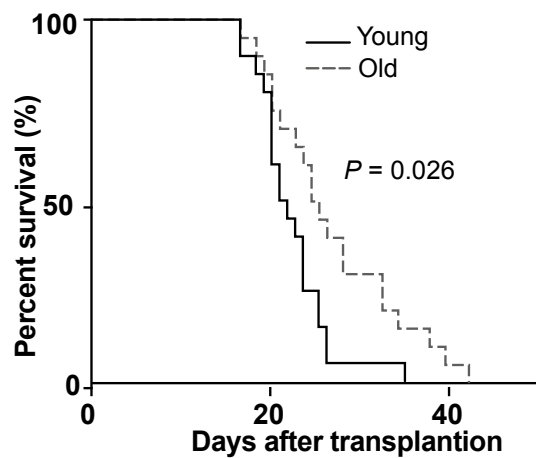


Figure 10 B-cell acute lymphoblastic leukaemia (B-ALL) induced in young and aged irradiated mice.

Kaplan-Meier-style survival curve for young (black) or old (gray) BALB/c recipient mice in the model of B-ALL. (*P* value is as indicated).

6.3 B-ALL can be induced without pre-conditioning irradiation

A common strategy for overcoming immunologic rejection and improving engraftment is to sublethally irradiate recipient mice before transplantation^{207,208}. As a result, we hypothesized that irradiation may have played a role in the observed phenotype (paragraphs 6.1 and 6.2). Therefore, trial experiments on recipient mice using various irradiation doses or no irradiation were conducted. CML was induced in irradiated C57BL/6 mice (50,100, 200, 450 cGy), and the disease was monitored over time. As figure 10A shows, with the lowest irradiation dose (50 cGy), induction of CML was not efficiently achieved. In the case of B-ALL (figure 10 B), BCR-ABL1-transduced doses of 1×10^6 , 2×10^6 , 3×10^6 and 2×10^6 , 3×10^6 and 5×10^6 BM cells for the BALB/c and C57BL/6 mouse strains, respectively, were transplanted into unirradiated and sublethally irradiated BALB/c and C57BL/6 young recipient mice. In both mouse strains, B-ALL was successfully induced in all conditions (figure 10 C-D). To test our hypothesis in paragraph 6.2. we chose to proceed with transducing BM cells with BCR-ABL1 and transplanting them into young and old unirradiated BALB/c recipient mice.

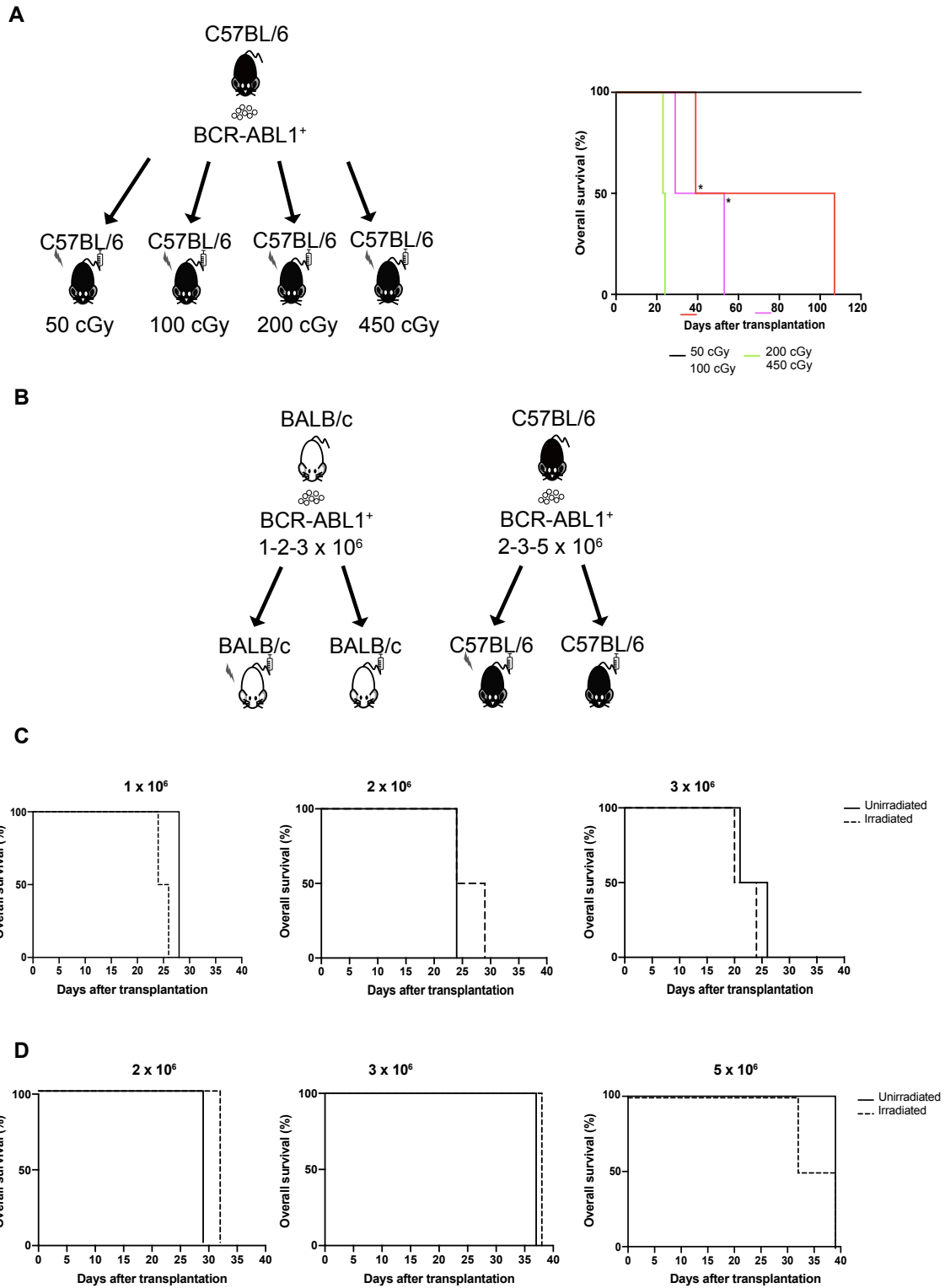


Figure 11 Induction of CML and B-ALL in irradiated and non-irradiated mice.

A) Kaplan-Meier-style survival curve of mice irradiated with different doses in the CML model. **B)** Outline of B-ALL induction in young BALB/c and C57BL/6J recipient mice **C)** and **D)** Kaplan-Meier-style survival curve for young non-irradiated (solid line) and irradiated (dashed line) of BCR-ABL1-transduced BM cells in the B-ALL model.

6.4 The contribution of an ageing BMM to B-ALL development

In the previous paragraphs, we showed that a young BMM contributes to the aggressiveness of B-ALL. However, we cannot rule out the possibility that young and/or old leukemia cells contribute to the clinical picture in humans. Hence, we quantified the contribution of LIC-intrinsic versus -extrinsic ageing effects on B-ALL development. We designed an experiment as shown in figure 12 A, in which BM cells from 3, 6- and 78-week old mice were transduced with BCR-ABL1 in the B-ALL model and transplanted into either young or old unirradiated recipient mice. When comparing the transplants, in which BM cells from 3- and 78-weeks old mice were transplanted into young and old recipient mice, we were able to demonstrate that the disease was more aggressive in young mice transplanted with BM cells from 3 week old mice (figure 12 B left). In contrast, BM cells from 78-week old mice transplanted into young and old recipients did not show significant differences (figure 12 B right). To simply assess the effect of a young and old BMM, 6 weeks old donor BM cells were transplanted into young and old mice, and a significant acceleration of disease was observed in young mice compared to their older counterparts (figure 12 B middle). These findings suggest that the combined contribution of young leukemia cells and a young BMM influences disease aggressiveness and accurately reflects clinical B-ALL development in paediatric versus adult patients.

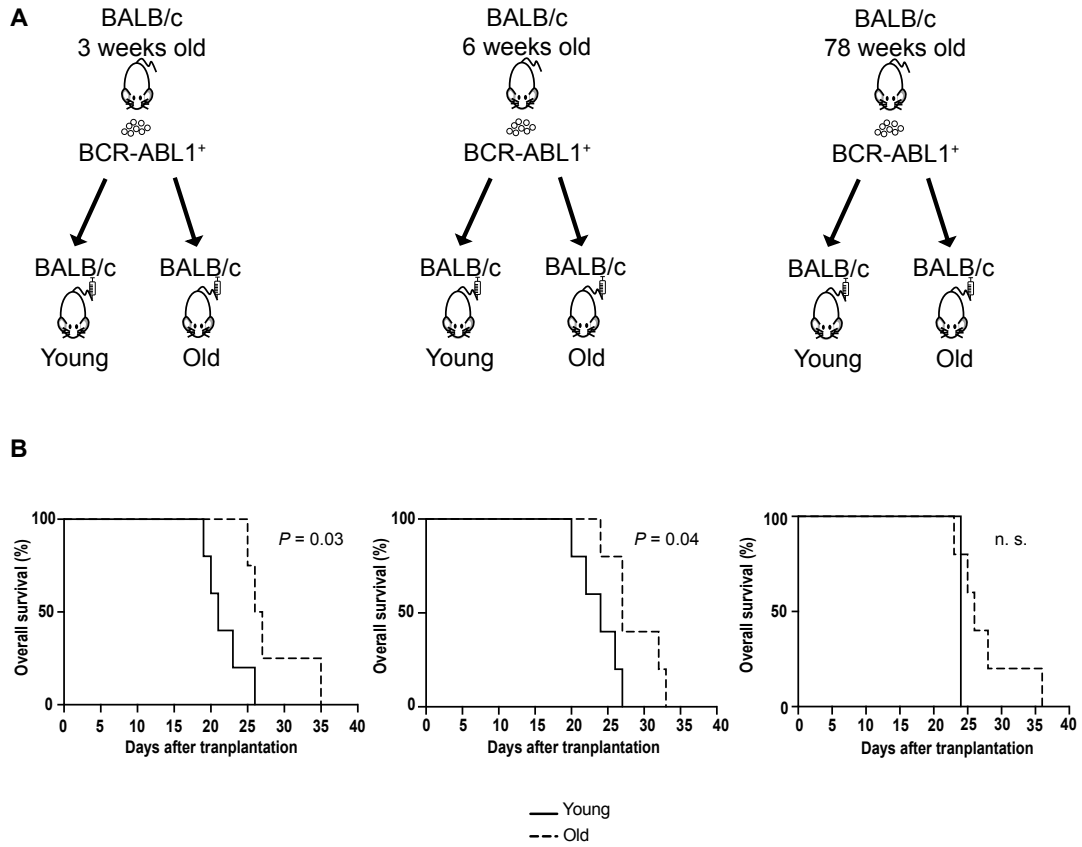


Figure 12 B-cell acute lymphoblastic leukaemia (B-ALL) is influenced by LIC-intrinsic

A) Outline of B-ALL induction in **B)** BALB/c young and old recipient mice. **B)** Kaplan-Meier-style survival curves for young (solid line) and old (dashed line) in BALB/c unirradiated recipient mice transplanted with 2×10^6 BCR-ABL1-transduced BM cells from 3- (left), 6- (middle) or 78- (right) week old mice in the B-ALL model (P values are as indicated).

6.5 B-ALL is more aggressive in young unirradiated mice

As seen above, we recapitulated the preponderance of B-ALL in children (versus adults) in young sublethally irradiated mice. Considering the above trial experiments, we were able to exclude irradiation from our experimental settings. Therefore, B-ALL was induced in two different mouse strains (BALB/c and C57BL/6) without irradiation of recipients. For this we transplanted BM cells (from 6 week old donors), transduced with BCR-ABL1 into young and old BALB/c recipient mice (Figure 13A). This led to a significantly higher number of leukocytes (figure 13 B) and BCR-ABL1⁺ BP-1⁺ cells (figure 13 C), representing the tumor load, in the peripheral blood of young recipients on day 13, as well as over time (figure 13 D). In addition, higher spleen weight was observed in young mice with B-ALL (figure 13 E). As suggested already (figure 12 middle), an acceleration of the disease was confirmed in young unirradiated mice in the BALB/c, as well as in the C57BL/6 strains (figure 13 F-G). In addition, a homing experiment showed that the percentage (figure 13 I), but not the number, of BCR-ABL1⁺ BP-1⁺ cells (figure 13 H), which had homed to the BMM, was higher in in young compared to old mice. No differences were observed in the spleen.

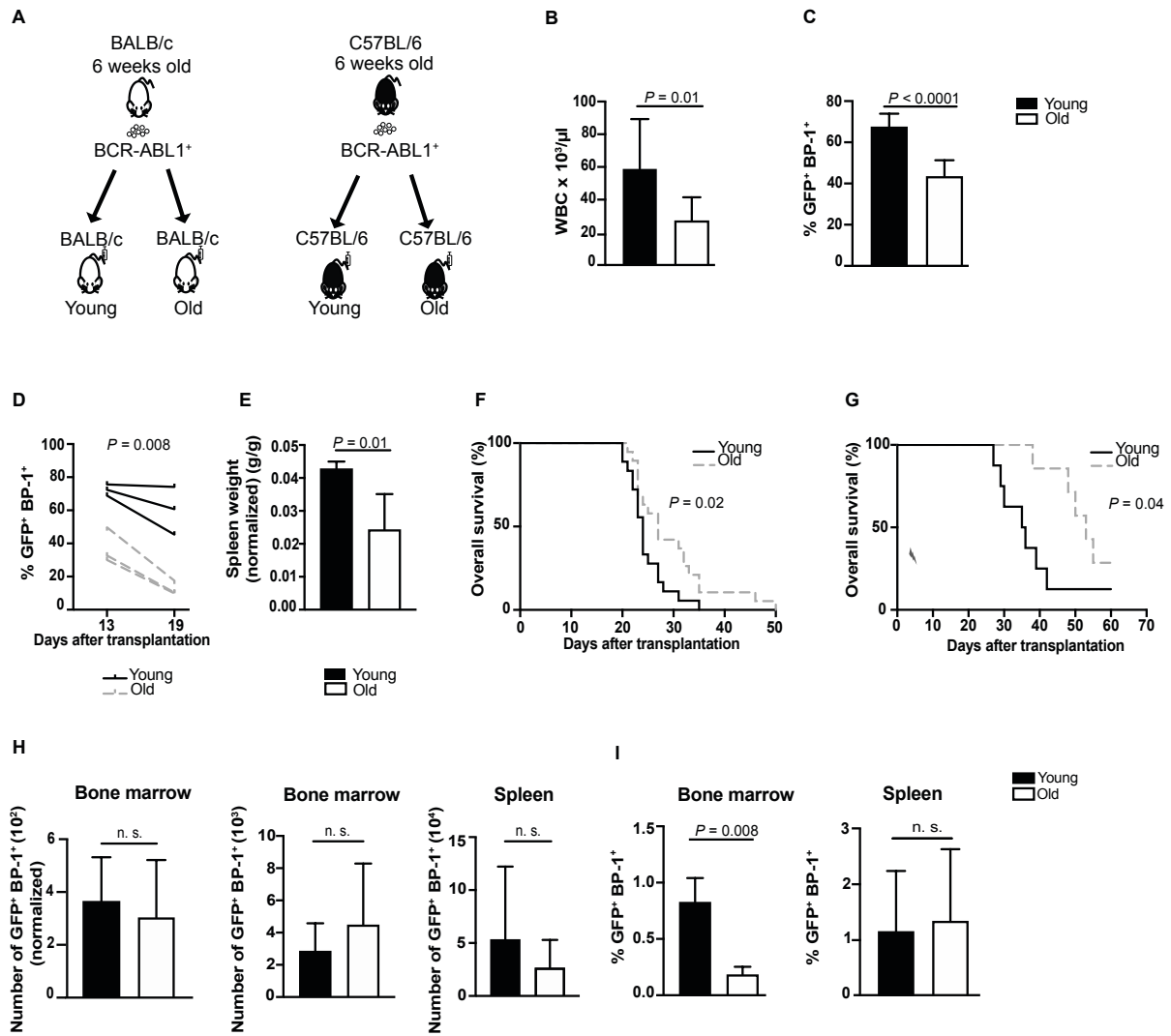


Figure 13 The efficiency of induction of B-ALL in a young versus old BMM differs.

A) Outline of experiments in **(F)** and **(G)**. **B)** White blood cell (WBC) count and **C)** percentage of GFP⁺ (BCR-ABL1) BP-1⁺ cells in the PB of young (white) and old (black) mice. **D)** Percentage of GFP⁺ (BCR-ABL1) BP-1⁺ cells over time in young and old mice. **E)** Spleen weights of young and old mice. **F-G)** Kaplan-Meier survival curves for young (black solid line) and old (grey dashed line) in BALB/c **(F)** and C57BL/6J **(G)** unirradiated mice. **H-G)** Number **(H)** and **(I)** percentage of GFP⁺ (BCR-ABL1) BP-1⁺ cells of total leukocytes which homed to the BM and spleen 18 hours after transplantation (*P* values are as indicated).

Since leukaemia cells can disseminate into different organs as explained in paragraph 3.2.2, the distribution of leukaemia cells was determined in different organs by flow cytometry on day 18 post transplantation (figure 14 A). In young recipient mice, flow cytometry (gating strategy in figure 14 B) and its quantification (figure 14 C) show an increase in tumour burden in peripheral blood, BM and spleen. These overall findings further confirm that a young environment has an impact on the maintenance, progression and aggressiveness of B-ALL.

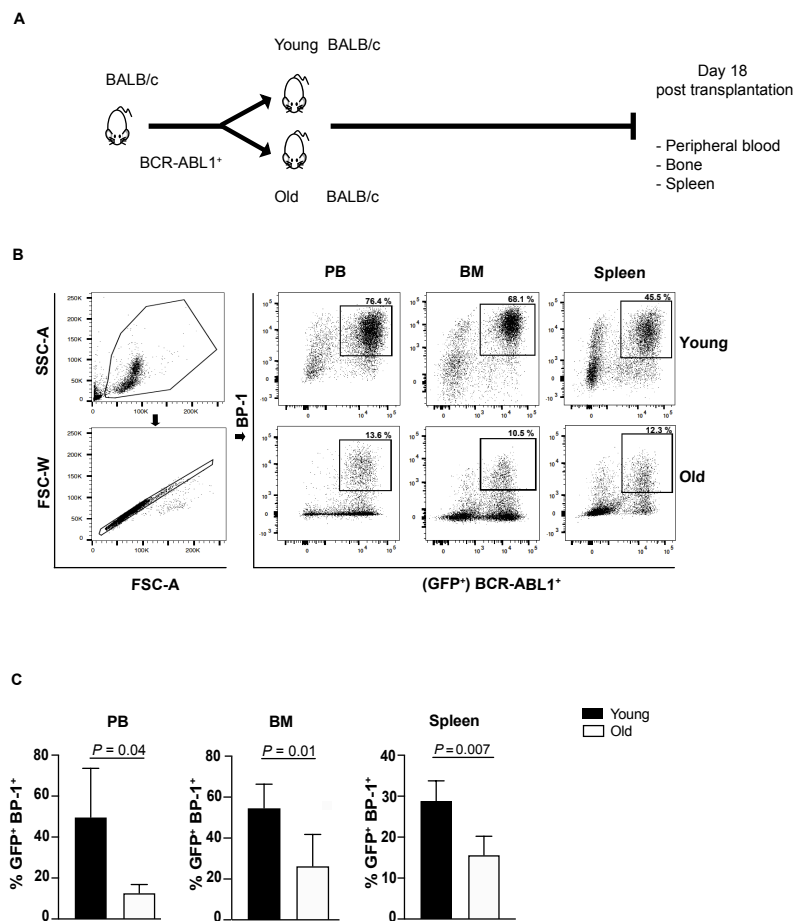


Figure 14 B-ALL cells infiltrate in different organs.

A) Outline of experiment. **B)** Flow cytometry gating strategy and quantification of GFP⁺ (BCR-ABL1⁺) BP-1⁺ cells **(C)** in PB, BM and spleen of young versus old unirradiated recipient BALB/c mice on day 18 after transplantation of BCR-ABL1- transduced bone marrow in the B-ALL model (*P* values are as indicated).

6.6 The engraftment of human primary B-ALL cells is higher in young versus old NOD/SCID IL-2receptor gamma KO mice

To confirm the survival differences between young and old mice observed in our syngeneic mouse model (page 68) and to develop a model more likely to mimic human leukaemia, we used the patient derived xenograft (PDX) transplantation model. Therefore, we transplanted primary human B-ALL cells into young versus old NSG recipient mice. Disease progression was followed by analysis of hCD45⁺ CD19⁺ cells in the peripheral blood (figure 15 C). This revealed a higher engraftment of human CD45⁺ leukocytes in young mice (figure 15 B and D) and a shorter survival in young mice (figure 15 E). This study validated our findings in our murine transduction/transplantation model, in which a young BMM has a supportive role in the engraftment and maintenance of B-ALL cells.

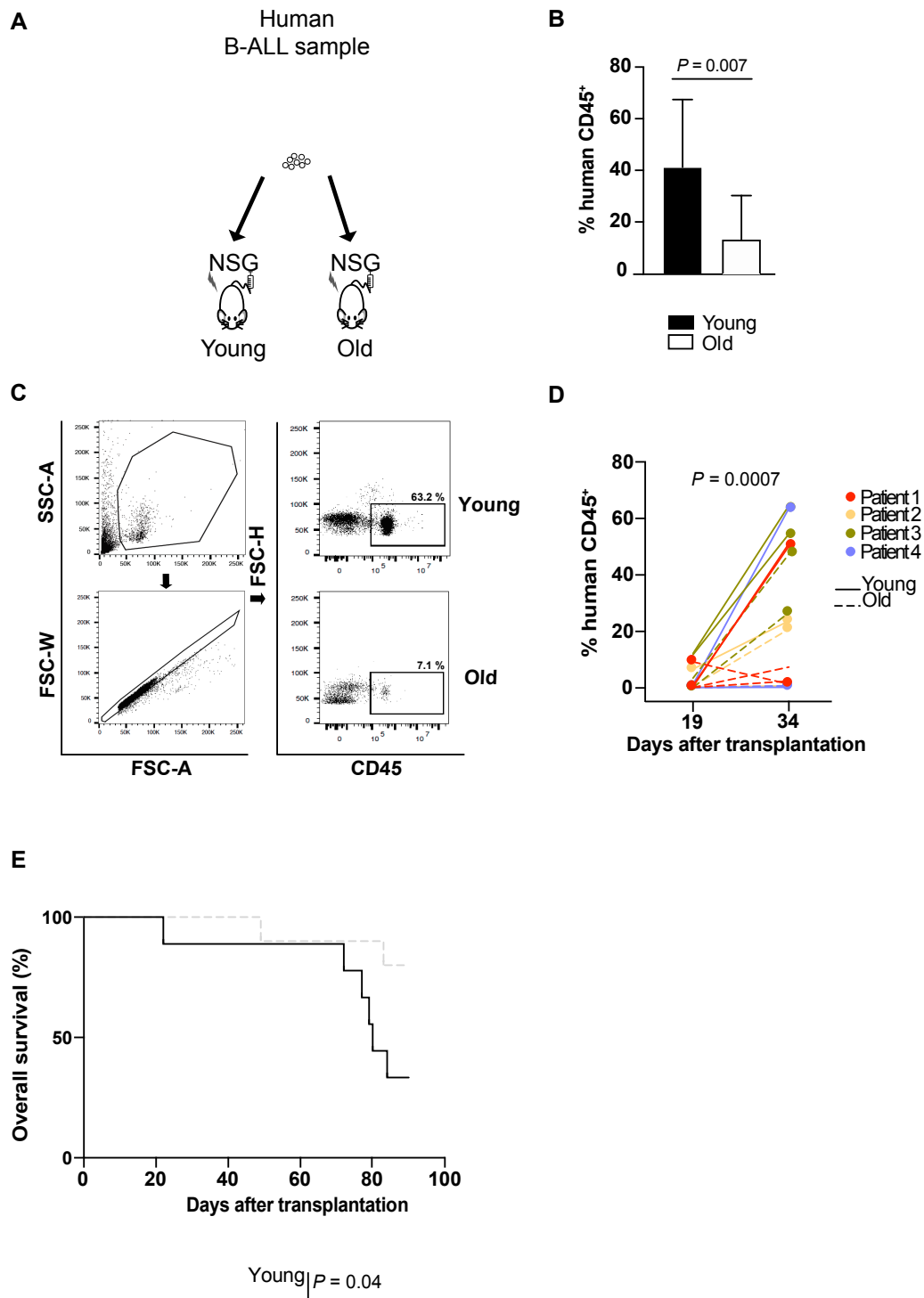


Figure 15 A young microenvironment supports the engraftment and maintenance of B-ALL cells.

A) Outline of experiment **B**) Percentage of human CD45⁺ leukocytes in the PB of young (black) versus old (white) NOD SCID interleukin-2 receptor γ knockout (NSG) mice transplanted with 2×10^6 human B-ALL cells on day 34 post transplantation **(D)** and over time (days 19 and 34 after transplantation). The gating strategy is shown in **C**). Individual patients in **(D)** are indicated by distinct colors. **E**) Kaplan-Meier-style survival curve for young (black solid line) or old (gray dashed line) NSG mice.

6.7 The location and characteristics of B-ALL-initiating cells differ in a young versus an old BMM

The location of leukaemia cells in the bone marrow has been linked to disease aggressiveness, progression, and/or chemotherapy resistance, as also shown by us^{174,176}. In light of our previous findings we monitored the location and behaviour of BCR-ABL1+ B-ALL cells and normal lineage-negative cells in young and old mice using *in vivo* microscopy, imaging B-ALL cells in the young and old murine calvarium (a schematic outline of the experiment is illustrated in figure 16 A) representative image of the localization of leukaemia cells in respect to vessels and bone in the murine calvarium is shown in figure 16 B.

We observed that B-ALL injected into young mice homed to locations closer to the endosteum compared to old counterparts as shown in figure 16 C. However, no differences were observed in normal lineage-negative cells. In particular, the speed of spontaneous movement of B-ALL cells was found to be faster in young mice (figure 16 D). When we tracked individual B-ALL cells in young mice, we discovered that the movement of any given cell was less random than the movement of any given cell in the calvarium of old mice, which may indicate that the cells have more migratory features in a young environment (figure 17). Our imaging methodology suggests that the location and migration of B-ALL-initiating cells differ between young and old BMMs, and that the cell path may be linked to specific interactions with the niche.

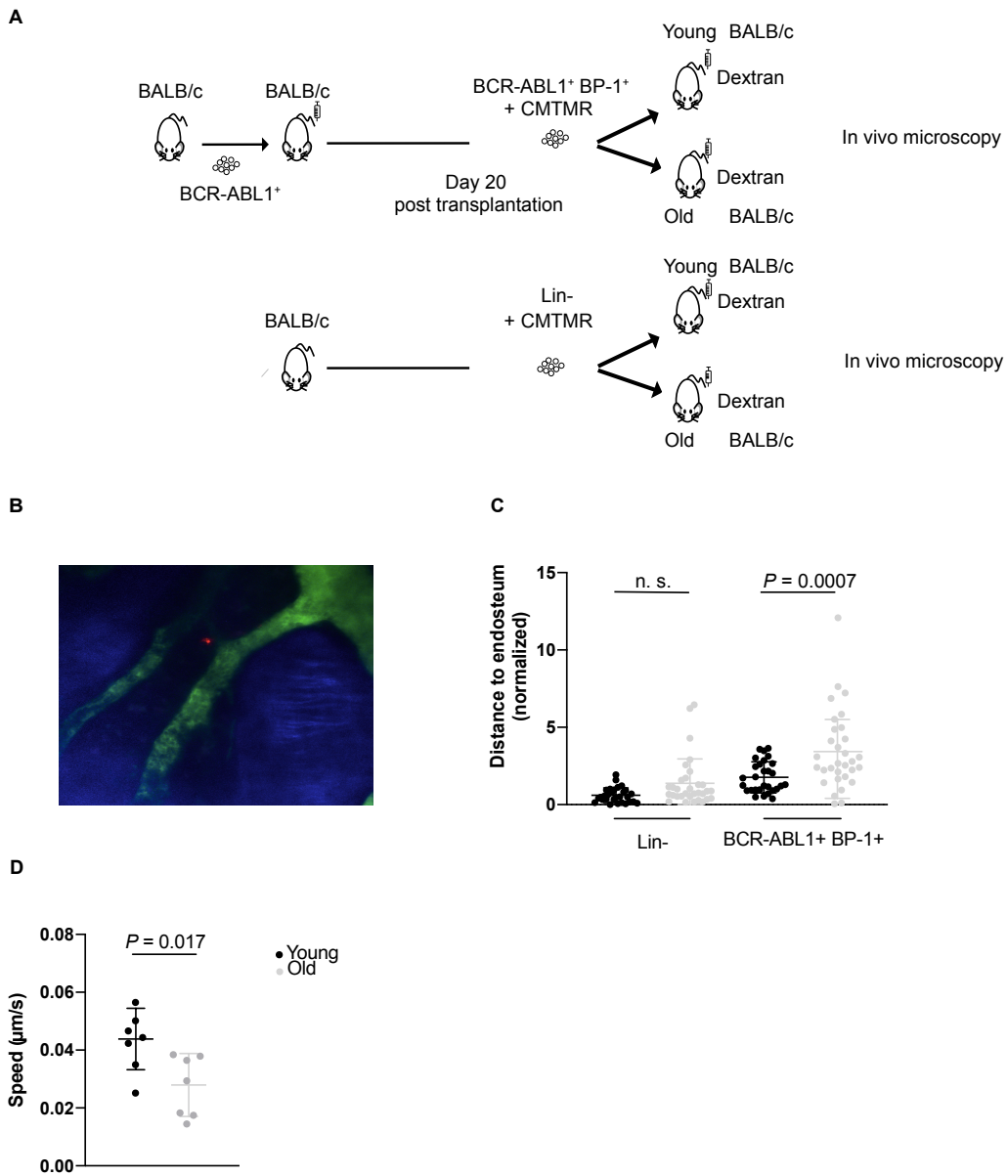


Figure 16 The location and behaviour of B-ALL cells differ in a young versus and old BMM.

A) Schematic of the imaging experiments with two-photon *in vivo* microscopy. **B)** Representative two-photon *in vivo* microscopy image of the BM calvarium **C)** Distance of sorted BCR-ABL1⁺ BP-1⁺ B-ALL cells or lineage negative cells (Lin-) to the endosteum. **D)** Speed of sorted BCR-ABL1⁺ BP-1⁺ B-ALL cells from BALB/c mice with established disease in $\mu\text{m/s}$ (P values are as indicated).

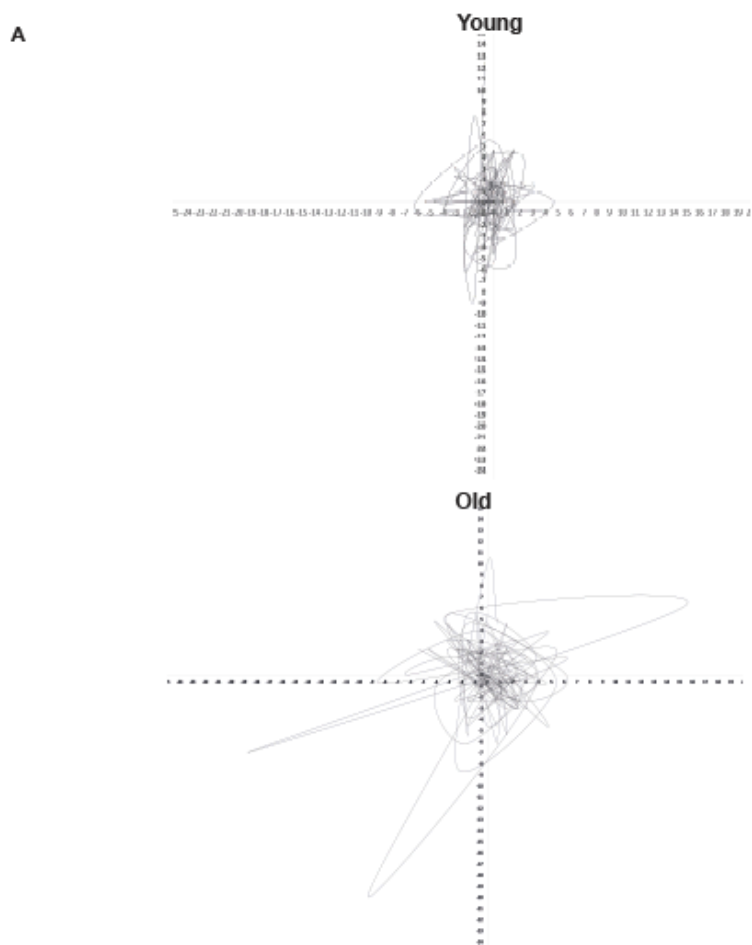


Figure 17 The movement of B-ALL cells is less random in young mice.

A) Representative track plot showing the random migration of sorted GFP+ (BCR-ABL1+) BP-1+ B-ALL cells from BALB/c mice with established disease labelled with CMTMR and injected into young (top) or old (bottom) non-irradiated BALB/c mice.

6.8 BCR-ABL1+ cells proliferate more on young BM derived macrophages compared to old counterparts.

Given the observed contribution of the young BMM to leukaemia, we investigated the role of macrophages in young and old BMMs, as we previously had demonstrated that macrophages influence normal haematopoiesis²⁰⁹. Multiple proliferation assays were performed using primary murine BCR-ABL1+ BP1+ cells or BA/F3 cells transduced with BCR-ABL1, plated on young and old F4/80+ CD11b+ BM-derived macrophages (figure 18 A illustrates the immunophenotyping of the cultured cells from young and old mice). Taking into account the preponderance of B-ALL in children versus adults (paragraph 3.2.2) we plated leukaemia cells onto macrophages from mice of increasing age as shown in figure 18 B left. A gradual but significant decline in proliferation of BCR-ABL1+ BA/F3 cells was observed when leukaemia cells were plated on BM macrophages from 11- to 16-week-old compared to 3-week-old mice figure 18 B (right). In line with this experiment and the prolonged survival of old recipient mice used in the murine B-ALL experiments (paragraph 5.2), we plated BCR-ABL1+ BP1+ cells on macrophages from 3week-old versus 78 week-old mice. Indeed, young BM macrophages supported the growth and survival of leukaemia cells (figure 18 C). To confirm the proliferative advantage, cells were harvested, and cell cycle was assessed. The cell cycle analysis revealed that a greater proportion of leukaemia cells are found in the G2-M phases of the cell cycle when plated on young compared to old macrophages (figure 18 D). The beneficial effect of young macrophages was further evaluated by isolating leukaemia cells from a young and old recipient environment on day 21 post-transplantation and exposing them *in vitro* to young and old macrophages (figure 18 E). Over time, we observed that the leukaemia cells grow rapidly; in fact, leukaemia cells exposed to an old BMM and then plated on young BM macrophages grew faster than those plated on old macrophages (figure 18 F). All of these data

suggest that, of all the cell types in the BMM, young macrophages have an effect on the growth of leukaemia cells.

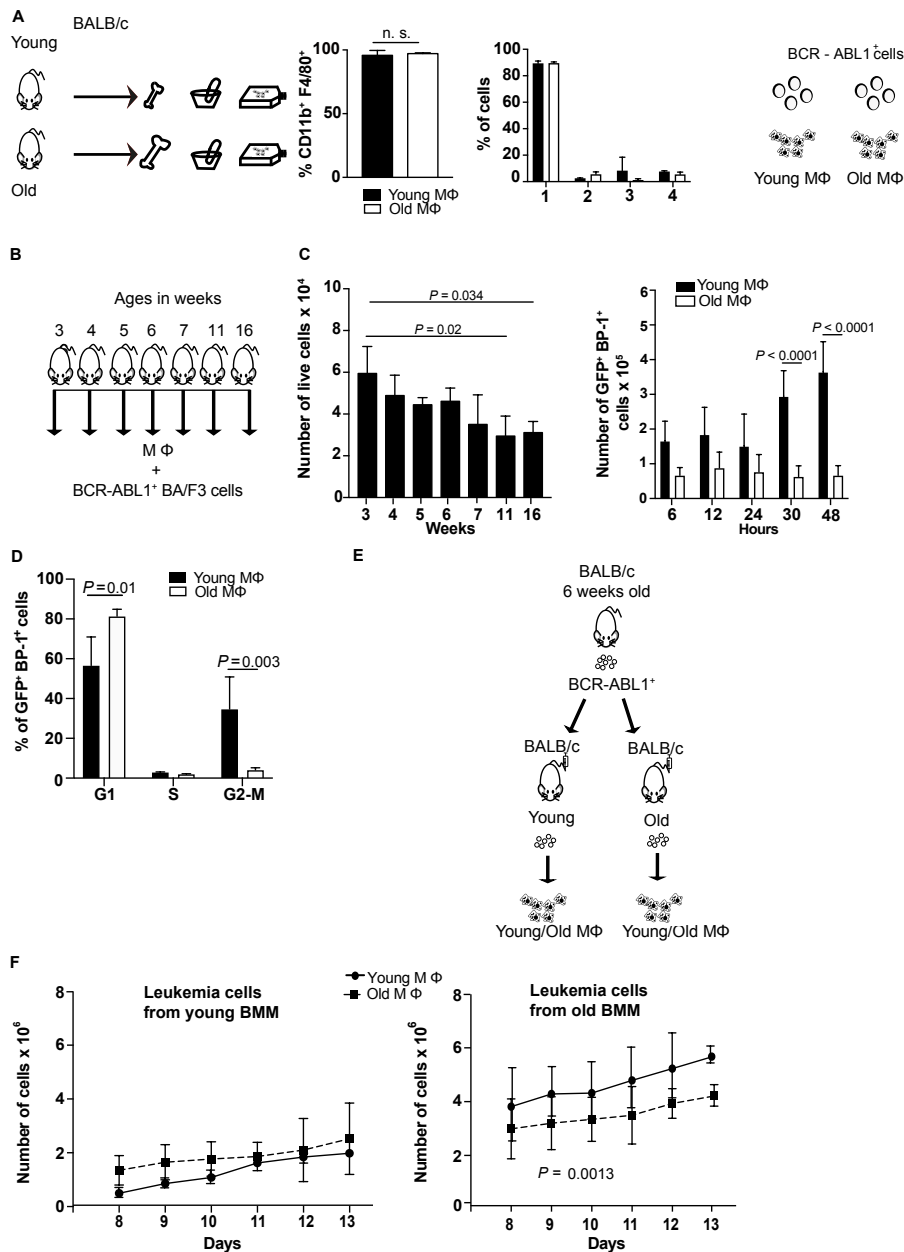


Figure 18 Leukaemia cells proliferate more on young macrophages

A) Schematic representation of the isolation and quantification of CD11b⁺F4/80⁺ cells (left). Percentage of macrophages (1), monocytes (2), dendritic cells (3) and neutrophils (4) in young (white) and old (black) mice. **B)** Number of BCR-ABL1⁺ BA/F3 cells plated on macrophages from mice of increasing ages (3-16 weeks). **C)** Number of primary BCR-ABL1⁺ (GFP⁺) BP-1⁺ cells and cell cycle status (**D**) plated on macrophages from young (black) versus old (white) mice. **E)** Schematic representation of the experiment and (**F**) number of primary BCR-ABL1⁺ (GFP⁺) BP-1⁺ B-ALL cells from young or old mice with established B-ALL plated on young versus old macrophages (*P* values are as indicated).

6.9 Leukaemia cells migrate faster towards young BM derived macrophages

Numerous studies have established the critical role of HSC or LSC adhesion and migration in the BMM (details in paragraph 3.3). Adhesion and migration assays were performed to determine whether leukaemia cells differentially adhere or migrate towards young or old macrophages. To either young or old macrophages, no difference in B-ALL cell adhesion was observed (figure 19 A). Therefore, excluding direct cell-cell interactions as mediators, we hypothesized that potential factors released from young BM-derived macrophages may be contributors to the migration of leukaemia cells. To examine migration, a transwell system with leukaemia cells in the top chamber and macrophages in the bottom chamber demonstrated that leukaemia cells migrate more quickly towards young BM-derived macrophages than they do towards older BM-derived macrophages (figure 19 B-C). These findings suggest that young BM-derived macrophages release chemokines and/or factors that contribute to the observed phenotype. Additionally, this effect could be explained by our previous *in vivo* findings (figure 17) in which we discovered that leukaemia cells in a young microenvironment exhibit less random migration.

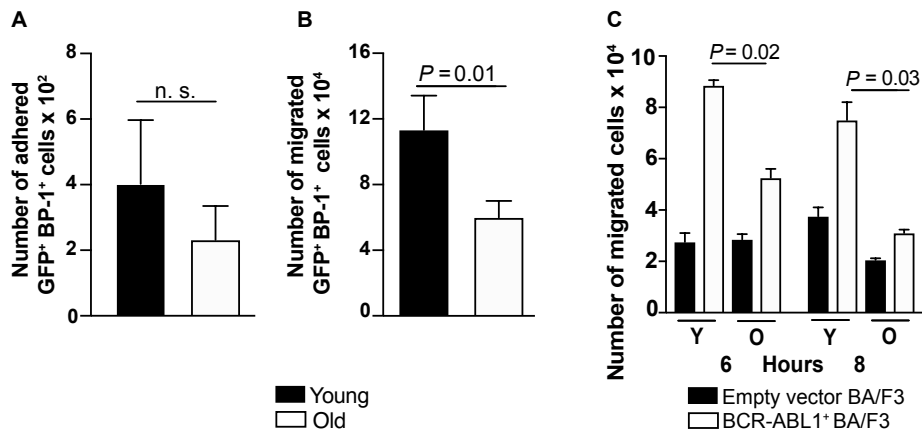


Figure 19 Migration of leukaemia cells towards young versus old macrophages differs

A) Number of primary BCR-ABL1+ (GFP+) BP-1+ cells adhering to macrophages from young (black) versus old (white) mice for 6 hours. **B)** Number of primary BCR-ABL1+ (GFP+) BP-1+ cells which had migrated towards macrophages from young (black) versus old (white) mice after 24 hours. **C)** Number of empty vector (black) or BCR-ABL1-transduced (white) BA/F3 cells which had migrated towards young (Y) versus old (O) macrophages after 6 or 8 hours (*P* values are as indicated).

6.10 Released factors from young macrophages may be responsible for the proliferation of leukaemia cells.

Based on the observations in the previous paragraph, we hypothesized and tested if soluble factors from young macrophages might be responsible for a proliferative advantage of leukaemia cells and disease progression. Therefore, leukaemia cells were co-cultured with conditioned medium from young and old macrophages. In confirmation of our hypothesis, leukaemia cells exposed to conditioned medium from young macrophages proliferated more compared to leukaemia cells exposed to conditioned medium from old mice (figure 20 A). In addition, we isolated leukaemia cells from young and old mice and co-cultured them with conditioned medium from young or old BM macrophages. We observed that leukaemia cells from an old microenvironment and exposed to young BM-derived conditioned medium alter their proliferation ability over time (figure 20 C). Leukaemia cells from a young microenvironment exposed to old BM-derived macrophages, on the other hand, were unable

to maintain their proliferation rate (figure 20 B). The potential effects of released factors from young macrophages on promoting migration but also influencing proliferation, as seen in the previous paragraph, confirms the supportive role of macrophages, which may be linked to a more aggressive disease in young recipient mice (figure 13).

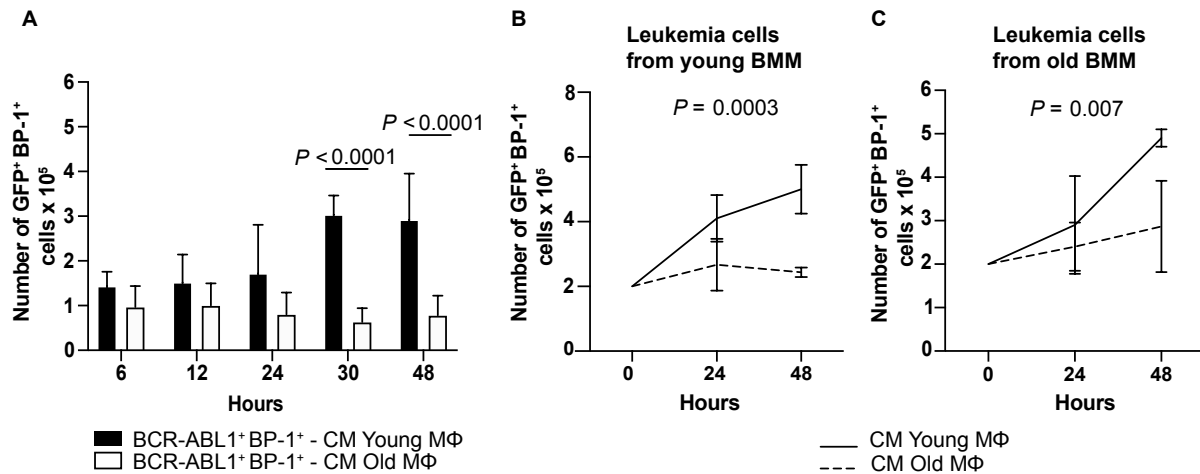


Figure 20 Conditioned medium from young macrophages influence the proliferation of leukaemia cells.

A) Number of BCR-ABL1+ (GFP+) BP-1+ cells plated in the conditioned medium of macrophages from young (black) versus old (white) mice. **B)** Number of BCR-ABL1+ (GFP+) BP-1+ cells from young (left) versus old (right) mice with established B-ALL plated in the conditioned medium of macrophages from young (black solid line) versus old (black dashed line) mice (*P* values are as indicated).

6.11 Age-related differences between macrophages from the BMM of young versus old mice

Given the differences in support of BCR-ABL1+ B-ALL cells between young and old macrophages, we hypothesized that young versus old macrophages might exhibit distinct ageing characteristics, including proliferation and genomic and epigenetic changes. The characteristics of ageing were discussed in paragraphs 3.4 and 3.4.1. As shown in figure 21A, the proliferation capacity of old macrophages declines, whereas the proliferation capacity of young macrophages increases from passage 1 to 2 (figure 21 B). Increases of ROS and DNA damage are critical characteristics with respect to cell death and ageing, and indeed we

observed an increase of ROS and γ H2AX staining in old compared to young macrophages (figure 21 C-D). Abnormal staining for TOM20 has also been observed as a result of possible mitochondrial stress in aged macrophages. Consistently, in old macrophages, figure 21 E demonstrates a decrease in the staining and elongation of mitochondria in old macrophages²¹⁰.

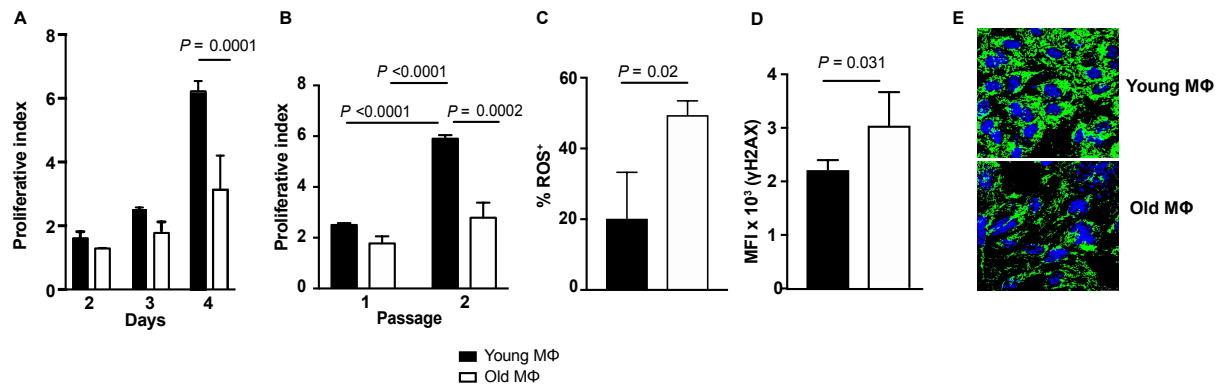


Figure 21 Ageing effects in BM macrophages from old mice.

A) Proliferative index of first passage macrophages from young or old mice on days 2, 3 and 4 after plating. **B)** Proliferative index as in (A) of first and second passage macrophages from young or old mice on day 3 after plating. **C and D)** Percentage of macrophages from young (black) or old (white) mice positive for ROS (C) or gammaH2AX MFI (D). **E)** Representative confocal images of macrophages from young (top) or old (bottom) mice stained with an antibody to TOM20 (green) to visualize mitochondria. Nuclei are stained with DAPI (blue) (P values are as indicated).

In order to test possible differences in the genomic landscape between young and old macrophages, we performed RNA sequencing. This revealed pronounced global differences and overall 473 up- and 569 downregulated differentially expressed genes (DEG) between cultured young versus old macrophages (figure 22 A). Non-redundant enrichment analysis of DEGs revealed significant enrichment of terms related to cytokine function such as chemotaxis, virus response and inflammation (figure 22 B). Investigating whether epigenetic changes regulate macrophage function, we performed ATAC sequencing to determine the open chromatin landscape in young versus old macrophages. This revealed pronounced global differences in genome-wide chromatin accessibility patterns (figure 22 C). On a global scale the differentially accessible region (DAR)s were associated with the gene expression changes observed between young and old macrophages (figure 22 D). In summary, these data suggest

that functional differences exist between macrophages isolated from young and old BM, in particular with regards to proliferation, ROS content, DNA damage, mitochondria and inflammatory response.

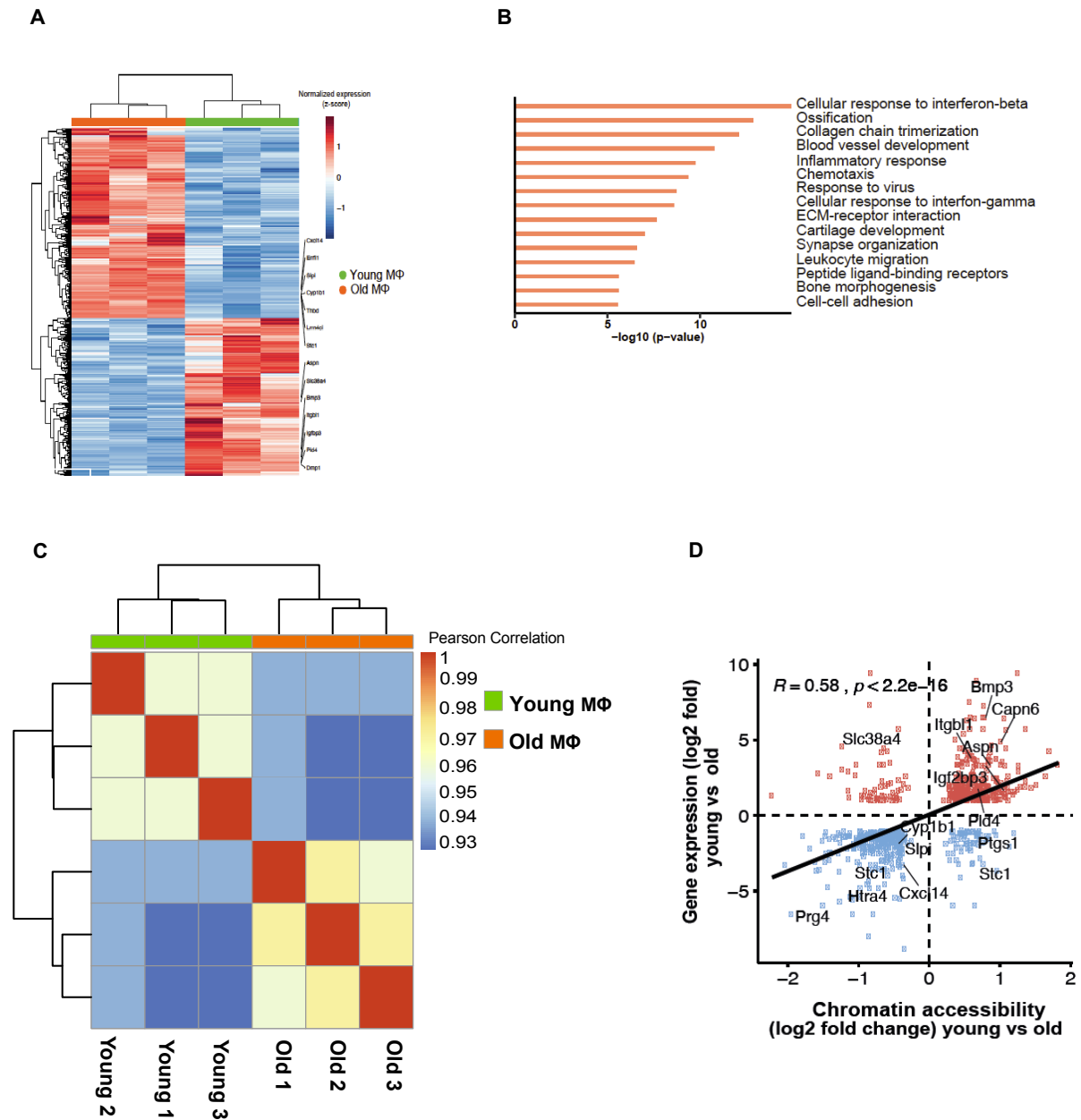


Figure 22 Young and old macrophages differ with regards to their transcriptome and epigenetic signature

A) Heatmap of differentially expressed genes (DEGs) showing z-scores of normalized gene expression in cultured macrophages from young (green) versus old (orange) mice. **B)** Enrichment analysis of DEGs of macrophages from young vs old mice. **C)** Heatmap depicting the Pearson correlation of normalized reads per peak (ATAC-seq). **D)** Scatterplot of chromatin accessibility versus normalized gene expression including all promoter-associated DARs from young versus old macrophages.

6.12 Young BM-derived macrophages produce higher levels of CXCL13

The effect of conditioned medium on proliferation and migration of leukaemia cells in experiments with young macrophages suggests that cytokines and/or chemokines could be responsible for the observed phenotype. Given that CXCL13 is involved in B cell migration and is a diagnostic marker in the cerebrospinal fluid of patients with neuroborreliosis (paragraph 3.5.1), we analysed and compared the level of CXCL13 in young versus old macrophages. While RTqPCR analysis revealed no differences in *Cxcl13* expression between young and old macrophages (figure 23 A), immunoblot analysis revealed a significant upregulation of CXCL13 protein in young compared to old macrophages (figure 23 B-C). CXCL13 was detected at a higher level in the flushed bone marrow of young compared to old healthy mice (figure 23 D), as well as in the conditioned medium of young and old BM-derived macrophages (figure 23 E). In summary, these results indicate that post-transcriptional regulation may occur, as no difference in gene expression levels was observed; however, additional suggestions will be made in the discussion. Notably, and consistent with our hypothesis, a higher CXCL13 protein level was detected in young BMM. Considering that CXCL13 may play a role in the aggressiveness of B-ALL in a young environment and taking into consideration that B-ALL acceleration was observed in both sub-lethally irradiated and unirradiated mice, we analysed CXCL13 expression after irradiation. Therefore, given the transplant in paragraph 6.2, the level of CXCL13 was assessed by ELISA on day 19 post transplantation. We observed that irradiation before leukaemia induction induces an overall increase of secreted CXCL13 when compared to healthy condition as shown in the previous paragraph, but no significant changes were observed between young and old recipient mice (figure 24).

These findings support the notion that pro-inflammatory cytokines such as CXCL13 are released in equal amounts by young and old mice in response to exogenous stress such as irradiation.

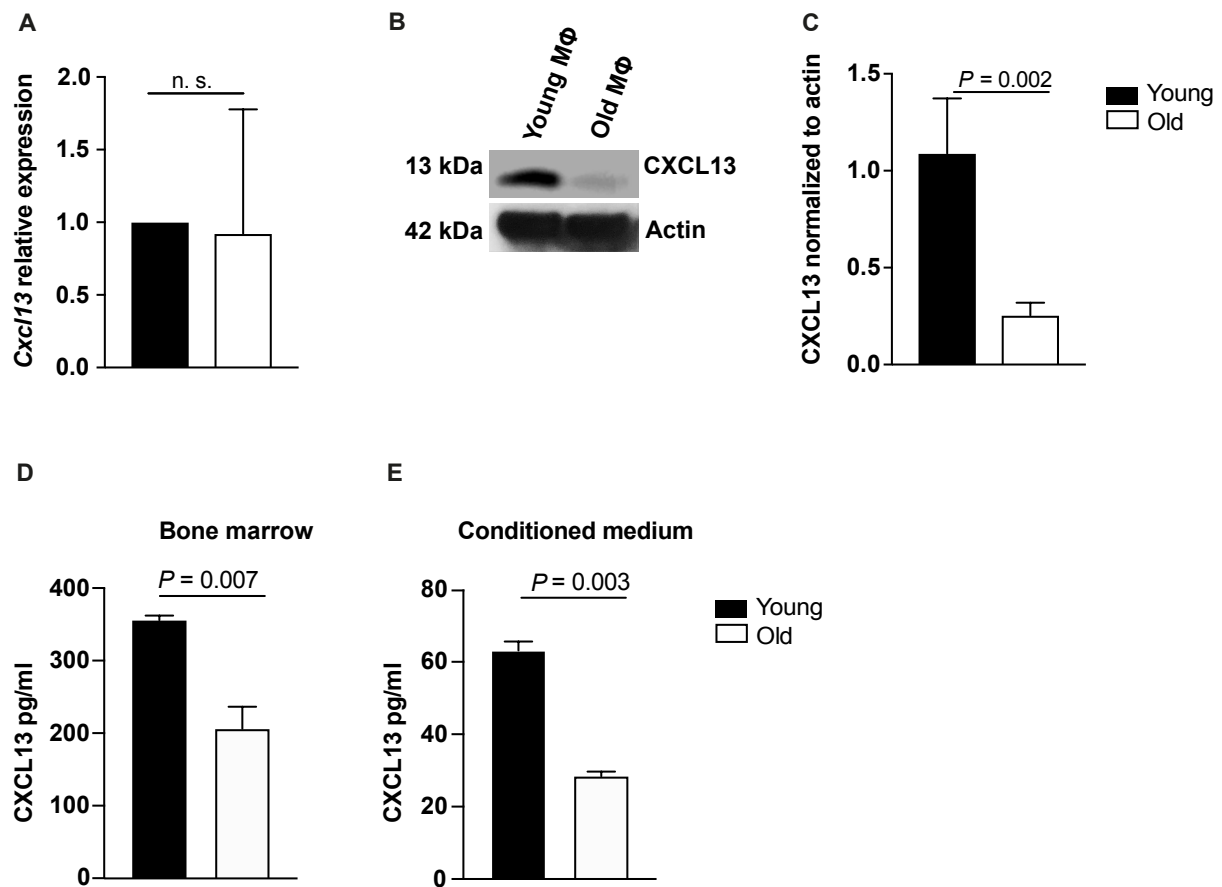


Figure 23 CXCL13 is higher in macrophages and the bone marrow of young mice

A) Relative expression of CxCl13 in macrophages from young (black) versus old (white) mice **B)** Western blot of protein lysates of macrophages from young versus old mice stained with an antibody to CXCL13 (13 kDa) and integrated density of the CXCL13 band **(C), D and E)** Concentration of CXCL13 in pg/ml in flushed bone **(D)** or conditioned medium from macrophages **(E)** from healthy young (black) versus aged (white) mice (*P* values are as indicated).

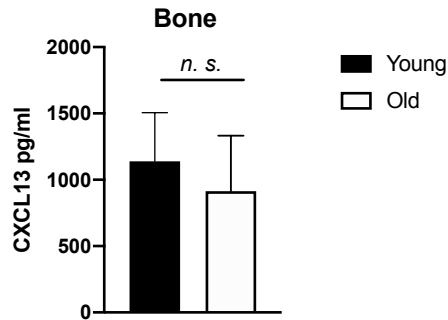


Figure 24 CXCL13 levels do not change with irradiation.

Concentration of CXCL13 in pg/ml in flushed bone of young and old irradiated recipient mice with B-ALL.

6.12.1 CXCL13 level is higher in young unirradiated leukaemic mice

Due to our observation of CXCL13 levels in healthy mice, we tested whether the difference was maintained during B-ALL. The level of CXCL13 showed to be maintained and to be higher in plasma and BM in young leukaemic mice (figure 25 A-B). In addition, young BM derived macrophages in a leukaemic environment show to release more CXCL13 compared to old macrophages (figure 25 C). This final data regarding the expression level of CXCL13 proposes that CXCL13 is a released factor which may be responsible for the aggressiveness of the disease.

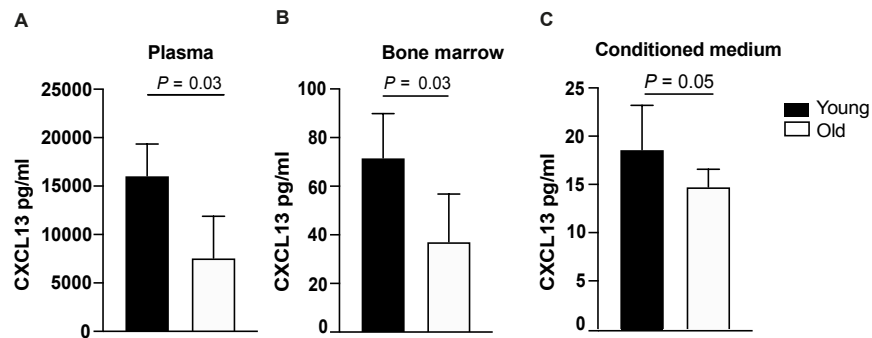


Figure 25 CXCL13 level does not change upon irradiation

A-C) Concentration of CXCL13 in pg/ml in the plasma of PB (A), flushed BM (B) or conditioned medium of macrophages (C) from young (black) versus old (white) non-irradiated BALB/c recipient mice transplanted with BCR-ABL1-transduced bone marrow on day 18 after transplantation (*P* values are as indicated).

6.13 CXCL13 supports the proliferation of B-ALL cells in vitro

As mentioned in paragraph 3.5, chemokines are known to form chemotactic gradients in order to orchestrate cell migration, homing, and cell proliferation in a variety of biological processes. We investigated the functional role of CXCL13 in light of our previous observation of a higher concentration of CXCL13 in a young microenvironment. As a result, we conducted co-culture experiments in which BCR-ABL1⁺ BP1⁺ and BCR-ABL1⁺ BA/F3 cells cocultured with young or old BM-derived macrophages were exposed to a CXCL13 neutralizing antibody as shown in figure 26 left or recombinant CXCL13 figure 26 right. When leukaemia cells were plated on young macrophages, inhibition of CXCL13 significantly reduced their proliferation. However, inhibition was not observed when an isotype control antibody was used (figure 26 B-C). When recombinant CXCL13 was added to the coculture system, BCR-ABL1⁺ BP1⁺ cells proliferated more rapidly on both young and old macrophages (figure 26 C). However, when BCR-ABL1 BA/F3 cells were exposed to young macrophages, the addition of recombinant CXCL13 increased the proliferation (figure 26 D) of leukaemia cells. In line with this, treatment of BCR-ABL1⁺ BP1⁺ cells, which had been exposed to a young or an old BMM, with established leukaemia, with recombinant CXCL13 significantly promoted the growth of leukaemia cells (figure 26 E). These results confirm that CXCL13 is an important chemokine released from young macrophages which contributes to the progression of B-ALL.

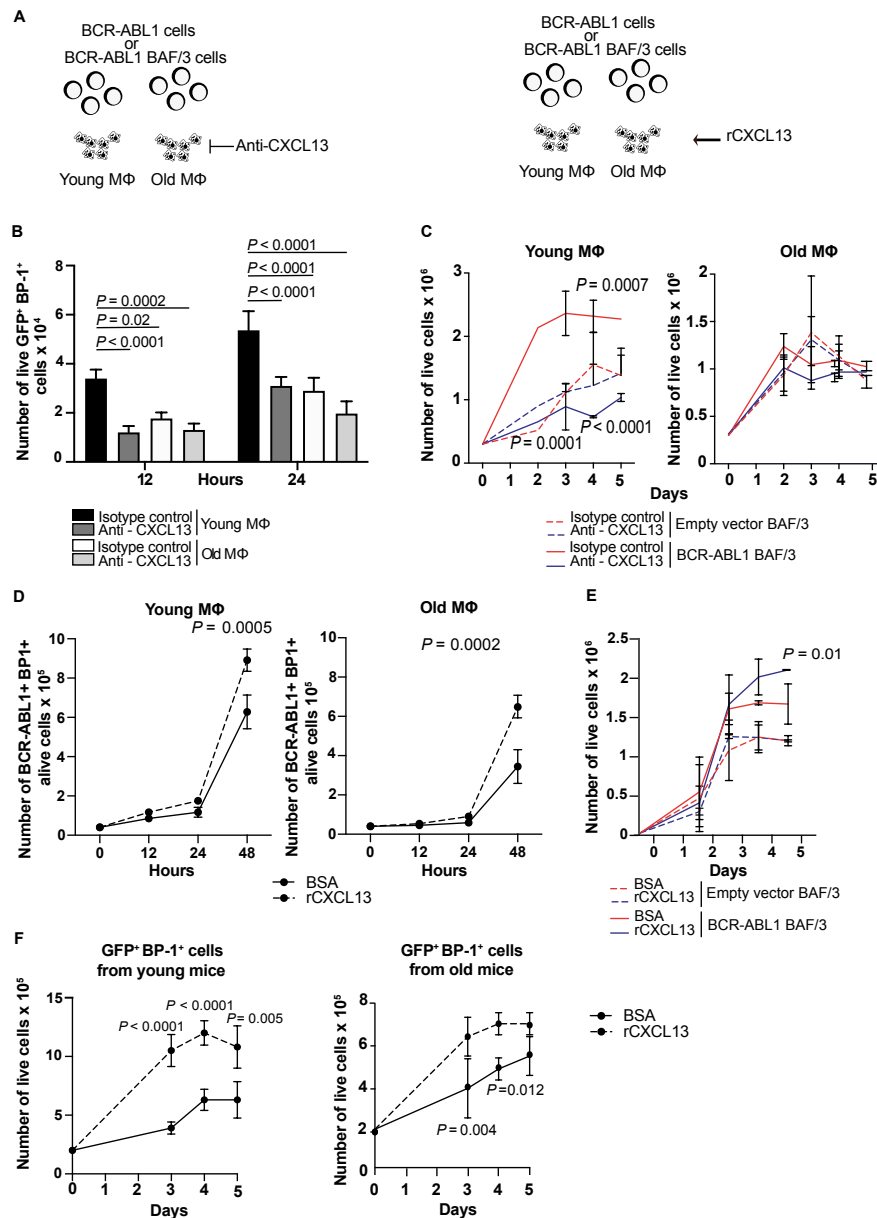


Figure 26 CXCL13 supports the proliferation of B-ALL cells.

A) Outline of experiments in (B-C) left and (D-F) right. **B-C)** Number of GFP+ (BCR-ABL1+) BP-1+ cells **(B)** and BA/F3 cells **(C)** plated on macrophages from young versus old mice in the presence of isotype control or anti-CXCL13 antibody. **D-E)** Number of primary GFP+ (BCR-ABL1+) BP-1+ cells **(D)** and BA/F3 cells **(E)** plated on macrophages from young versus old mice in the presence of BSA or rCXCL13. **F)** Number of GFP+ (BCR-ABL1+) BP-1+ cells from young (left) or old (right) mice with established B-ALL cultured in the presence of BSA or rCXCL13 (*P* values are as indicated).

6.14 CXCL13 increases the migration of leukaemia cells

In light of the chemotactic properties of CXCL13, as discussed in paragraph 3.5.1, we performed a migration assay in which we assessed leukaemia cells' ability to migrate towards recombinant CXCL13 or the effect of CXCL13 inhibition on B-ALL cell migration using a neutralizing antibody (figure 27 A). Recombinant CXCL13 enhanced the migration of leukaemia cells (figure 27 B). However, the primary activity of CXCL13 was determined by using the transwell system to block free-CXCL13 released from young and old macrophages at the bottom chamber. We discovered that CXCL13 promoted the migration of BCR-ABL1+ BP1+ cells as well as BCR-ABL1+ BA/F3 cells (figure 27 B-C). These findings demonstrate that CXCL13 is capable of inducing a migratory response of B-ALL cells.

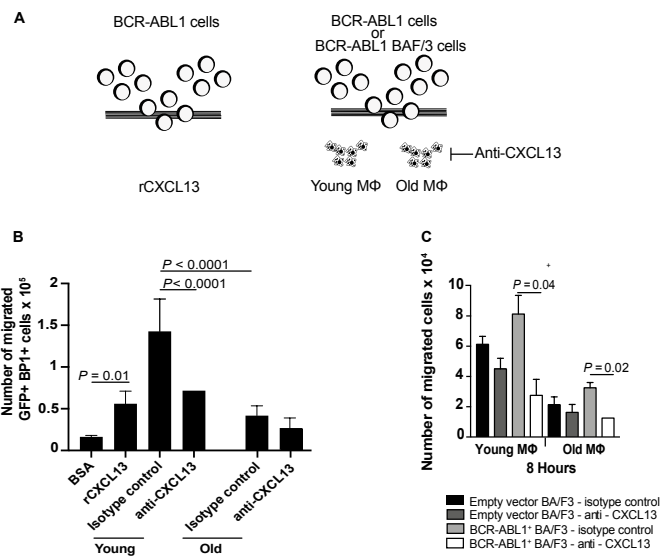


Figure 27 CXCL13 regulates migration of leukaemia cells.

A) Schematic representation of experiments in **(B)** and **(C)**. **B)** Number of GFP+ (BCR-ABL1+) BP-1+ cells which had migrated towards BSA or rCXCL13 or young versus old macrophages in the presence of isotype control or anti-CXCL13 antibody after 24 hours. **C)** Number of empty vector- or BCR-ABL1-transduced BA/F3 cells migrated towards young versus old macrophages in the presence of isotype control or anti-CXCL13 antibody after 8 hours (*P* values are as indicated).

6.15 CXCL13 induces pAKT upregulation in B-ALL cells

The signalling pathway downstream of BCR-ABL1 and CXCR5 are characterized by phosphorylation of downstream proteins – albeit by different mechanisms. One such example is PI3K/Akt signalling. Therefore, we assessed the level of pAKT in our experiment settings. Co-culture of BCR-ABL1+ BA/F3 cells with young BM-derived macrophages led to higher levels of pAKT compared to a coculture of BCR-ABL1+ BA/F3 cells with old macrophages figure 26 C. In addition, inhibition of CXCL13 reduced the level of pAKT in BCR-ABL1+ BA/F3 cells (figure 28 A-B). To further assess the phosphorylation of pAKT, we treated BCR-ABL1+ BA/F3 for 10 minutes with 100 or 1000 ng/ml of recombinant CXCL13. Immunoblot analysis showed an increased level of pAKT. However, no differences in pAKT levels were observed if recombinant CXCL13 was supplied in a dynamic range (figure 28 C).

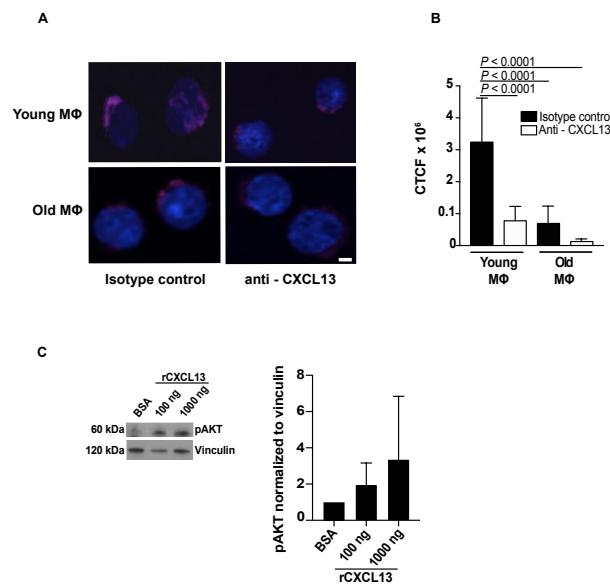


Figure 28 CXCL13 induces pAKT upregulation.

A) Representative confocal images of BCR-ABL1+ BA/F3 cells plated on macrophages from young or old mice stained with an antibody to pAKT (red) after treatment with isotype control or anti-CXCL13 antibody **B)** Corrected total cell fluorescence (CTCF) for nuclear pAKT, as in (A). **C)** Western blot of protein lysates of BCR-ABL1+ BA/F3 cells cultured in the presence of BSA or rCXCL13 for 10 minutes. Cells were stained with an antibody to phospho-AKT (60 kDa) (left). Integrated density of the phospho-AKT band from 3 independent Western blots (right) (*P* values are as indicated).

6.16 Young BM derived macrophages and CXCL13 are supportive factors in B-ALL in vivo

Our *in vitro* experiments indicate that young macrophages have a direct effect on leukaemia cells via CXCL13 (paragraph 6.13). To test the contribution of CXCL13 and macrophages *in vivo*, we induced B-ALL in young and old mice (as in figure 13 G) followed by administration of clodronate, a well-established method to deplete macrophages²⁰⁹. A schematic representation of the experiment is shown in figure 29 A. We were able to show a significant decrease in the tumour burden (figure 29 B) and prolongation of murine survival in young mice treated with clodronate (figure 29 C), while no significant changes were observed in old mice (figure 29 D). To determine whether CXCL13 contributes to progression of B-ALL, we measured CXCL13 levels following clodronate treatment using an ELISA. CXCL13 levels in the plasma and in the bone marrow of young recipient mice with clodronate-ablated macrophages were decreased (figure 29 E-F).

Finally, to confirm the pro-proliferative effect of CXCL13 *in vivo*, we pre-treated B-ALL cells with recombinant CXCL13 or vehicle for 18 hours prior to transplantation as shown in figure 29G. Prior treatment of LIC with CXCL13 markedly shortened the survival of recipient mice compared to LIC pre-treated with vehicle (figure 29 H). Taken together, these findings suggest that macrophages act as a supportive niche for B-ALL cells within the BMM via CXCL13 secretion.

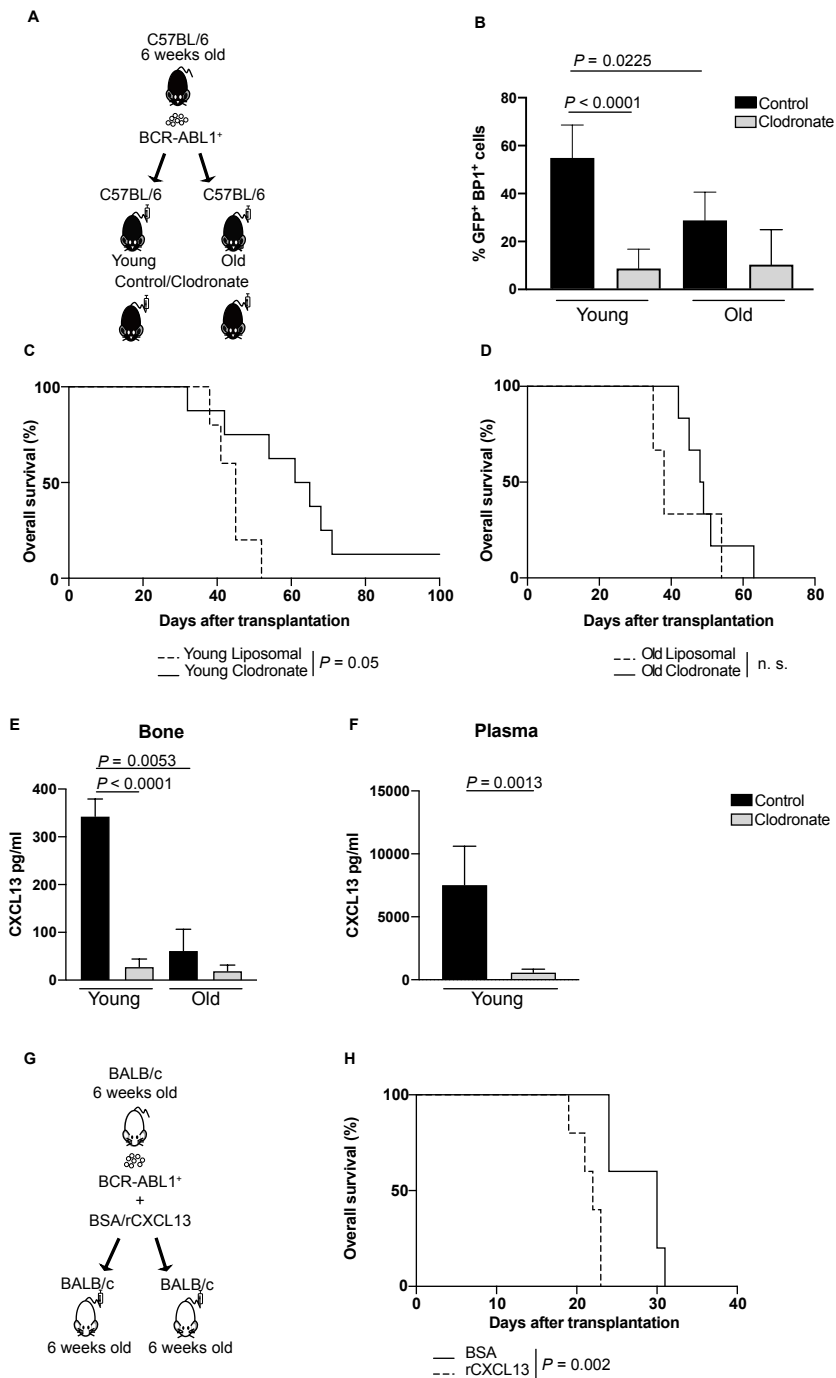


Figure 29 Young macrophages and CXCL13 are supportive factors in B-ALL.

A) Schematic representation of the transplant in (B-D). **B)** Percentage of GFP⁺ (BCR-ABL1⁺) BP-1⁺ cells in PB on day 21. **C-D)** Kaplan-Meier-style survival curves of young (C) and old (D) non-irradiated C57BL/6J recipient mice, treated with control liposomes or clodronate liposomes. **E-F)** Concentration of CXCL13 in pg/ml in the flushed bone (E) and plasma (F) of young C57BL/6J recipient mice. **G)** Schematic representation of the transplant in (H). **H)** Kaplan-Meier-style survival curve of non-irradiated BALB/c recipient mice transplanted with BM cells pretreated with BSA or rCXCL13 for 18 hours prior to transplantation (P values are as indicated).

6.17 CXCL13 expression is higher in human macrophages and in non-classical human monocytes

We demonstrated that CXCL13 is expressed at a higher level in young BM compared to older BM, specifically in young macrophages, where it acts as a promoter of leukaemia cell migration and proliferation. To determine the clinical relevance of our findings in mice, we stained human bone sections for monocyte/macrophage markers and CXCL13. In agreement with our findings in mice, we demonstrated that human CD68⁺ macrophages and CXCL13 staining was significantly higher in bone sections from paediatric versus adult B-ALL patients (figure 30 A). Additionally, as previously stated on page 27, we attempted to identify non-classical monocytes, a population that emerges during diagnosis and relapse in B-ALL¹⁷⁷, in our settings. In bone sections from patients with pediatric versus adult B-ALL we observed an increased frequency of this cell population, that is CD14^{dim} CD16⁺, in pediatric patients (figure 30 B). Also, flow cytometry of human B-ALL cells revealed increased CXCL13 expression in non-classical monocytes (figure 30 C). These data corroborate our findings in mice suggesting that CXCL13 is produced in greater amounts in macrophages from pediatric compared to adult patients with B-ALL.

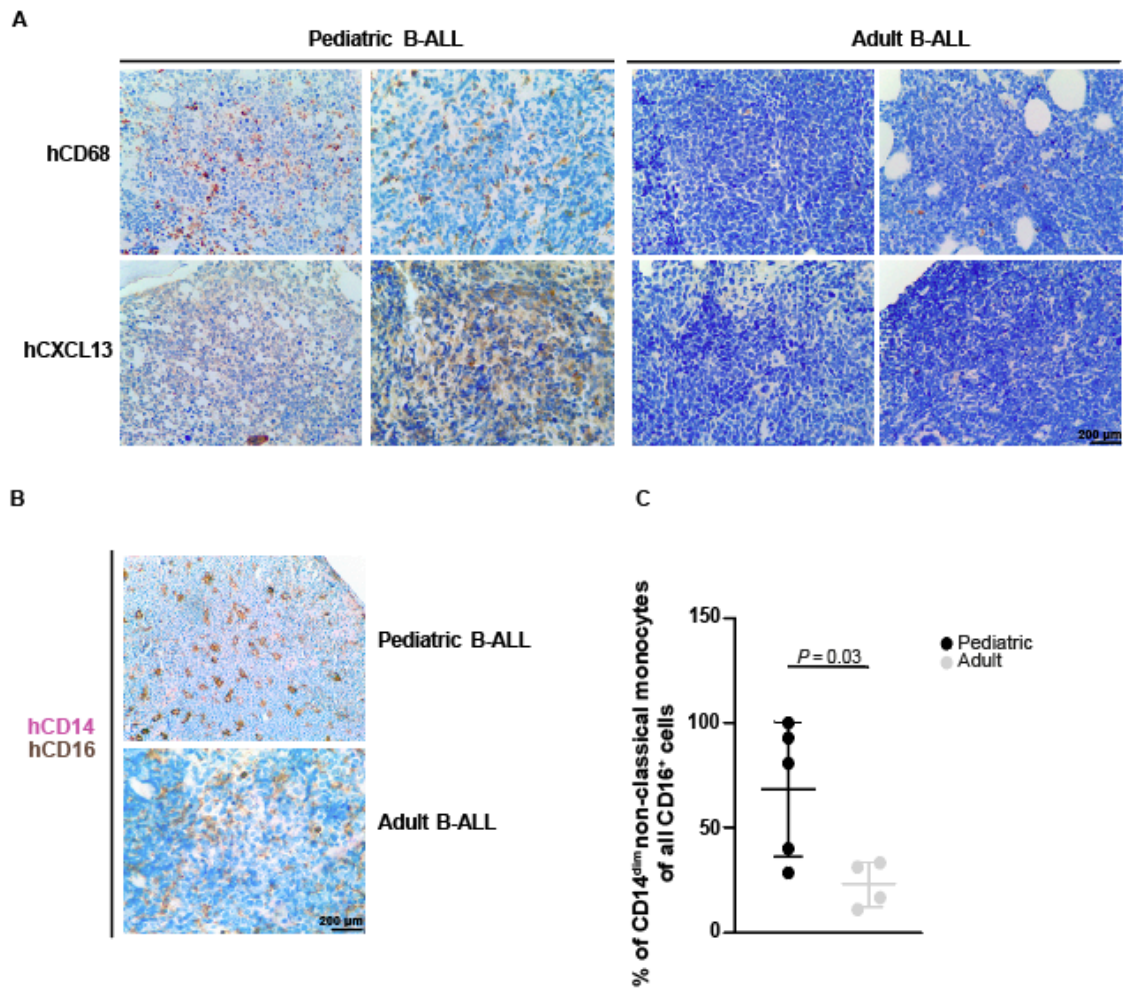


Figure 30 Increased staining for macrophages and CXCL13 in bone sections from paediatric versus adult patients with B-ALL

A) Representative bone sections of two human paediatric (left) or adult (right) patients with B-ALL stained with antibodies to CD68 labeling macrophages or CXCL13. **B)** Representative bone sections of human paediatric (top) or adult (bottom) patients with B-ALL stained with antibodies to CD14 (pink) and CD16 (brown), depicting CD14^{dim} CD16⁺ non-classical monocytes. **C)** Percentage of CXCL13⁺ CD14⁺ CD16^{dim} (classical monocytes) versus CXCL13⁺ CD14^{dim} CD16⁺ (non-classical monocytes) in bone marrow aspirates of human paediatric patients with B-ALL.

6.18 CXCR5 expression is higher on leukaemia cells from a young BMM

As explained in paragraph 3.5.1, CXCR5 is the cognate receptor of CXCL13. Therefore, we also studied the expression of CXCR5 on leukaemia cells from young and old recipient mice. We observed that BCR-ABL1+ BP1+ cells from young mice express higher levels of CXCR5 in the PB and spleen on day 21 post transplantation (figure 31). In conclusion, due to the higher expression of CXCL13 and CXCR5 in a leukaemic young environment we suggest that CXCL13-CXCR5 may be an important axis in B-ALL.

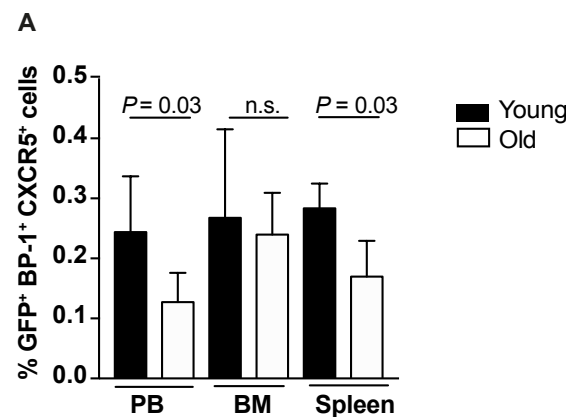


Figure 31: Expression of CXCR5 on leukaemia cells

A) Percentage of GFP+ (BCR-ABL1+) BP-1+ CXCR5+ cells in peripheral blood (PB), bone marrow (BM) and spleen in young (white) and old (black) recipient mice.

6.18.1 CXCR5 impacts survival in murine B-ALL

In light of the findings presented in the previous paragraph, we sought to characterize the CXCR5-CXCL13 axis *in vivo* by use of our retroviral transduction/transplantation model. As a result, we transplanted BCR-ABL1+ wildtype donor BM or CXCR5-deficient donor BM into wildtype recipient mice, both young and old (figure 32 A). We observed a significant prolongation of survival of recipients of CXCR5-deficient compared to wildtype B-ALL cells (figure 32 B) in young mice, but no differences were observed in old mice (figure 32 C). In

order to rule out any homing defects, we performed a homing experiment. Homing of CXCR5-deficient BCR-ABL1+ BP1+ cells to BM or spleen was not compromised compared to wildtype control (figure 32 D). Overall, using CXCR5-deficient B-ALL cells we were able to confirm the relevance of CXCR5 for B-ALL induction and progression.

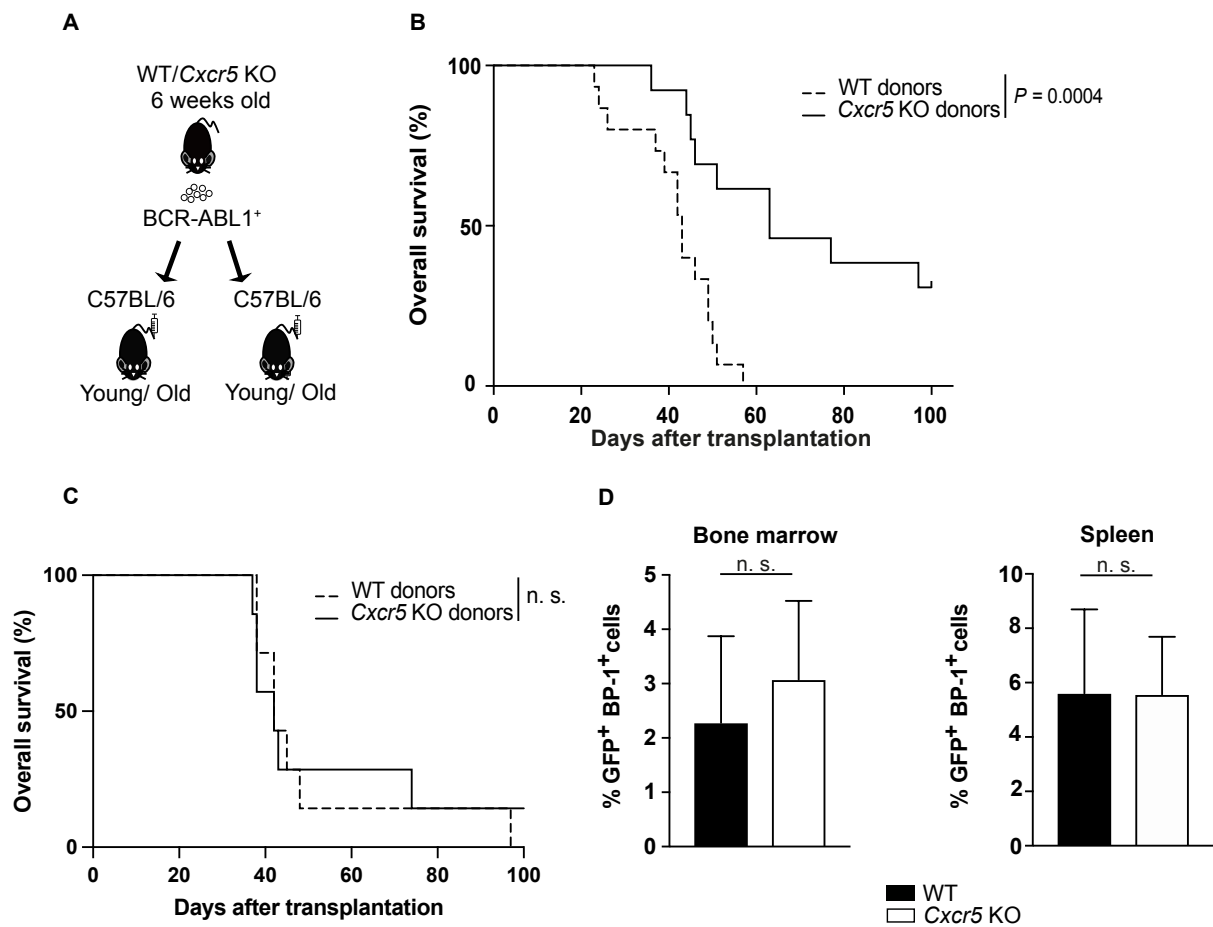


Figure 32: CXCR5 expression on B-ALL cells impacts outcome in the murine model .

A) Schematic representation of the transplant in **B-C)** Kaplan-Meier-style survival curve for young (**B)** and old (**C)** (WT) (dashed line) wildtype or *Cxcr5* knockout (KO) (solid line) recipients of BCR-ABL1-transduced donor bone marrow (BM) cells in the B-ALL model. **D)** Percentage of GFP⁺ (BCR-ABL1⁺) BP-1⁺ cells of total leukocytes which homed to the bone marrow (left) or spleen (right) of wildtype (black) versus *Cxcr5* knockout (KO) (white) mice 18 hours after transplantation in the B-ALL model (P values are as indicated).

6.18.2 CXCR5 expression may predict outcome in the human setting

Given the relevance of CXCR5 in the syngeneic model (previous paragraph), we tested whether the expression of CXCR5 may act as a predictive marker in the clinical setting. We used the retrospective data from the Pan-B-ALL study²¹¹ and stratified the patients according to age and high or low expression of CXCR5 based on the RNA-sequencing results. In the B-ALL subset ‘hyperdiploid’ we could demonstrate that low expression of CXCR5 was associated with improved EFS in the adolescent and young adult (AYA) group (figure 33 A). However, the number of patients was small. No significant differences were observed with regards to EFS in the low CXCR5 expression group in other B-ALL subtypes (data not shown).

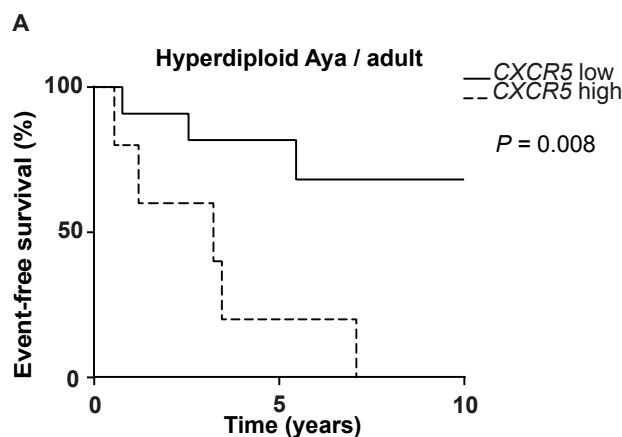


Figure 33: CXCR5 expression may predict outcome in the human setting.

A) Kaplan-Meier-style curves for event-free survival (EFS) for patients in the adolescent/young adult (AYA) and adult age groups with the hyperdiploid subset of B-ALL. Patients are stratified by low (solid line) or high (dashed line) expression of CXCR5.

6.18.1 CXCR5 expression may predict central nervous system relapse of B-ALL

Given the role of CXCL13 and CXCR5 for the homing of B cells to the CNS in neuroborreliosis, as explained in paragraph 3.5.1, and the role of the CNS as a relapse site, as explained in paragraph 3.2.2, we hypothesized that *CXCR5* expression may be predictive of B-ALL relapse in the CNS. Indeed, using the analysis of a publicly available clinical dataset of B-ALL blasts from patients with CNS and BM relapses¹⁸⁷, we observed a significantly increased expression of *CXCR5* on B-ALL blasts from patients with a CNS compared to an isolated BM relapse (figure 34 A). Taken together, these findings suggest that increased *CXCR5* expression may be associated with CNS relapse in human B-ALL. However, additional research is required to substantiate this hypothesis.

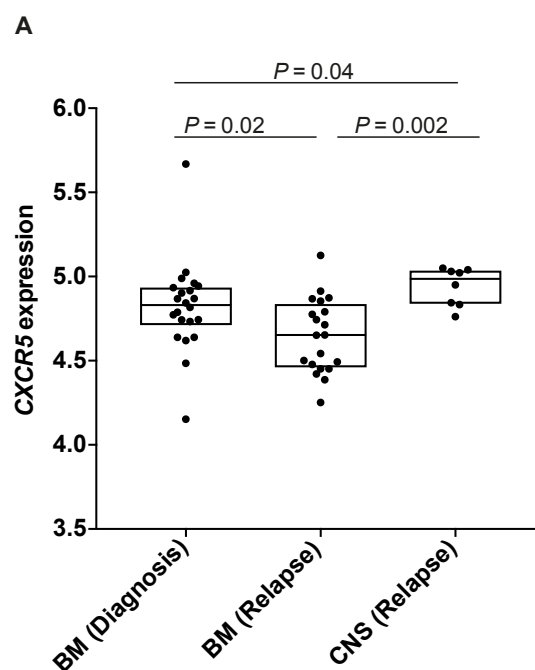


Figure 34: CXCR5 expression on B-ALL blasts may predict CNS relapse of human B-ALL.

A) Comparison of gene expression of *CXCR5* on B-ALL blasts retrieved from bone marrow (BM) at diagnosis, bone marrow at relapse and the central nervous system (CNS) at CNS relapse (*P* values are as indicated).

7 Discussion

The role of a young versus old BMM in CML but mainly in B-ALL was investigated in this thesis. We demonstrated that B-ALL has a more aggressive phenotype in young mice transplanted with B-ALL cells compared to old mice, whereas CML has a more aggressive disease course in aged mice compared to young mice. As a result, we recapitulated the human situation in which B-ALL is more prevalent in children and CML is more common in adults (Cancer Research UK). We observed that young BM-derived macrophages act as a supportive niche for the progression of B-ALL, partially via the involvement of the CXCR5-CXCL13 axis. Additionally, we propose that CXCR5-CXCL13 may act as prognostic markers and may be used as therapeutic targets in human B-ALL. The paragraphs below summarize our findings in relation to the literature.

7.1 Differential progression of CML and B-ALL in young and aged mice

The BMM's role in haematological disorders as a factor influencing disease initiation, progression, therapy resistance, and relapse has been investigated over the last two decades. Using new technologies and mouse models researchers have been able to identify a crosstalk between malignant cells and the BMM²¹². In the future this approach might be important in the development of novel therapeutic strategies. The incidence of leukaemia differs by pathological types and among different populations, but a significant decrease in incidence was observed between 1990 and 2017²¹³. Geographical location, gender, and ethnicity do not appear to play a role in the incidence of leukaemia. However, it is clear that age is a risk factor for the development of the disease. CML is one of the most common type of leukaemia among older people as CLL, despite the fact that it can occur in anyone²¹⁴. In contrast, B-ALL is frequent in children with a peak between 2 and 5 years of age²¹⁵. The precise cause of such discrepancies is unknown. Despite numerous efforts at solving this conundrum, the question

of whether alterations in "young" or "aged" HSCs are caused by HSC-intrinsic changes capable of influencing the development of leukaemia continues to be debated. Recent findings identified alteration in metabolic programs and loss of epigenetic identity as major drivers of old HSC dysfunction and their role in promoting leukaemia onset in the context of age-related clonal haematopoiesis (ARCH)²¹⁶. Additionally, there is a shift in the differentiation potential of HSCs as they age, and HSC exhibit a bias toward the production of more myeloid cells^{217,218,219}. However, the contribution of the microenvironment is largely underappreciated. In recent years, age-related changes in stromal and immune populations have been investigated as they may act synergistically to promote tumour cell progression²²⁰. Variations in secreted factors, as well as changes in the biophysical architecture of the microenvironment, are the result of these changes²²¹⁻²²³.

Given the importance of the BMM and the incidence of B-ALL predominantly in children, we hypothesized that a young versus an old microenvironment may differentially influence disease progression. In our preliminary experiment, we assessed the HSC-intrinsic versus extrinsic effects of ageing. As mentioned in paragraph 6.4, young, middle and old BCR-ABL1+ BM donor cells, which were transplanted into young versus old mice, led to a faster disease course in young mice transplanted with young BM cells.

This finding is partially consistent with a previous study²²⁴, in which the penetrance of B-ALL was negatively correlated with age. In their case, young, middle-aged and old BCR-ABL1+ BM cells were transplanted into young mice. The incidence of the disease in recipients was 63%, when young, 25% when middle-aged and 0%, when old BCR-ABL1+ donor BM cells²²⁴ were transplanted. The difference between our findings and this study can be explained by the use of immunodeficient irradiated mice (Rag1 -/-) in comparison to syngeneic, unirradiated mice used in our settings. As a result, the absence of mature B and T lymphocytes²²⁵, as well as the possible effect of irradiation, may have contributed to the observed phenotype.

Additionally, our data add valuable information to these data, as our middle-aged BCR-ABL1+ BM cells induced more aggressive disease in young mice than in older mice, implying that, despite the contribution of young leukaemia cells, the young microenvironment is critical for the induction and maintenance of B-ALL. Our study, therefore, focused primarily on the role of young and old BMM.

In our murine transplantation studies, we initially used irradiated young and aged recipient mice and transplanted either 5-FU pre-treated or non-treated, BCR-ABL1-transduced BM in the respective models of B-ALL versus CML. Irradiation in its traditional sense is thought to be essential for transplantation, as it promotes the engraftment of donor cells and prevents immunological rejection. Due to the fact that irradiation can cause reversible or irreversible damage to the BMM, which is further dependent on the age of the BMM, alternative methods for conducting such experiments are required. Another strategy for improving engraftment is an antibody-based strategy in which a blocking antibody against c-Kit or CD45 is used as a non-myeloablative conditioning approach²²⁶⁻²²⁸. In our case, we considered an antibody-based approach, but the following reasons led us to exclude this method; a) the vast majority of immune cells, including macrophages, express CD45²²⁹. Any CD45-specific antibody would also deplete macrophages, the object of our study. b) It was recently discovered that c-KIT is expressed on cells involved in the maintenance of the bone skeleton, and c-Kit inhibition can have pleiotropic effects. In particular, fetal c-Kit⁺ cells give rise to 20% of Leptin Receptor (LEPR)⁺, if not done before, stromal cells in adult BM, forming nearly half of all osteoblasts²³⁰. In addition, populations expressing higher c-Kit levels are able to generate bone-resorbing osteoclasts, macrophages and dendritic cells²³¹. We also found that young and old BM-derived macrophages express CD11b, F4/80⁺ and c-Kit (data not shown). Thus, we opted out of performing the experiment in which B-ALL was induced in unirradiated mice, but with prior condition with c-Kit-depleting antibodies (trial experiments are shown in paragraph 6.3).

Additionally, among closer recapitulation to the human settings, young unirradiated mice, resulted to die faster compared to old mice in both strains, BALB/c and C57BL/6J (paragraph 6.5) suggesting that young BMM influences the disease.

The impact of a young versus an elderly microenvironment has not been thoroughly investigated in leukaemia. However, few data are available in other tumours. For example, in prostate cancer, the aged prostatic microenvironment regulates malignant prostate cell growth and metastasis by remodelling the ECM²³². There is limited research in AML that suggests that an older BMM is more permissive to disease progression, consistent with the disease's increased incidence in the elderly. For instance, Vas and colleagues discovered that transplanting AML-ETO⁺ HSC into a murine system increased the number of early progenitors in the bone marrow of old mice relative to young mice²³³. Another study reported that AML blasts induce a senescent phenotype in the stromal cells within the BM microenvironment and that the BM stromal cell senescence is driven by p16INK4a expression²³⁴. Additionally, MLL-AF9 cells in the adult microenvironment maintained a myeloid phenotype, possibly via CCL5, whereas the neonatal microenvironment was favourable for the development of mixed early B cell/myeloid leukaemia²³⁵. All of these studies imply that the BMM, more precisely a young versus an old BMM, has an effect on the development and/or maintenance of malignant cells. However, no data on the role of the young versus the old BMM in B-ALL and CML are available; thus, it is worth noting that, while our study demonstrates a permissive role of an old BMM in CML, we also emphasize the supportive role of a young BMM (specifically macrophages, see paragraph below) for the progression of B-ALL, in close correlation with the phenotype in humans.

7.2 Macrophages as a supportive niche for leukaemia

Monocytes and macrophages have been described as supportive niches for the progression of acute leukaemias, which is consistent with our *in vitro* and *in vivo* observations (paragraphs 6.8 and 6.16). Witkowski et al. demonstrated that an increase of a monocyte population, specifically non-classical monocytes is a predictive factor in B-ALL. Also, an increased absolute monocyte count (AMC) in combination with bulk RNA seq in paediatric patients at diagnosis is a predictive factor in B-ALL.

In line we identified higher number of macrophages and specifically non-classical monocytes in paediatric patients with B-ALL and that they have higher expression of CXCL13 (paragraph 6.17). In Witkowski's study, the combination of anti-CSF1R (which targets monocytes) and nilotinib not only prolonged survival but also decreased the incidence of leukaemia relapse in mice¹⁷⁷. This study closely replicates our *in vivo* experiment, in which we used clodronate to deplete phagocytes and we observed a reduction in tumour burden and prolongation of survival of young mice (paragraph 6.16). Additionally, a recent study in T-ALL highlights the importance of myeloid cells/macrophages. Depletion of multiple myeloid subsets in mice with established T-ALL resulted in a significant decrease in circulating T-ALL blasts and cell dissemination in extramedullary organs¹⁷⁸. Additionally, evaluation of published clinical data²³⁶ revealed a correlation between an elevated macrophage signature and decreased event-free survival rates in paediatric T-ALL patients. Furthermore, it was observed that the myeloid compartment's effect on T-ALL growth was not dependent on suppression of anti-tumour T cell responses. This is in contrast to a previously published report²³⁷, which showed that myeloid depletion significantly decreased T-ALL tumour burden even in immunodeficient mice such as Rag2^{-/-} mice.

The concept that myeloid cells (macrophages included) promote tumour progression through immunosuppressive mechanisms was also reported few decades ago; later on these cells were

classified as myeloid-derived suppressor cells (MDSC)s²³⁸. While the role of MDSCs as suppressors of both innate and adaptive immune responses is well established in solid tumours²³⁹⁻²⁴¹, the role of MDSCs in haematological malignancies, particularly B-ALL, is poorly understood. However, it is well established that MDSCs are significantly overrepresented in the peripheral blood and bone marrow of patients with B-ALL when compared to age-matched healthy controls²⁴². It is important to point out that in our study we did not attempt to elucidate a potential role of macrophages as MDSCs. In other haematological disorders, for example in acute promyelocytic leukaemia (APL) a significant expansion of activated MDSCs is observed²⁴³. In myelodysplastic syndromes (MDS) the expansion of MDSCs was shown to be partially driven by the S100A9/CD33 pathway²⁴⁴. Additionally, in CML a significant expansion of MDSC was observed at diagnosis, which subsequently decreased to normal levels after imatinib treatment²⁴⁵. With the strong evidence that leukaemia cells benefit from the support of young macrophages in our study, a possible role of macrophages as immune suppressors may be contributing in our B-ALL model. However, it should be considered that we have established a novel B-ALL mouse model in which recipient mice are not irradiated and in which recipient mice retain their complete innate and adaptive immune system. Considering that we have also observed a shortened survival of young NSG mice in B-ALL (paragraph 6.6), where the majority of the immune compartment, namely B, T and NK cells are absent, young macrophages may not play a supportive role in the immune system by suppressing it. Depletion of macrophages in young and old NSG mice with established B-ALL may have aided the interpretation of this point. While the examination of the role of MDSCs and other immune cells was beyond the scope of our study, such an investigation could provide critical insight into the role of these cells for B-ALL progression.

7.3 CXCL13 levels are higher in a young BMM

We implicated the CXCR5-CXCL13 axis as responsible pathway for the accelerated progression of B-ALL in young mice, with CXCL13 being more highly secreted by young macrophages (paragraphs 6.12 and 6.16). In our study, however, we did not observe differences in transcriptional expression of *Cxcl13* between young and old macrophages, but rather an increase in protein levels in a young healthy BMM (paragraph 6.12). An increase of CXCL13 protein was also observed in leukaemic mice (6.12.1).

Because the CXCL13 protein identified by Western blotting was already upregulated in young macrophages from healthy mice (Figure 23), potential post transcriptional modifications may occur with age. Mazumber's research group has devoted considerable effort to understanding the role of the ribosomal protein L13a from the 60S ribosomal subunit as a mechanism of transcript-specific translational control²⁴⁶. Deficiency of L13a in macrophages led to an overproduction of CXCL13 upon endotoxin treatment²⁴⁷. According to this data, the most perspicuous explanation for the increased protein expression of CXCL13 in young macrophages might be that the L13a protein is downregulated and its function might be altered in old macrophages, resulting in a decrease in CXCL13 protein production. However, it is worth noting that the abundance of mRNA for numerous genes encoding ribosomal (proteins such as L13a) is significantly associated with the decline associated with aging in humans²⁴⁸. Additionally, as protein levels are maintained by a balance of protein synthesis and degradation, these mechanisms could also account for the higher levels of CXCL13 in macrophages of young mice observed in our study. However, it has been reported that proteolytic activity and proteasome function are decreased during ageing^{249,250}. Taking these findings into account, additional analyses are required, as our data are insufficient to draw definitive conclusions about the equal expression of CXCL13 at an RNA level and differences between macrophages from young versus old mice on a protein level. When our attention is

shifted to the expression and possible role of CXCL13 in solid cancers, other haematological tumours and immune diseases, the available data corroborate our findings. CXCL13 was found to be elevated in the cerebrospinal fluid (CSF) in the majority of pediatric patients (73%) with Lyme neuroborreliosis¹⁶⁵. Thus, the levels of CXCL13 seem to be negatively related to an increased age, in line with our finding (paragraph 6.12). Also, CXCL13 was found to be overexpressed, at both mRNA and protein levels, in breast cancer tissue as well as in the PB of patients with advanced stage of the disease.

In addition to the notion that CXCL13 acts as a chemoattracting agent¹⁵⁷, we have observed that a higher migration of leukaemia cells towards young BM-derived macrophages, partially due to the secretion of CXCL13. However, other proteins and mechanisms can regulate cell migration. For example, it was shown that ALL cells are highly motile and capable of rapid migration within marrow stroma, largely via very late antigen (VLA)-4 and VLA-5²⁵¹. Additionally, MSCs isolated from B-cell precursor (BCP)-ALL, BCP patients' bone marrow produce more ActivinA than healthy MSCs, which may result in increased BCP-ALL cell motility via CXCL12²⁵². Moreover, CXCL12, in conjunction with its cognate receptor CXCR4, regulates survival, migration, homing, and interaction of leukaemia cells with the microenvironment²⁵³. As such, it should be emphasized that CXCL12 produced by young BM-derived macrophages may also induce leukaemia cell migration in a similar manner as CXCL13, as it was also found to decrease with advancing age²⁵⁴.

Additionally, CXCL13 was detected in the supernatants of CLL cells co-cultured with macrophages²⁵⁵ as well as in angioimmunoblastic T-cell lymphoma (AITL)²⁵⁶. Due to the critical role of CXCL13 in the progression of the disease, the World Health Organization included CXCL13 as diagnostic marker for AITL²⁵⁷.

We have identified the role of CXCL13, released primarily by young macrophages which acts as a pro-tumorigenic factor in B-ALL. However, our experiments were conducted on BM-

derived macrophages, and given the enormous heterogeneity of cells found in the BMM, it would have been interesting to evaluate additional BM-associated cells for the production of CXCL13. To substantiate this hypothesis, it was demonstrated using single-cell transcriptomic data that *Cxcl13* is expressed in the BM of a population of cells with adipogenesis-associated markers⁶⁷. However, although adipocytes are known to be generated via differentiation of MSC, opened chromatin at the position of *Cxcl13* was not detected in our ATAC sequencing of young and old MSCs (data not shown).

As discussed previously, this does not rule out differential regulation of CXCL13 at the protein level even in MSCs, as observed in BM-derived macrophages. Thus, quantification of CXCL13 at both the RNA and protein levels would be beneficial in clarifying the single-cell transcriptomic data also in MSCs. However, it is worth noting that in the above-mentioned transcriptomic analysis⁶⁷ for mice under haematopoietic stress due to administration of 5-FU, the level of CXCL13 was found to be increased in comparison to steady state. Considering irradiation as a stress condition, and in line with this report, we observed an increase in the level of CXCL13 on day 19 post-transplant compared to young or old healthy mice (paragraphs 6.12 and 6.12.1). In conclusion, despite discrepancies in published research regarding the source of CXCL13, which may also vary according to the stress, we were able to provide additional evidence indicating that a young BMM is more permissive for the development and progression of B-ALL due to the release of CXCL13.

7.1 CXCR5

As previously stated, CXCL13 is at least partially released by young macrophages and is involved in the proliferation and migration of leukaemia cells, as well as the disease's aggressiveness in young recipient mice. Leukaemia cells with CXCR5 deficiency, led to a

significant prolongation of survival of young mice, confirming the importance of the CXCL13-CXCR5 axis in B-ALL (paragraphs 6.18.1).

According to studies on CLL, B cells express a high level of functional CXCR5²⁵⁵. Additionally, the authors observed a significant, transient increase in F-actin in response to CXCL13 binding, as well as CXCR5 internalization and prolonged p44/42 MAPK activation. Along with the changes in pAKT observed in leukaemia cells following treatment with recombinant CXCL13, it would have been interesting to examine potential changes in the MAPK complex of leukaemia cells when co-cultured with young and old macrophages.

Similarly, in other haematological diseases such as lymphoma long-term anti-CXCR5 antibody treatment prevented tumour growth in a xenotransplantation assay in mice and prolonged murine survival²⁵⁸. This result may be consistent with our observation of prolonged survival of murine recipients of CXCR5-deficient B-ALL LIC. In addition, to improve the treatment efficacy in nodal B-cell Non-Hodgkin-Lymphoma (B-NHL)s, chimeric antigen receptor (CAR) cells have been engineered targeting CXCR5, which efficiently inhibit lymphoma growth in a murine xenograft model²⁵⁹.

In breast cancer, similar to CXCL13, CXCR5 was notably associated with metastasis to lymph nodes, but patient age was considered an independent factor²⁶⁰. However, the patients in this study were divided into two separate cohorts: 31-56 and 56-82 years old. Thus, a cohort of young patients is missing. According to our findings, there may be a link between CXCR5 expression and relapse of B-ALL in the CNS. This is consistent with previously published data on the migration of precursor B-ALL cell lines with higher CXCR5 expression to the CNS, where it was discovered that CXCL13 was expressed by the meninges²⁶¹.

While survival rates for ALL have increased, CNS relapse continues to be a significant cause of treatment failure and morbidity associated with treatment²⁶². In addition, especially in children, CNS-directed therapy is partially toxic to the developing brain²⁶³. Until now the

mechanistic explanation of CNS infiltration of B-ALL cells is poorly understood. Using data from a published study, we demonstrated that expression of *CXCR5* on B-ALL blasts is higher in those patients who suffer relapse in the CNS compared to the BM. Additionally, CNS infiltration mechanisms are unknown, as are the timing, frequency, and properties of BCP-ALL blasts entering the CNS compartment, but two models have been proposed²⁶¹. In the first model, only specific clones are able to leave the BM, migrate and enter the CNS, whereas the second model proposes that all leukaemia cells may have the ability to leave the BM and reach the CNS. Based on their data²⁶¹, only the cells more “adaptable” to a new microenvironment are involved in the CNS relapse, thus refuting the first model. Thus, the high rate of infiltration and the absence of selective trafficking, CNS tropism is a universal property of leukaemic cells and CNS infiltration is not selective at the time of B-ALL diagnosis. This model appears to support our observations even more, as *CXCR5* expression was detected during relapse. Therefore, *CXCR5*-expressing B-ALL cells in the CNS may have adapted to their new environment and may evade B-ALL-directed therapy and immune surveillance. To further verify this statement, we might speculate that *CXCR5*-expressing B-ALL cells acquired molecular changes in the microenvironment of the CNS, in order to seed and possibly cause disease relapse. At the same time, we can also assume that the infiltration to the CNS might be higher due to chemoattraction if the concentration of *CXCL13* in CNS is higher, as it was shown in lymphoma²⁶⁴. However, this hypothesis may argue against the model previously explained since CNS infiltration is a generic property of B-ALL cells. However, additional experiments from our side could further refine the hypothesis. Due to the small size of our patient cohort, additional in-depth studies are necessary to characterize this. However, our data may be used to develop novel treatment strategies for the prevention of B-ALL relapse in the CNS.

8 Conclusion

In our work, we show that the age of the BMM influences the maintenance and the progression of CML and B-ALL. In particular, we show through a variety of *in vitro* and *in vivo* experiments that a young BMM, specifically macrophages, act as a supportive niche for the progression of B-ALL. We identified CXCL13 to be more highly expressed in young murine macrophages, bone marrow and plasma. In line with our findings in mice, we found that the number of human macrophages and CXCL13 levels were higher in paediatric B-ALL patients than in adults. CXCL13 appears to be a promoter of proliferation and migration of B-ALL cells, influencing survival in B-ALL via its receptor CXCR5. In our murine model, we demonstrate that the CXCL13-CXCR5 axis, specifically in young mice, plays a role in the progression of B-ALL. In conclusion, the CXCR5-CXCL13 axis may be relevant in human B-ALL, and higher *CXCR5* expression in human B-ALL may serve as a predictive marker.

9 References

- 1 Cheng, H., Zheng, Z. & Cheng, T. New paradigms on hematopoietic stem cell differentiation. *Protein Cell* **11**, 34-44, doi:10.1007/s13238-019-0633-0 (2020).
- 2 Kazanietz, M. G., Durando, M. & Cooke, M. CXCL13 and Its Receptor CXCR5 in Cancer: Inflammation, Immune Response, and Beyond. *Front Endocrinol (Lausanne)* **10**, 471, doi:10.3389/fendo.2019.00471 (2019).
- 3 Berman, I., Maloney, W. J., Weissmann, I. L. & Rossi, D. J. Stem cells and the aging hematopoietic system. *Curr Opin Immunol* **22**, 500-506, doi:10.1016/j.coi.2010.06.007 (2010).
- 4 Lopez-Otin, C., Blasco, M. A., Partridge, L., Serrano, M. & Kroemer, G. The hallmarks of aging. *Cell* **153**, 1194-1217, doi:10.1016/j.cell.2013.05.039 (2013).
- 5 Krause, D. S. & Scadden, D. T. A hostel for the hostile: the bone marrow niche in hematologic neoplasms. *Haematologica* **100**, 1376-1387, doi:10.3324/haematol.2014.113852 (2015).
- 6 Galloway, J. L. & Zon, L. I. Ontogeny of hematopoiesis: examining the emergence of hematopoietic cells in the vertebrate embryo. *Curr Top Dev Biol* **53**, 139-158, doi:10.1016/s0070-2153(03)53004-6 (2003).
- 7 Tavian, M. & Peault, B. Embryonic development of the human hematopoietic system. *Int J Dev Biol* **49**, 243-250, doi:10.1387/ijdb.041957mt (2005).
- 8 Orkin, S. H. & Zon, L. I. Hematopoiesis: an evolving paradigm for stem cell biology. *Cell* **132**, 631-644, doi:10.1016/j.cell.2008.01.025 (2008).
- 9 Morrison, S. J., Uchida, N. & Weissman, I. L. The biology of hematopoietic stem cells. *Annu Rev Cell Dev Biol* **11**, 35-71, doi:10.1146/annurev.cb.11.110195.000343 (1995).
- 10 Orkin, S. H. Diversification of haematopoietic stem cells to specific lineages. *Nat Rev Genet* **1**, 57-64, doi:10.1038/35049577 (2000).
- 11 Reya, T., Morrison, S. J., Clarke, M. F. & Weissman, I. L. Stem cells, cancer, and cancer stem cells. *Nature* **414**, 105-111, doi:10.1038/35102167 (2001).
- 12 Dick, J. E. Stem cells: Self-renewal writ in blood. *Nature* **423**, 231-233, doi:10.1038/423231a (2003).
- 13 Seita, J. & Weissman, I. L. Hematopoietic stem cell: self-renewal versus differentiation. *Wiley Interdiscip Rev Syst Biol Med* **2**, 640-653, doi:10.1002/wsbm.86 (2010).
- 14 Akashi, K., Traver, D., Miyamoto, T. & Weissman, I. L. A clonogenic common myeloid progenitor that gives rise to all myeloid lineages. *Nature* **404**, 193-197, doi:10.1038/35004599 (2000).
- 15 Yanez, A. *et al.* Granulocyte-Monocyte Progenitors and Monocyte-Dendritic Cell Progenitors Independently Produce Functionally Distinct Monocytes. *Immunity* **47**, 890-902 e894, doi:10.1016/j.immuni.2017.10.021 (2017).
- 16 Pronk, C. J. *et al.* Elucidation of the phenotypic, functional, and molecular topography of a myeloerythroid progenitor cell hierarchy. *Cell Stem Cell* **1**, 428-442, doi:10.1016/j.stem.2007.07.005 (2007).
- 17 Kondo, M., Weissman, I. L. & Akashi, K. Identification of clonogenic common lymphoid progenitors in mouse bone marrow. *Cell* **91**, 661-672, doi:10.1016/s0092-8674(00)80453-5 (1997).
- 18 Morrison, S. J., Wandycz, A. M., Hemmati, H. D., Wright, D. E. & Weissman, I. L. Identification of a lineage of multipotent hematopoietic progenitors. *Development* **124**, 1929-1939 (1997).
- 19 Lo Celso, C. *et al.* Live-animal tracking of individual haematopoietic stem/progenitor cells in their niche. *Nature* **457**, 92-96, doi:10.1038/nature07434 (2009).

- 20 Wu, M. *et al.* Imaging hematopoietic precursor division in real time. *Cell Stem Cell* **1**, 541-554, doi:10.1016/j.stem.2007.08.009 (2007).
- 21 Morrison, S. J. & Weissman, I. L. The long-term repopulating subset of hematopoietic stem cells is deterministic and isolatable by phenotype. *Immunity* **1**, 661-673, doi:10.1016/1074-7613(94)90037-x (1994).
- 22 Laurenti, E. & Gottgens, B. From haematopoietic stem cells to complex differentiation landscapes. *Nature* **553**, 418-426, doi:10.1038/nature25022 (2018).
- 23 Zhang, Y., Gao, S., Xia, J. & Liu, F. Hematopoietic Hierarchy - An Updated Roadmap. *Trends Cell Biol* **28**, 976-986, doi:10.1016/j.tcb.2018.06.001 (2018).
- 24 Velten, L. *et al.* Human haematopoietic stem cell lineage commitment is a continuous process. *Nat Cell Biol* **19**, 271-281, doi:10.1038/ncb3493 (2017).
- 25 Moignard, V. *et al.* Characterization of transcriptional networks in blood stem and progenitor cells using high-throughput single-cell gene expression analysis. *Nat Cell Biol* **15**, 363-372, doi:10.1038/ncb2709 (2013).
- 26 Morrison, S. J. & Scadden, D. T. The bone marrow niche for haematopoietic stem cells. *Nature* **505**, 327-334, doi:10.1038/nature12984 (2014).
- 27 Crane, G. M., Jeffery, E. & Morrison, S. J. Adult haematopoietic stem cell niches. *Nat Rev Immunol* **17**, 573-590, doi:10.1038/nri.2017.53 (2017).
- 28 Dohner, H., Weisdorf, D. J. & Bloomfield, C. D. Acute Myeloid Leukemia. *N Engl J Med* **373**, 1136-1152, doi:10.1056/NEJMra1406184 (2015).
- 29 Valent, P. *et al.* Clonal Hematopoiesis with Oncogenic Potential (CHOP): Separation from CHIP and Roads to AML. *Int J Mol Sci* **20**, doi:10.3390/ijms20030789 (2019).
- 30 Parcells, B. W., Ikeda, A. K., Simms-Waldrup, T., Moore, T. B. & Sakamoto, K. M. FMS-like tyrosine kinase 3 in normal hematopoiesis and acute myeloid leukemia. *Stem Cells* **24**, 1174-1184, doi:10.1634/stemcells.2005-0519 (2006).
- 31 Falini, B. *et al.* Cytoplasmic nucleophosmin in acute myelogenous leukemia with a normal karyotype. *N Engl J Med* **352**, 254-266, doi:10.1056/NEJMoa041974 (2005).
- 32 Dombret, H. Gene mutation and AML pathogenesis. *Blood* **118**, 5366-5367, doi:10.1182/blood-2011-09-379081 (2011).
- 33 Ley, T. J. *et al.* DNMT3A mutations in acute myeloid leukemia. *N Engl J Med* **363**, 2424-2433, doi:10.1056/NEJMoa1005143 (2010).
- 34 Kantarjian, H. *et al.* Acute myeloid leukemia: current progress and future directions. *Blood Cancer J* **11**, 41, doi:10.1038/s41408-021-00425-3 (2021).
- 35 Hallek, M., Shanafelt, T. D. & Eichhorst, B. Chronic lymphocytic leukaemia. *Lancet* **391**, 1524-1537, doi:10.1016/S0140-6736(18)30422-7 (2018).
- 36 Groffen, J. *et al.* Philadelphia chromosomal breakpoints are clustered within a limited region, bcr, on chromosome 22. *Cell* **36**, 93-99, doi:10.1016/0092-8674(84)90077-1 (1984).
- 37 Rowley, J. D. Letter: A new consistent chromosomal abnormality in chronic myelogenous leukaemia identified by quinacrine fluorescence and Giemsa staining. *Nature* **243**, 290-293, doi:10.1038/243290a0 (1973).
- 38 Quintas-Cardama, A. & Cortes, J. Molecular biology of bcr-abl1-positive chronic myeloid leukemia. *Blood* **113**, 1619-1630, doi:10.1182/blood-2008-03-144790 (2009).
- 39 Faderl, S. *et al.* The biology of chronic myeloid leukemia. *N Engl J Med* **341**, 164-172, doi:10.1056/NEJM199907153410306 (1999).
- 40 Janossy, G., Coustan-Smith, E. & Campana, D. The reliability of cytoplasmic CD3 and CD22 antigen expression in the immunodiagnosis of acute leukemia: a study of 500 cases. *Leukemia* **3**, 170-181 (1989).

- 41 Jain, N. *et al.* Early T-cell precursor acute lymphoblastic leukemia/lymphoma (ETP-ALL/LBL) in adolescents and adults: a high-risk subtype. *Blood* **127**, 1863-1869, doi:10.1182/blood-2015-08-661702 (2016).
- 42 Chessells, J. M. *et al.* Down's syndrome and acute lymphoblastic leukaemia: clinical features and response to treatment. *Arch Dis Child* **85**, 321-325, doi:10.1136/adc.85.4.321 (2001).
- 43 Shah, A., John, B. M. & Sondhi, V. Acute lymphoblastic leukemia with treatment-naive Fanconi anemia. *Indian Pediatr* **50**, 508-510 (2013).
- 44 Ratnaparkhe, M. *et al.* Genomic profiling of Acute lymphoblastic leukemia in ataxia telangiectasia patients reveals tight link between ATM mutations and chromothripsis. *Leukemia* **31**, 2048-2056, doi:10.1038/leu.2017.55 (2017).
- 45 Harrison, C. J. Cytogenetics of paediatric and adolescent acute lymphoblastic leukaemia. *Br J Haematol* **144**, 147-156, doi:10.1111/j.1365-2141.2008.07417.x (2009).
- 46 Mullighan, C. G. *et al.* Genome-wide analysis of genetic alterations in acute lymphoblastic leukaemia. *Nature* **446**, 758-764, doi:10.1038/nature05690 (2007).
- 47 Hunger, S. P. & Mullighan, C. G. Acute Lymphoblastic Leukemia in Children. *N Engl J Med* **373**, 1541-1552, doi:10.1056/NEJMra1400972 (2015).
- 48 Schultz, K. R. *et al.* Improved early event-free survival with imatinib in Philadelphia chromosome-positive acute lymphoblastic leukemia: a children's oncology group study. *J Clin Oncol* **27**, 5175-5181, doi:10.1200/JCO.2008.21.2514 (2009).
- 49 Aur, R. J. *et al.* Central nervous system therapy and combination chemotherapy of childhood lymphocytic leukemia. *Blood* **37**, 272-281 (1971).
- 50 Lewis, J. M. & Schwartz, M. A. Integrins regulate the association and phosphorylation of paxillin by c-Abl. *J Biol Chem* **273**, 14225-14230, doi:10.1074/jbc.273.23.14225 (1998).
- 51 Sawyers, C. L., McLaughlin, J., Goga, A., Havlik, M. & Witte, O. The nuclear tyrosine kinase c-Abl negatively regulates cell growth. *Cell* **77**, 121-131, doi:10.1016/0092-8674(94)90240-2 (1994).
- 52 Laneuville, P. Abl tyrosine protein kinase. *Semin Immunol* **7**, 255-266, doi:10.1006/smim.1995.0030 (1995).
- 53 Melo, J. V. The diversity of BCR-ABL fusion proteins and their relationship to leukemia phenotype. *Blood* **88**, 2375-2384 (1996).
- 54 Mandanas, R. A. *et al.* Role of p21 RAS in p210 bcr-abl transformation of murine myeloid cells. *Blood* **82**, 1838-1847 (1993).
- 55 Deininger, M. W., Goldman, J. M. & Melo, J. V. The molecular biology of chronic myeloid leukemia. *Blood* **96**, 3343-3356 (2000).
- 56 Skorski, T. *et al.* Phosphatidylinositol-3 kinase activity is regulated by BCR/ABL and is required for the growth of Philadelphia chromosome-positive cells. *Blood* **86**, 726-736 (1995).
- 57 Schofield, R. The relationship between the spleen colony-forming cell and the haemopoietic stem cell. *Blood Cells* **4**, 7-25 (1978).
- 58 Cox, D. N. *et al.* A novel class of evolutionarily conserved genes defined by piwi are essential for stem cell self-renewal. *Genes Dev* **12**, 3715-3727, doi:10.1101/gad.12.23.3715 (1998).
- 59 Xie, T. & Spradling, A. C. A niche maintaining germ line stem cells in the Drosophila ovary. *Science* **290**, 328-330, doi:10.1126/science.290.5490.328 (2000).
- 60 Ding, L. & Morrison, S. J. Haematopoietic stem cells and early lymphoid progenitors occupy distinct bone marrow niches. *Nature* **495**, 231-235, doi:10.1038/nature11885 (2013).

- 61 Kuhn, R., Schwenk, F., Aguet, M. & Rajewsky, K. Inducible gene targeting in mice. *Science* **269**, 1427-1429, doi:10.1126/science.7660125 (1995).
- 62 Kalajzic, I. *et al.* Use of type I collagen green fluorescent protein transgenes to identify subpopulations of cells at different stages of the osteoblast lineage. *J Bone Miner Res* **17**, 15-25, doi:10.1359/jbmr.2002.17.1.15 (2002).
- 63 Mizoguchi, T. *et al.* Osterix marks distinct waves of primitive and definitive stromal progenitors during bone marrow development. *Dev Cell* **29**, 340-349, doi:10.1016/j.devcel.2014.03.013 (2014).
- 64 Hawkins, E. D. *et al.* T-cell acute leukaemia exhibits dynamic interactions with bone marrow microenvironments. *Nature* **538**, 518-522, doi:10.1038/nature19801 (2016).
- 65 Duarte, D. *et al.* Inhibition of Endosteal Vascular Niche Remodeling Rescues Hematopoietic Stem Cell Loss in AML. *Cell Stem Cell* **22**, 64-77 e66, doi:10.1016/j.stem.2017.11.006 (2018).
- 66 Baccin, C. *et al.* Combined single-cell and spatial transcriptomics reveal the molecular, cellular and spatial bone marrow niche organization. *Nat Cell Biol* **22**, 38-48, doi:10.1038/s41556-019-0439-6 (2020).
- 67 Tikhonova, A. N. *et al.* The bone marrow microenvironment at single-cell resolution. *Nature* **569**, 222-228, doi:10.1038/s41586-019-1104-8 (2019).
- 68 Zanetti, C. & Krause, D. S. "Caught in the net": the extracellular matrix of the bone marrow in normal hematopoiesis and leukemia. *Exp Hematol* **89**, 13-25, doi:10.1016/j.exphem.2020.07.010 (2020).
- 69 Schepers, K., Campbell, T. B. & Passegue, E. Normal and leukemic stem cell niches: insights and therapeutic opportunities. *Cell Stem Cell* **16**, 254-267, doi:10.1016/j.stem.2015.02.014 (2015).
- 70 Simmons, P. J. *et al.* Vascular cell adhesion molecule-1 expressed by bone marrow stromal cells mediates the binding of hematopoietic progenitor cells. *Blood* **80**, 388-395 (1992).
- 71 Wright, D. E., Wagers, A. J., Gulati, A. P., Johnson, F. L. & Weissman, I. L. Physiological migration of hematopoietic stem and progenitor cells. *Science* **294**, 1933-1936, doi:10.1126/science.1064081 (2001).
- 72 Chow, A. *et al.* Bone marrow CD169⁺ macrophages promote the retention of hematopoietic stem and progenitor cells in the mesenchymal stem cell niche. *J Exp Med* **208**, 261-271, doi:10.1084/jem.20101688 (2011).
- 73 Winkler, I. G. *et al.* Bone marrow macrophages maintain hematopoietic stem cell (HSC) niches and their depletion mobilizes HSCs. *Blood* **116**, 4815-4828, doi:10.1182/blood-2009-11-253534 (2010).
- 74 Mendez-Ferrer, S. *et al.* Mesenchymal and haematopoietic stem cells form a unique bone marrow niche. *Nature* **466**, 829-834, doi:10.1038/nature09262 (2010).
- 75 Kunisaki, Y. *et al.* Arteriolar niches maintain haematopoietic stem cell quiescence. *Nature* **502**, 637-643, doi:10.1038/nature12612 (2013).
- 76 Itkin, T. *et al.* Distinct bone marrow blood vessels differentially regulate haematopoiesis. *Nature* **532**, 323-328, doi:10.1038/nature17624 (2016).
- 77 Winkler, I. G. *et al.* Vascular niche E-selectin regulates hematopoietic stem cell dormancy, self renewal and chemoresistance. *Nat Med* **18**, 1651-1657, doi:10.1038/nm.2969 (2012).
- 78 Visnjic, D. *et al.* Hematopoiesis is severely altered in mice with an induced osteoblast deficiency. *Blood* **103**, 3258-3264, doi:10.1182/blood-2003-11-4011 (2004).
- 79 Zhu, J. *et al.* Osteoblasts support B-lymphocyte commitment and differentiation from hematopoietic stem cells. *Blood* **109**, 3706-3712, doi:10.1182/blood-2006-08-041384 (2007).

- 80 Stier, S. *et al.* Osteopontin is a hematopoietic stem cell niche component that negatively regulates stem cell pool size. *J Exp Med* **201**, 1781-1791, doi:10.1084/jem.20041992 (2005).
- 81 Kollet, O. *et al.* Osteoclasts degrade endosteal components and promote mobilization of hematopoietic progenitor cells. *Nat Med* **12**, 657-664, doi:10.1038/nm1417 (2006).
- 82 Mansour, A. *et al.* Osteoclasts promote the formation of hematopoietic stem cell niches in the bone marrow. *J Exp Med* **209**, 537-549, doi:10.1084/jem.20110994 (2012).
- 83 Sacchetti, B. *et al.* Self-renewing osteoprogenitors in bone marrow sinusoids can organize a hematopoietic microenvironment. *Cell* **131**, 324-336, doi:10.1016/j.cell.2007.08.025 (2007).
- 84 Ding, L., Saunders, T. L., Enikolopov, G. & Morrison, S. J. Endothelial and perivascular cells maintain haematopoietic stem cells. *Nature* **481**, 457-462, doi:10.1038/nature10783 (2012).
- 85 van Furth, R. & Cohn, Z. A. The origin and kinetics of mononuclear phagocytes. *J Exp Med* **128**, 415-435, doi:10.1084/jem.128.3.415 (1968).
- 86 Schulz, C. *et al.* A lineage of myeloid cells independent of Myb and hematopoietic stem cells. *Science* **336**, 86-90, doi:10.1126/science.1219179 (2012).
- 87 McKercher, S. R. *et al.* Targeted disruption of the PU.1 gene results in multiple hematopoietic abnormalities. *EMBO J* **15**, 5647-5658 (1996).
- 88 Ginhoux, F. *et al.* Fate mapping analysis reveals that adult microglia derive from primitive macrophages. *Science* **330**, 841-845, doi:10.1126/science.1194637 (2010).
- 89 Hashimoto, D. *et al.* Tissue-resident macrophages self-maintain locally throughout adult life with minimal contribution from circulating monocytes. *Immunity* **38**, 792-804, doi:10.1016/j.immuni.2013.04.004 (2013).
- 90 Lavin, Y. *et al.* Tissue-resident macrophage enhancer landscapes are shaped by the local microenvironment. *Cell* **159**, 1312-1326, doi:10.1016/j.cell.2014.11.018 (2014).
- 91 Kurotaki, D., Uede, T. & Tamura, T. Functions and development of red pulp macrophages. *Microbiol Immunol* **59**, 55-62, doi:10.1111/1348-0421.12228 (2015).
- 92 Boyle, W. J., Simonet, W. S. & Lacey, D. L. Osteoclast differentiation and activation. *Nature* **423**, 337-342, doi:10.1038/nature01658 (2003).
- 93 Kaur, S. *et al.* Self-repopulating recipient bone marrow resident macrophages promote long-term hematopoietic stem cell engraftment. *Blood* **132**, 735-749, doi:10.1182/blood-2018-01-829663 (2018).
- 94 Jones, C. V. & Ricardo, S. D. Macrophages and CSF-1: implications for development and beyond. *Organogenesis* **9**, 249-260, doi:10.4161/org.25676 (2013).
- 95 Kandalla, P. K. *et al.* M-CSF improves protection against bacterial and fungal infections after hematopoietic stem/progenitor cell transplantation. *J Exp Med* **213**, 2269-2279, doi:10.1084/jem.20151975 (2016).
- 96 Crimmins, E. M. Lifespan and Healthspan: Past, Present, and Promise. *Gerontologist* **55**, 901-911, doi:10.1093/geront/gnv130 (2015).
- 97 Mortimer, R. K. & Johnston, J. R. Life span of individual yeast cells. *Nature* **183**, 1751-1752, doi:10.1038/1831751a0 (1959).
- 98 Fabrizio, P. & Longo, V. D. The chronological life span of *Saccharomyces cerevisiae*. *Methods Mol Biol* **371**, 89-95, doi:10.1007/978-1-59745-361-5_8 (2007).
- 99 Koks, S. *et al.* Mouse models of ageing and their relevance to disease. *Mech Ageing Dev* **160**, 41-53, doi:10.1016/j.mad.2016.10.001 (2016).
- 100 Moskalev, A. A. *et al.* The role of DNA damage and repair in aging through the prism of Koch-like criteria. *Ageing Res Rev* **12**, 661-684, doi:10.1016/j.arr.2012.02.001 (2013).

- 101 Saretzki, G. Telomeres, Telomerase and Ageing. *Subcell Biochem* **90**, 221-308, doi:10.1007/978-981-13-2835-0_9 (2018).
- 102 Blackburn, E. H., Greider, C. W. & Szostak, J. W. Telomeres and telomerase: the path from maize, Tetrahymena and yeast to human cancer and aging. *Nat Med* **12**, 1133-1138, doi:10.1038/nm1006-1133 (2006).
- 103 Dechat, T., Adam, S. A. & Goldman, R. D. Nuclear lamins and chromatin: when structure meets function. *Adv Enzyme Regul* **49**, 157-166, doi:10.1016/j.advenzreg.2008.12.003 (2009).
- 104 Gruenbaum, Y., Margalit, A., Goldman, R. D., Shumaker, D. K. & Wilson, K. L. The nuclear lamina comes of age. *Nat Rev Mol Cell Biol* **6**, 21-31, doi:10.1038/nrm1550 (2005).
- 105 Dahl, K. N. *et al.* Distinct structural and mechanical properties of the nuclear lamina in Hutchinson-Gilford progeria syndrome. *Proc Natl Acad Sci U S A* **103**, 10271-10276, doi:10.1073/pnas.0601058103 (2006).
- 106 Heilbronn, L. K. & Ravussin, E. Calorie restriction and aging: review of the literature and implications for studies in humans. *Am J Clin Nutr* **78**, 361-369, doi:10.1093/ajcn/78.3.361 (2003).
- 107 Roth, G. S., Ingram, D. K. & Lane, M. A. Slowing ageing by caloric restriction. *Nat Med* **1**, 414-415, doi:10.1038/nm0595-414 (1995).
- 108 McCay, C. M., Crowell, M. F. & Maynard, L. A. The effect of retarded growth upon the length of life span and upon the ultimate body size. 1935. *Nutrition* **5**, 155-171; discussion 172 (1989).
- 109 Feser, J. *et al.* Elevated histone expression promotes life span extension. *Mol Cell* **39**, 724-735, doi:10.1016/j.molcel.2010.08.015 (2010).
- 110 Wallace, D. C. A mitochondrial paradigm for degenerative diseases and ageing. *Novartis Found Symp* **235**, 247-263; discussion 263-246, doi:10.1002/0470868694.ch20 (2001).
- 111 Park, C. B. & Larsson, N. G. Mitochondrial DNA mutations in disease and aging. *J Cell Biol* **193**, 809-818, doi:10.1083/jcb.201010024 (2011).
- 112 Edgar, D. *et al.* Random point mutations with major effects on protein-coding genes are the driving force behind premature aging in mtDNA mutator mice. *Cell Metab* **10**, 131-138, doi:10.1016/j.cmet.2009.06.010 (2009).
- 113 Wickens, A. P. Ageing and the free radical theory. *Respir Physiol* **128**, 379-391, doi:10.1016/s0034-5687(01)00313-9 (2001).
- 114 Barja, G. The mitochondrial free radical theory of aging. *Prog Mol Biol Transl Sci* **127**, 1-27, doi:10.1016/B978-0-12-394625-6.00001-5 (2014).
- 115 Retta, S. F., Chiarugi, P., Trabalzini, L., Pinton, P. & Belkin, A. M. Reactive oxygen species: friends and foes of signal transduction. *J Signal Transduct* **2012**, 534029, doi:10.1155/2012/534029 (2012).
- 116 Van Remmen, H. *et al.* Life-long reduction in MnSOD activity results in increased DNA damage and higher incidence of cancer but does not accelerate aging. *Physiol Genomics* **16**, 29-37, doi:10.1152/physiolgenomics.00122.2003 (2003).
- 117 Zhang, Y. *et al.* Mice deficient in both Mn superoxide dismutase and glutathione peroxidase-1 have increased oxidative damage and a greater incidence of pathology but no reduction in longevity. *J Gerontol A Biol Sci Med Sci* **64**, 1212-1220, doi:10.1093/gerona/64.11.1212 (2009).
- 118 Kujoth, G. C. *et al.* Mitochondrial DNA mutations, oxidative stress, and apoptosis in mammalian aging. *Science* **309**, 481-484, doi:10.1126/science.1112125 (2005).
- 119 Campisi, J. & d'Adda di Fagagna, F. Cellular senescence: when bad things happen to good cells. *Nat Rev Mol Cell Biol* **8**, 729-740, doi:10.1038/nrm2233 (2007).

- 120 Schmeer, C., Kretz, A., Wengerodt, D., Stojiljkovic, M. & Witte, O. W. Dissecting Aging and Senescence-Current Concepts and Open Lessons. *Cells* **8**, doi:10.3390/cells8111446 (2019).
- 121 Kuilman, T. *et al.* Oncogene-induced senescence relayed by an interleukin-dependent inflammatory network. *Cell* **133**, 1019-1031, doi:10.1016/j.cell.2008.03.039 (2008).
- 122 Acosta, J. C. *et al.* Chemokine signaling via the CXCR2 receptor reinforces senescence. *Cell* **133**, 1006-1018, doi:10.1016/j.cell.2008.03.038 (2008).
- 123 Kuilman, T. & Peeper, D. S. Senescence-messaging secretome: SMS-ing cellular stress. *Nat Rev Cancer* **9**, 81-94, doi:10.1038/nrc2560 (2009).
- 124 Franceschi, C. *et al.* Inflamm-aging. An evolutionary perspective on immunosenescence. *Ann N Y Acad Sci* **908**, 244-254, doi:10.1111/j.1749-6632.2000.tb06651.x (2000).
- 125 Geiger, H., de Haan, G. & Florian, M. C. The ageing haematopoietic stem cell compartment. *Nat Rev Immunol* **13**, 376-389, doi:10.1038/nri3433 (2013).
- 126 Morrison, S. J., Wandycz, A. M., Akashi, K., Globerson, A. & Weissman, I. L. The aging of hematopoietic stem cells. *Nat Med* **2**, 1011-1016, doi:10.1038/nm0996-1011 (1996).
- 127 Chambers, S. M. & Goodell, M. A. Hematopoietic stem cell aging: wrinkles in stem cell potential. *Stem Cell Rev* **3**, 201-211, doi:10.1007/s12015-007-0027-1 (2007).
- 128 Dykstra, B., Olthof, S., Schreuder, J., Ritsema, M. & de Haan, G. Clonal analysis reveals multiple functional defects of aged murine hematopoietic stem cells. *J Exp Med* **208**, 2691-2703, doi:10.1084/jem.20111490 (2011).
- 129 de Haan, G., Nijhof, W. & Van Zant, G. Mouse strain-dependent changes in frequency and proliferation of hematopoietic stem cells during aging: correlation between lifespan and cycling activity. *Blood* **89**, 1543-1550 (1997).
- 130 Kuranda, K. *et al.* Age-related changes in human hematopoietic stem/progenitor cells. *Aging Cell* **10**, 542-546, doi:10.1111/j.1474-9726.2011.00675.x (2011).
- 131 Miller, J. P. & Allman, D. Linking age-related defects in B lymphopoiesis to the aging of hematopoietic stem cells. *Semin Immunol* **17**, 321-329, doi:10.1016/j.smim.2005.05.003 (2005).
- 132 Allman, D. & Miller, J. P. The aging of early B-cell precursors. *Immunol Rev* **205**, 18-29, doi:10.1111/j.0105-2896.2005.00269.x (2005).
- 133 Miller, J. P. & Allman, D. The decline in B lymphopoiesis in aged mice reflects loss of very early B-lineage precursors. *J Immunol* **171**, 2326-2330, doi:10.4049/jimmunol.171.5.2326 (2003).
- 134 Plowden, J., Renshaw-Hoelscher, M., Engleman, C., Katz, J. & Sambhara, S. Innate immunity in aging: impact on macrophage function. *Aging Cell* **3**, 161-167, doi:10.1111/j.1474-9728.2004.00102.x (2004).
- 135 Sebastian, C., Espia, M., Serra, M., Celada, A. & Lloberas, J. MacrophAging: a cellular and molecular review. *Immunobiology* **210**, 121-126, doi:10.1016/j.imbio.2005.05.006 (2005).
- 136 Renshaw, M. *et al.* Cutting edge: impaired Toll-like receptor expression and function in aging. *J Immunol* **169**, 4697-4701, doi:10.4049/jimmunol.169.9.4697 (2002).
- 137 Ogawa, T., Kitagawa, M. & Hirokawa, K. Age-related changes of human bone marrow: a histometric estimation of proliferative cells, apoptotic cells, T cells, B cells and macrophages. *Mech Ageing Dev* **117**, 57-68, doi:10.1016/s0047-6374(00)00137-8 (2000).
- 138 Wang, C. Q., Udupa, K. B., Xiao, H. & Lipschitz, D. A. Effect of age on marrow macrophage number and function. *Aging (Milano)* **7**, 379-384, doi:10.1007/BF03324349 (1995).

- 139 Albright, J. W. & Albright, J. F. Ageing alters the competence of the immune system to control parasitic infection. *Immunol Lett* **40**, 279-285, doi:10.1016/0165-2478(94)00066-2 (1994).
- 140 Bradley, S. F. & Kauffman, C. A. Aging and the response to Salmonella infection. *Exp Gerontol* **25**, 75-80, doi:10.1016/0531-5565(90)90012-q (1990).
- 141 De La Fuente, M. Changes in the macrophage function with aging. *Comp Biochem Physiol A Comp Physiol* **81**, 935-938, doi:10.1016/0300-9629(85)90933-8 (1985).
- 142 Linehan, E. *et al.* Aging impairs peritoneal but not bone marrow-derived macrophage phagocytosis. *Aging Cell* **13**, 699-708, doi:10.1111/accel.12223 (2014).
- 143 Chen, C., Liu, Y., Liu, Y. & Zheng, P. mTOR regulation and therapeutic rejuvenation of aging hematopoietic stem cells. *Sci Signal* **2**, ra75, doi:10.1126/scisignal.2000559 (2009).
- 144 Florian, M. C. *et al.* Cdc42 activity regulates hematopoietic stem cell aging and rejuvenation. *Cell Stem Cell* **10**, 520-530, doi:10.1016/j.stem.2012.04.007 (2012).
- 145 Vas, V., Senger, K., Dorr, K., Niebel, A. & Geiger, H. Aging of the microenvironment influences clonality in hematopoiesis. *PLoS One* **7**, e42080, doi:10.1371/journal.pone.0042080 (2012).
- 146 Tuljapurkar, S. R. *et al.* Changes in human bone marrow fat content associated with changes in hematopoietic stem cell numbers and cytokine levels with aging. *J Anat* **219**, 574-581, doi:10.1111/j.1469-7580.2011.01423.x (2011).
- 147 Thelen, M. & Stein, J. V. How chemokines invite leukocytes to dance. *Nat Immunol* **9**, 953-959, doi:10.1038/ni.f.207 (2008).
- 148 Rollins, B. J. Chemokines. *Blood* **90**, 909-928 (1997).
- 149 Mackay, C. R. Chemokines: what chemokine is that? *Curr Biol* **7**, R384-386, doi:10.1016/s0960-9822(06)00181-3 (1997).
- 150 Murphy, P. M. *et al.* International union of pharmacology. XXII. Nomenclature for chemokine receptors. *Pharmacol Rev* **52**, 145-176 (2000).
- 151 Zlotnik, A. & Yoshie, O. Chemokines: a new classification system and their role in immunity. *Immunity* **12**, 121-127, doi:10.1016/s1074-7613(00)80165-x (2000).
- 152 Moser, B. & Willmann, K. Chemokines: role in inflammation and immune surveillance. *Ann Rheum Dis* **63 Suppl 2**, ii84-ii89, doi:10.1136/ard.2004.028316 (2004).
- 153 Malik, I. A. *et al.* Single-dose gamma-irradiation induces up-regulation of chemokine gene expression and recruitment of granulocytes into the portal area but not into other regions of rat hepatic tissue. *Am J Pathol* **176**, 1801-1815, doi:10.2353/ajpath.2010.090505 (2010).
- 154 Schaeue, D., Kachikwu, E. L. & McBride, W. H. Cytokines in radiobiological responses: a review. *Radiat Res* **178**, 505-523, doi:10.1667/RR3031.1 (2012).
- 155 Blanchet, X., Langer, M., Weber, C., Koenen, R. R. & von Hundelshausen, P. Touch of chemokines. *Front Immunol* **3**, 175, doi:10.3389/fimmu.2012.00175 (2012).
- 156 Stone, M. J., Hayward, J. A., Huang, C., Z, E. H. & Sanchez, J. Mechanisms of Regulation of the Chemokine-Receptor Network. *Int J Mol Sci* **18**, doi:10.3390/ijms18020342 (2017).
- 157 Legler, D. F. *et al.* B cell-attracting chemokine 1, a human CXC chemokine expressed in lymphoid tissues, selectively attracts B lymphocytes via BLR1/CXCR5. *J Exp Med* **187**, 655-660, doi:10.1084/jem.187.4.655 (1998).
- 158 Gunn, M. D. *et al.* A B-cell-homing chemokine made in lymphoid follicles activates Burkitt's lymphoma receptor-1. *Nature* **391**, 799-803, doi:10.1038/35876 (1998).

- 159 Dobner, T., Wolf, I., Emrich, T. & Lipp, M. Differentiation-specific expression of a novel G protein-coupled receptor from Burkitt's lymphoma. *Eur J Immunol* **22**, 2795-2799, doi:10.1002/eji.1830221107 (1992).
- 160 Ansel, K. M. *et al.* A chemokine-driven positive feedback loop organizes lymphoid follicles. *Nature* **406**, 309-314, doi:10.1038/35018581 (2000).
- 161 Muller, G. & Lipp, M. Signal transduction by the chemokine receptor CXCR5: structural requirements for G protein activation analyzed by chimeric CXCR1/CXCR5 molecules. *Biol Chem* **382**, 1387-1397, doi:10.1515/BC.2001.171 (2001).
- 162 Heinig, K. *et al.* Access to follicular dendritic cells is a pivotal step in murine chronic lymphocytic leukemia B-cell activation and proliferation. *Cancer Discov* **4**, 1448-1465, doi:10.1158/2159-8290.CD-14-0096 (2014).
- 163 Hu, C. *et al.* PEG10 activation by co-stimulation of CXCR5 and CCR7 essentially contributes to resistance to apoptosis in CD19+CD34+ B cells from patients with B cell lineage acute and chronic lymphocytic leukemia. *Cell Mol Immunol* **1**, 280-294 (2004).
- 164 Hussain, M. *et al.* CXCL13/CXCR5 signaling axis in cancer. *Life Sci* **227**, 175-186, doi:10.1016/j.lfs.2019.04.053 (2019).
- 165 Henningson, A. J., Lager, M., Brannstrom, R., Tjernberg, I. & Skogman, B. H. The chemokine CXCL13 in cerebrospinal fluid in children with Lyme neuroborreliosis. *Eur J Clin Microbiol Infect Dis* **37**, 1983-1991, doi:10.1007/s10096-018-3334-3 (2018).
- 166 Barstad, B. *et al.* Cerebrospinal fluid cytokines and chemokines in children with Lyme neuroborreliosis; pattern and diagnostic utility. *Cytokine* **130**, 155023, doi:10.1016/j.cyto.2020.155023 (2020).
- 167 Fritze, J. *et al.* Loss of Cxcr5 alters neuroblast proliferation and migration in the aged brain. *Stem Cells* **38**, 1175-1187, doi:10.1002/stem.3207 (2020).
- 168 Lisignoli, G. *et al.* Age-associated changes in functional response to CXCR3 and CXCR5 chemokine receptors in human osteoblasts. *Biogerontology* **4**, 309-317, doi:10.1023/a:1026203502385 (2003).
- 169 Publicover, J. *et al.* Age-dependent hepatic lymphoid organization directs successful immunity to hepatitis B. *J Clin Invest* **123**, 3728-3739, doi:10.1172/JCI68182 (2013).
- 170 Lowenberg, B. *et al.* Effect of priming with granulocyte colony-stimulating factor on the outcome of chemotherapy for acute myeloid leukemia. *N Engl J Med* **349**, 743-752, doi:10.1056/NEJMoa025406 (2003).
- 171 Nervi, B. *et al.* Chemosensitization of acute myeloid leukemia (AML) following mobilization by the CXCR4 antagonist AMD3100. *Blood* **113**, 6206-6214, doi:10.1182/blood-2008-06-162123 (2009).
- 172 Hoellenriegel, J. *et al.* The Spiegelmer NOX-A12, a novel CXCL12 inhibitor, interferes with chronic lymphocytic leukemia cell motility and causes chemosensitization. *Blood* **123**, 1032-1039, doi:10.1182/blood-2013-03-493924 (2014).
- 173 Krause, D. S. *et al.* Differential regulation of myeloid leukemias by the bone marrow microenvironment. *Nat Med* **19**, 1513-1517, doi:10.1038/nm.3364 (2013).
- 174 Kumar, R. *et al.* Specific, targetable interactions with the microenvironment influence imatinib-resistant chronic myeloid leukemia. *Leukemia* **34**, 2087-2101, doi:10.1038/s41375-020-0866-1 (2020).
- 175 Verma, D. *et al.* Bone marrow niche-derived extracellular matrix-degrading enzymes influence the progression of B-cell acute lymphoblastic leukemia. *Leukemia* **34**, 1540-1552, doi:10.1038/s41375-019-0674-7 (2020).
- 176 Godavarthy, P. S. *et al.* The vascular bone marrow niche influences outcome in chronic myeloid leukemia via the E-selectin - SCL/TAL1 - CD44 axis. *Haematologica* **105**, 136-147, doi:10.3324/haematol.2018.212365 (2020).

- 177 Witkowski, M. T. *et al.* Extensive Remodeling of the Immune Microenvironment in B Cell Acute Lymphoblastic Leukemia. *Cancer Cell* **37**, 867-882 e812, doi:10.1016/j.ccell.2020.04.015 (2020).
- 178 Lyu, A. *et al.* Tumor-associated myeloid cells provide critical support for T-ALL. *Blood* **136**, 1837-1850, doi:10.1182/blood.2020007145 (2020).
- 179 Karantanou, C., Godavarthy, P. S. & Krause, D. S. Targeting the bone marrow microenvironment in acute leukemia. *Leuk Lymphoma* **59**, 2535-2545, doi:10.1080/10428194.2018.1434886 (2018).
- 180 Richman, C. *et al.* Postnatal and pubertal skeletal changes contribute predominantly to the differences in peak bone density between C3H/HeJ and C57BL/6J mice. *J Bone Miner Res* **16**, 386-397, doi:10.1359/jbmr.2001.16.2.386 (2001).
- 181 Van Etten, R. A. Models of chronic myeloid leukemia. *Curr Oncol Rep* **3**, 228-237, doi:10.1007/s11912-001-0055-y (2001).
- 182 Wolff, N. C. & Ilaria, R. L., Jr. Establishment of a murine model for therapy-treated chronic myelogenous leukemia using the tyrosine kinase inhibitor STI571. *Blood* **98**, 2808-2816, doi:10.1182/blood.v98.9.2808 (2001).
- 183 Li, S., Ilaria, R. L., Jr., Million, R. P., Daley, G. Q. & Van Etten, R. A. The P190, P210, and P230 forms of the BCR/ABL oncogene induce a similar chronic myeloid leukemia-like syndrome in mice but have different lymphoid leukemogenic activity. *J Exp Med* **189**, 1399-1412, doi:10.1084/jem.189.9.1399 (1999).
- 184 Friedl, P., Wolf, K., von Andrian, U. H. & Harms, G. Biological second and third harmonic generation microscopy. *Curr Protoc Cell Biol* **Chapter 4**, Unit 4 15, doi:10.1002/0471143030.cb0415s34 (2007).
- 185 Mohr, J. *et al.* The cell fate determinant Scribble is required for maintenance of hematopoietic stem cell function. *Leukemia* **32**, 1211-1221, doi:10.1038/s41375-018-0025-0 (2018).
- 186 Gu, C., Kim, G. B., Kim, W. J., Kim, H. U. & Lee, S. Y. Current status and applications of genome-scale metabolic models. *Genome Biol* **20**, 121, doi:10.1186/s13059-019-1730-3 (2019).
- 187 van der Velden, V. H. *et al.* New cellular markers at diagnosis are associated with isolated central nervous system relapse in paediatric B-cell precursor acute lymphoblastic leukaemia. *Br J Haematol* **172**, 769-781, doi:10.1111/bjh.13887 (2016).
- 188 Corces, M. R. *et al.* An improved ATAC-seq protocol reduces background and enables interrogation of frozen tissues. *Nat Methods* **14**, 959-962 (2017).
- 189 Krueger, F. Trim Galore! version 0.4.4. . *Bioinformatics Group, Babraham Institute, Cambridge, United Kingdom*: http://www.bioinformatics.babraham.ac.uk/projects/trim_galore. (2017).
- 190 Martin, M. Cutadapt removes adapter sequences from high-throughput sequencing reads. *EMBnet.journal* **17**, 10-12 (2011).
- 191 Langmead, B. & Salzberg, S. L. Fast gapped-read alignment with Bowtie 2. *Nat Methods* **9**, 357-359 (2012).
- 192 Li, H. *et al.* The Sequence Alignment/Map format and SAMtools. *Bioinformatics* **25**, 2078-2079 (2009).
- 193 Institute, B. Picard Tools version 2.17.4. . *Broad Institute, Cambridge, Massachusetts*: <http://broadinstitute.github.io/picard/> (2018).
- 194 Adey, A. *et al.* Rapid, low-input, low-bias construction of shotgun fragment libraries by high-density in vitro transposition. *Genome Biology* **11** (2010).
- 195 Zhang, Y. *et al.* Model-based Analysis of ChIP-Seq (MACS). *Genome Biology* **9** (2008).

- 196 Amstutz, P. *et al.* Common Workflow Language, v1.0. UC Davis
<http://dx.doi.org/10.6084/m9.figshare.3115156.v2> (2016).
- 197 Stark, R. & Brown, G. DiffBind: differential binding analysis of ChIP-seq peak data. .
Bioconductor (2011).
- 198 Robinson, M. D., McCarthy, D. J. & Smyth, G. K. edgeR: a Bioconductor package for
differential expression analysis of digital gene expression data. *Bioinformatics* **26**, 139-
140 (2010).
- 199 Yu, G., Wang, L. G. & He, Q. Y. ChIPseeker: an R/Bioconductor package for ChIP
peak annotation, comparison and visualization. *Bioinformatics* **31**, 2382-2383 (2015).
- 200 Berest, P. *et al.* Quantification of differential transcription factor activity and
multiomics-based classification into activators and repressors: diffTF. *bioRxiv*
<https://doi.org/10.1101/368498> (2018).
- 201 Kulakovskiy, I. V. *et al.* HOCOMOCO: expansion and enhancement of the collection
of transcription factor binding sites models. *Nucleic acids research* **44**, D116-125
(2016).
- 202 Heinz, S. *et al.* Simple combinations of lineage-determining transcription factors prime
cis-regulatory elements required for macrophage and B cell identities. *Mol Cell* **38**,
576-589 (2010).
- 203 Sheffield, N. C. & Bock, C. LOLA: enrichment analysis for genomic region sets and
regulatory elements in R and Bioconductor. *Bioinformatics* **32**, 587-589 (2016).
- 204 Subramanian, A. *et al.* Gene set enrichment analysis: a knowledge-based approach for
interpreting genome-wide expression profiles. *Proceedings of the National Academy of
Sciences of the United States of America* **102**, 15545-15550 (2005).
- 205 Blanche, P., Dartigues, J. F. & Jacqmin-Gadda, H. Estimating and comparing time-
dependent areas under receiver operating characteristic curves for censored event times
with competing risks. *Statistics in medicine* **32**, 5381-5397 (2013).
- 206 Team, R. C. R: A language and environment for statistical computing. *R Foundation
for Statistical Computing*. Vienna, Austria. (2018).
- 207 Down, J. D., Tarbell, N. J., Thames, H. D. & Mauch, P. M. Syngeneic and allogeneic
bone marrow engraftment after total body irradiation: dependence on dose, dose rate,
and fractionation. *Blood* **77**, 661-669 (1991).
- 208 Duran-Struuck, R. & Dysko, R. C. Principles of bone marrow transplantation (BMT):
providing optimal veterinary and husbandry care to irradiated mice in BMT studies. *J
Am Assoc Lab Anim Sci* **48**, 11-22 (2009).
- 209 Verma, D. *et al.* Vitamin K antagonism impairs the bone marrow microenvironment
and hematopoiesis. *Blood* **134**, 227-238, doi:10.1182/blood.2018874214 (2019).
- 210 Gomes, L. C., Di Benedetto, G. & Scorrano, L. During autophagy mitochondria
elongate, are spared from degradation and sustain cell viability. *Nat Cell Biol* **13**, 589-
598, doi:10.1038/ncb2220 (2011).
- 211 Gu, Z. *et al.* PAX5-driven subtypes of B-progenitor acute lymphoblastic leukemia. *Nat
Genet* **51**, 296-307, doi:10.1038/s41588-018-0315-5 (2019).
- 212 Mendez-Ferrer, S. *et al.* Bone marrow niches in haematological malignancies. *Nat Rev
Cancer* **20**, 285-298, doi:10.1038/s41568-020-0245-2 (2020).
- 213 Dong, Y. *et al.* Leukemia incidence trends at the global, regional, and national level
between 1990 and 2017. *Exp Hematol Oncol* **9**, 14, doi:10.1186/s40164-020-00170-6
(2020).
- 214 Hehlmann, R., Hochhaus, A., Baccarani, M. & European, L. Chronic myeloid
leukaemia. *Lancet* **370**, 342-350, doi:10.1016/S0140-6736(07)61165-9 (2007).
- 215 Inaba, H., Greaves, M. & Mullighan, C. G. Acute lymphoblastic leukaemia. *Lancet*
381, 1943-1955, doi:10.1016/S0140-6736(12)62187-4 (2013).

- 216 Verovskaya, E. V., Dellorusso, P. V. & Passegue, E. Losing Sense of Self and Surroundings: Hematopoietic Stem Cell Aging and Leukemic Transformation. *Trends Mol Med* **25**, 494-515, doi:10.1016/j.molmed.2019.04.006 (2019).
- 217 Frasca, D. *et al.* Aging down-regulates the transcription factor E2A, activation-induced cytidine deaminase, and Ig class switch in human B cells. *J Immunol* **180**, 5283-5290, doi:10.4049/jimmunol.180.8.5283 (2008).
- 218 Chong, Y. *et al.* CD27(+) (memory) B cell decrease and apoptosis-resistant CD27(-) (naive) B cell increase in aged humans: implications for age-related peripheral B cell developmental disturbances. *Int Immunol* **17**, 383-390, doi:10.1093/intimm/dxh218 (2005).
- 219 Dorshkind, K., Hofer, T., Montecino-Rodriguez, E., Pioli, P. D. & Rodewald, H. R. Do haematopoietic stem cells age? *Nat Rev Immunol* **20**, 196-202, doi:10.1038/s41577-019-0236-2 (2020).
- 220 Fane, M. & Weeraratna, A. T. How the ageing microenvironment influences tumour progression. *Nat Rev Cancer* **20**, 89-106, doi:10.1038/s41568-019-0222-9 (2020).
- 221 Nagelkerke, A., Bussink, J., Rowan, A. E. & Span, P. N. The mechanical microenvironment in cancer: How physics affects tumours. *Semin Cancer Biol* **35**, 62-70, doi:10.1016/j.semcancer.2015.09.001 (2015).
- 222 Krtolica, A. & Campisi, J. Cancer and aging: a model for the cancer promoting effects of the aging stroma. *Int J Biochem Cell Biol* **34**, 1401-1414, doi:10.1016/s1357-2725(02)00053-5 (2002).
- 223 Massaro, F. *et al.* Aging of Bone Marrow Mesenchymal Stromal Cells: Hematopoiesis Disturbances and Potential Role in the Development of Hematologic Cancers. *Cancers (Basel)* **13**, doi:10.3390/cancers13010068 (2020).
- 224 Signer, R. A., Montecino-Rodriguez, E., Witte, O. N., McLaughlin, J. & Dorshkind, K. Age-related defects in B lymphopoiesis underlie the myeloid dominance of adult leukemia. *Blood* **110**, 1831-1839, doi:10.1182/blood-2007-01-069401 (2007).
- 225 Mombaerts, P. *et al.* RAG-1-deficient mice have no mature B and T lymphocytes. *Cell* **68**, 869-877, doi:10.1016/0092-8674(92)90030-g (1992).
- 226 Czechowicz, A., Kraft, D., Weissman, I. L. & Bhattacharya, D. Efficient transplantation via antibody-based clearance of hematopoietic stem cell niches. *Science* **318**, 1296-1299, doi:10.1126/science.1149726 (2007).
- 227 Chhabra, A. *et al.* Hematopoietic stem cell transplantation in immunocompetent hosts without radiation or chemotherapy. *Sci Transl Med* **8**, 351ra105, doi:10.1126/scitranslmed.aae0501 (2016).
- 228 Czechowicz, A. *et al.* Selective hematopoietic stem cell ablation using CD117-antibody-drug-conjugates enables safe and effective transplantation with immunity preservation. *Nat Commun* **10**, 617, doi:10.1038/s41467-018-08201-x (2019).
- 229 Hermiston, M. L., Zikherman, J. & Zhu, J. W. CD45, CD148, and Lyp/Pep: critical phosphatases regulating Src family kinase signaling networks in immune cells. *Immunol Rev* **228**, 288-311, doi:10.1111/j.1600-065X.2008.00752.x (2009).
- 230 He, D. D. *et al.* C-KIT Expression Distinguishes Fetal from Postnatal Skeletal Progenitors. *Stem Cell Reports* **14**, 614-630, doi:10.1016/j.stemcr.2020.03.001 (2020).
- 231 Jacome-Galarza, C. E., Lee, S. K., Lorenzo, J. A. & Aguila, H. L. Identification, characterization, and isolation of a common progenitor for osteoclasts, macrophages, and dendritic cells from murine bone marrow and periphery. *J Bone Miner Res* **28**, 1203-1213, doi:10.1002/jbmr.1822 (2013).
- 232 Bianchi-Frias, D. *et al.* The Aged Microenvironment Influences the Tumorigenic Potential of Malignant Prostate Epithelial Cells. *Mol Cancer Res* **17**, 321-331, doi:10.1158/1541-7786.MCR-18-0522 (2019).

- 233 Vas, V., Wandhoff, C., Dorr, K., Niebel, A. & Geiger, H. Contribution of an aged microenvironment to aging-associated myeloproliferative disease. *PLoS One* **7**, e31523, doi:10.1371/journal.pone.0031523 (2012).
- 234 Abdul-Aziz, A. M. *et al.* Acute myeloid leukemia induces protumoral p16INK4a-driven senescence in the bone marrow microenvironment. *Blood* **133**, 446-456, doi:10.1182/blood-2018-04-845420 (2019).
- 235 Rowe, R. G. *et al.* The developmental stage of the hematopoietic niche regulates lineage in MLL-rearranged leukemia. *J Exp Med* **216**, 527-538, doi:10.1084/jem.20181765 (2019).
- 236 Liu, Y. *et al.* The genomic landscape of pediatric and young adult T-lineage acute lymphoblastic leukemia. *Nat Genet* **49**, 1211-1218, doi:10.1038/ng.3909 (2017).
- 237 Guth, A. M., Hafeman, S. D. & Dow, S. W. Depletion of phagocytic myeloid cells triggers spontaneous T cell- and NK cell-dependent antitumor activity. *Oncoimmunology* **1**, 1248-1257, doi:10.4161/onci.21317 (2012).
- 238 Talmadge, J. E. & Gabrilovich, D. I. History of myeloid-derived suppressor cells. *Nat Rev Cancer* **13**, 739-752, doi:10.1038/nrc3581 (2013).
- 239 Veglia, F., Perego, M. & Gabrilovich, D. Myeloid-derived suppressor cells coming of age. *Nat Immunol* **19**, 108-119, doi:10.1038/s41590-017-0022-x (2018).
- 240 Giese, M. A., Hind, L. E. & Huttenlocher, A. Neutrophil plasticity in the tumor microenvironment. *Blood* **133**, 2159-2167, doi:10.1182/blood-2018-11-844548 (2019).
- 241 Tesi, R. J. MDSC; the Most Important Cell You Have Never Heard Of. *Trends Pharmacol Sci* **40**, 4-7, doi:10.1016/j.tips.2018.10.008 (2019).
- 242 Liu, Y. F. *et al.* Expansion and activation of granulocytic, myeloid-derived suppressor cells in childhood precursor B cell acute lymphoblastic leukemia. *J Leukoc Biol* **102**, 449-458, doi:10.1189/jlb.5MA1116-453RR (2017).
- 243 Trabanelli, S. *et al.* Tumour-derived PGD2 and NKp30-B7H6 engagement drives an immunosuppressive ILC2-MDSC axis. *Nat Commun* **8**, 593, doi:10.1038/s41467-017-00678-2 (2017).
- 244 Chen, X. *et al.* Induction of myelodysplasia by myeloid-derived suppressor cells. *J Clin Invest* **123**, 4595-4611, doi:10.1172/JCI67580 (2013).
- 245 Giallongo, C. *et al.* Myeloid derived suppressor cells (MDSCs) are increased and exert immunosuppressive activity together with polymorphonuclear leukocytes (PMNs) in chronic myeloid leukemia patients. *PLoS One* **9**, e101848, doi:10.1371/journal.pone.0101848 (2014).
- 246 Mazumder, B. *et al.* Regulated release of L13a from the 60S ribosomal subunit as a mechanism of transcript-specific translational control. *Cell* **115**, 187-198, doi:10.1016/s0092-8674(03)00773-6 (2003).
- 247 Poddar, D. *et al.* An extraribosomal function of ribosomal protein L13a in macrophages resolves inflammation. *J Immunol* **190**, 3600-3612, doi:10.4049/jimmunol.1201933 (2013).
- 248 Peters, M. J. *et al.* The transcriptional landscape of age in human peripheral blood. *Nat Commun* **6**, 8570, doi:10.1038/ncomms9570 (2015).
- 249 Sarkis, G. J., Ashcom, J. D., Hawdon, J. M. & Jacobson, L. A. Decline in protease activities with age in the nematode *Caenorhabditis elegans*. *Mech Ageing Dev* **45**, 191-201, doi:10.1016/0047-6374(88)90001-2 (1988).
- 250 Saez, I. & Vilchez, D. The Mechanistic Links Between Proteasome Activity, Aging and Age-related Diseases. *Curr Genomics* **15**, 38-51, doi:10.2174/138920291501140306113344 (2014).

- 251 Makrynikola, V., Bianchi, A., Bradstock, K., Gottlieb, D. & Hewson, J. Migration of acute lymphoblastic leukemia cells into human bone marrow stroma. *Leukemia* **8**, 1734-1743 (1994).
- 252 Portale, F. *et al.* ActivinA: a new leukemia-promoting factor conferring migratory advantage to B-cell precursor-acute lymphoblastic leukemic cells. *Haematologica* **104**, 533-545, doi:10.3324/haematol.2018.188664 (2019).
- 253 Guo, F. *et al.* CXCL12/CXCR4: a symbiotic bridge linking cancer cells and their stromal neighbors in oncogenic communication networks. *Oncogene* **35**, 816-826, doi:10.1038/onc.2015.139 (2016).
- 254 Guang, L. G., Boskey, A. L. & Zhu, W. Age-related CXC chemokine receptor-4-deficiency impairs osteogenic differentiation potency of mouse bone marrow mesenchymal stromal stem cells. *Int J Biochem Cell Biol* **45**, 1813-1820, doi:10.1016/j.biocel.2013.05.034 (2013).
- 255 Burkle, A. *et al.* Overexpression of the CXCR5 chemokine receptor, and its ligand, CXCL13 in B-cell chronic lymphocytic leukemia. *Blood* **110**, 3316-3325, doi:10.1182/blood-2007-05-089409 (2007).
- 256 Dupuis, J. *et al.* Expression of CXCL13 by neoplastic cells in angioimmunoblastic T-cell lymphoma (AITL): a new diagnostic marker providing evidence that AITL derives from follicular helper T cells. *Am J Surg Pathol* **30**, 490-494, doi:10.1097/00000478-200604000-00009 (2006).
- 257 Swerdlow, S. H. *et al.* The 2016 revision of the World Health Organization classification of lymphoid neoplasms. *Blood* **127**, 2375-2390, doi:10.1182/blood-2016-01-643569 (2016).
- 258 Panjideh, H. *et al.* Immunotherapy of B-cell non-Hodgkin lymphoma by targeting the chemokine receptor CXCR5 in a preclinical mouse model. *Int J Cancer* **135**, 2623-2632, doi:10.1002/ijc.28893 (2014).
- 259 Bunse, M. *et al.* CXCR5 CAR-T cells simultaneously target B cell non-Hodgkin's lymphoma and tumor-supportive follicular T helper cells. *Nat Commun* **12**, 240, doi:10.1038/s41467-020-20488-3 (2021).
- 260 Jiang, L. *et al.* CXCL13/CXCR5 are potential biomarkers for diagnosis and prognosis for breast cancer. *J BUON* **25**, 2552-2561 (2020).
- 261 Williams, M. T. *et al.* The ability to cross the blood-cerebrospinal fluid barrier is a generic property of acute lymphoblastic leukemia blasts. *Blood* **127**, 1998-2006, doi:10.1182/blood-2015-08-665034 (2016).
- 262 Gossai, N. P. & Gordon, P. M. The Role of the Central Nervous System Microenvironment in Pediatric Acute Lymphoblastic Leukemia. *Front Pediatr* **5**, 90, doi:10.3389/fped.2017.00090 (2017).
- 263 Halsey, C. *et al.* The impact of therapy for childhood acute lymphoblastic leukaemia on intelligence quotients; results of the risk-stratified randomized central nervous system treatment trial MRC UKALL XI. *J Hematol Oncol* **4**, 42, doi:10.1186/1756-8722-4-42 (2011).
- 264 Rubenstein, J. L. *et al.* CXCL13 plus interleukin 10 is highly specific for the diagnosis of CNS lymphoma. *Blood* **121**, 4740-4748, doi:10.1182/blood-2013-01-476333 (2013).

Acknowledgment

I would like to thank my supervisor, Prof. D. S. Krause for giving me the opportunity to undertake this PhD and for all the support and encouragement I have received during the time I have spent in her laboratory. I would like to thank Prof. R. Marschalek for his guidance particularly during the PhD procedure.

To begin with my friends, I place my hand on my heart to express my gratitude to Rahul for his presence with his scientific knowledge and not which kept me on the track. Valentina for always showing the shining side of the medal, and Pablo for helping me to handle my over-a hundred percent. A big thanks to Chrissy for accepting my chaotic mind and for being an the most incomparable sympathetic friend. Raqui, who constantly reminded me that despite the exhaustion from a trying period, the outcome is worth it. Gody for the effective communication of unspoken conversations. All the guys for the nice time: Joscha, Kimena, Fabian, Celina, Roby, Minka, Theresa, Nina, Nathalie, Alessia, Max, Valerie, Luigi and Julian and Anjali for amazing cakes.

My friend Valenti P. because she's been a pilaster in FFM. I always feel your hug with your words. Valentina P. and Francesco, who daily reinforced my dandelion's point of view. In addition, I would like to thank Anna, Mark, Eli, Anto, Vera, Irene, Monika, Adri & Co, Mimmi, Isa, Trilly and Marty in Germany and in Italy from distracting me from the research. In particular, I want to thank Giu for showing me the beauty of Swing, which is part of myself now, and for teaching me the concept that mistakes do not exist, but there are only variations. My Turkish girls, Isil, because I knew that I needed to list the week's point to update you with our week's funny and lovely report at the end of the week. Bahar, Tudge and Dany Dany because from a rock step we rock our friendships.

Last but not least, my family. My parents for being so exceptional. Everyone should meet them once in life. My sisters because they constantly offered me invaluable love via distance. Even as the years passed, they kept transmitting to me the spirit of being the little sister who gave me strong energy. Cri for being my hexane cycle.

Bobby and Birba brightened my days in Germany and Italy because with their uncontrollable love keep the smile on my face, you are big gifts.

Without the support of such a diverse and international team, I'm not sure it would have been as meaningful this time.

CURRICULUM VITAE

Costanza Zanetti



Nationality: Italian

Date of birth: 06.08.1990

Home address: Dürerstraße 11
60596 Frankfurt am Main
Germany

Email address: costanza.zanetti@libero.it - zanetti@gsh.uni-frankfurt.de

Education

- 2017-present* **The influence of an aged bone marrow microenvironment in leukaemia**
- Dr. Prof. D. S. Krause**, Georg Speyer Haus (GSH), Frankfurt am Main Germany - Institut für Pharmazeutische Biologie, Goethe-Universität, Frankfurt am Main.
- 2016* Master Degree in Translational Oncology, University of Hull, England.
- 2014* Bachelor Degree in Biology, University of Rome Tor Vergata, Rome, Italy.
-
-

Awards and Scholarships

- December 2019* Urkunde für hervorragende leistungen für die untersuchung der Rolle des Alters des Knochenmarkmikromilieus bei den Leukämien.
Paul-Ehrlich-Förderpreis 2019
- November 2019* Travel Award des Biologischen Vereins.
- September 2018* Leuka International Travel Scholarships Support Young Leukaemia Researchers.
- September 2009* Erasmus scholarship for the Campus De Bizkaia - Campus of Biscay, (University of Bilbao, Spain).

Education and working experience

02/2017- present	<p>PhD Student “The age of the bone marrow microenvironment influences B-cell acute lymphoblastic leukemia progression via CXCR5-CXCL13”. GSH, Frankfurt am Main, Germany - Dr. Prof. D.S. Krause</p> <p>Instituts für Pharmazeutische Biologie, Goethe-Universität, Frankfurt am Main, Germany- Dr. Prof. R. Marschalek</p>
09/2016-01/2017	<p>Research Assistant Assesment of apoptotic biomarkers in oesophageal tumour University of Hull, England - Dr. I. M. Pires Trinity College, Dublin, Ireland - Dr. S.G. Maher</p>
09/2015-08/2016	<p>Master Student “Combined PS-341 and TRAIL treatment enhances the sensitivity of oesophageal tumour though the mitochondrial apoptotic pathways. University of Hull, England - Dr. S.G. Maher</p>
09/2012-06/2013	<p>Erasmus Student (Bachelor) University Campus De Bizkaia - Campus of Biscay (University of Bilbao, Spain).</p>
01/2010-05/2014	<p>Bachelor Student “Control of system in the partial resection of the kidney in the laparoscopy 3D”. University of Rome “Tor Vergata”, Rome-Italy Dr. M. Mattei</p>

Laboratory/Technical skills

- *In vivo* mouse: handling, manipulations, intraperitoneal, intravenous, gavage injections, stitching and blood withdrawal.
- Mouse bone marrow transduction/transplantation models.
- Patient-derived xenografts (PDX).
- Isolation and maintenance of murine primary cells from the BM: macrophages, mesenchymal stromal cells (MSC), endothelial cells (EC), fibroblasts and haematopoietic stem cells (HSC).
- Molecular Biology and Cell Biology techniques: Western Blots, qPCR, PCR, ELISA.
- Flow cytometry and cell sorting.
- Confocal imaging and live imaging by intravital microscope/2 photon microscope.

- Cell culture in normoxia and hypoxia conditions.
-
-

Software

- Adobe Illustrator
 - Fiji Image analysis
 - Imaris
 - FlowJo
 - Prism
 - EndNote
 - Microsoft Office Package
-
-

Additional Qualifications and Skills

Licenses and Courses

	Driving license category B
2021	Managing Scientific Projects course
2017	BD Flow cytometry course
2017	Animal experimental license-FELASA A and D
2016	International English Language Testing System (IELTS)

Supervising

- Trained and supervised Hiwi - 2017 to 2020
 - Trained and supervised PhD student for internship - 2019
-
-

Languages

- Italian: native speaker
 - English: fluent
 - Spanish: fluent
 - German: basic
-
-

Social engagement and community work

<i>November 2019-Present</i>	Vice representative of the Italian community, Frankfurt am Main.
<i>November 2018-2020</i>	PhD representative at the GSH, Frankfurt am Main (second term).
<i>May 2019</i>	Science Communication Day at the Italian community, Frankfurt am Main.

Conferences and Presentations

- January 2020* GSH - Research meeting, Frankfurt am Main.
Oral presentation: Bone marrow niche-derived extracellular matrix-degrading enzymes influence the progression of B-cell acute lymphoblastic leukemia.
- December 2019* ASH-American Society of Hematology
61st ASH Annual Meeting and Exposition, Orlando, Florida
Poster presentation: “The age of the bone marrow microenvironment influences B-cell acute lymphoblastic leukemia progression via CXCR5-CXCL13”.
- May 2019* Acute myeloid leukaemia consortium
Poster presentation: Bone marrow niche-derived extracellular matrix-degrading enzymes influence the progression of B cell acute lymphoblastic leukemia.
- October 2018* GSH - Research meeting, Frankfurt am Main.
Oral presentation: The influence of the age of the bone marrow microenvironment on leukaemia progression.
- September 2018* ESH-European School of Haematology
20th Annual John Goldman Conference on Chronic Myeloid Leukemia: Biology and Therapy, Miami, Florida (USA).
Oral presentation: The role of the growing bone marrow microenvironment in paediatric B-cell acute lymphoblastic and chronic myeloid leukaemia.
- January 2017* Postgraduate Student Conference 2017
University of Hull, England.
Oral presentation: The role of TRAIL as a therapeutic agent for cancer.

Manuscripts Published

1. **Zanetti et al., 2021** Blood Journal
The age of the bone marrow microenvironment influences B-cell acute lymphoblastic leukemia progression via CXCR5-CXCL13.
2. **Zanetti, C.** and Krause, D., 2020.
“Caught in the net”: the extracellular matrix of the bone marrow in normal hematopoiesis and leukemia. *Experimental Hematology*, 89, pp.13-25.
(Review article).
3. Kumar, R., Pereira, R.#, **Zanetti, C.** #, Minciacchi, V., Merten, M., Meister, M., Niemann, J., Dietz, M., Rüssel, N., Schnütgen, F., Tamai, M., Akahane, K., Inukai, T., Oellerich, T., Kvasnicka, H., Pfeifer, H., Nicolini, F., Heilemann, M., Van Etten, R. and Krause, D., 2020.
Specific, targetable interactions with the microenvironment influence imatinib-resistant chronic myeloid leukemia. *Leukemia*, 34(8), pp.2087-2101.

4. Verma, D.#, **Zanetti, C.#**, Godavarthy, P.#, Kumar, R., Minciacchi, V., Pfeiffer, J., Metzler, M., Lefort, S., Maguer-Satta, V., Nicolini, F., Burrioni, B., Fontenay, M. and Krause, D., 2020. Bone marrow niche-derived extracellular matrix-degrading enzymes influence the progression of B-cell acute lymphoblastic leukemia. *Leukemia*, 34(6), pp.1540-1552.
5. Verma, D., Kumar, R., S. Pereira, R., Karantanou, C., **Zanetti, C.**, Minciacchi, V., Fulzele, K., Kunz, K., Hoelper, S., Zia-Chahabi, S., Jabagi, M., Emmerich, J., Dray-Spira, R., Kuhlee, F., Hackmann, K., Schroeck, E., Wenzel, P., Müller, S., Filmann, N., Fontenay, M., Divieti-Pajevic, P. and Krause, D. (2019). Vitamin K-antagonism impairs the bone marrow microenvironment and hematopoiesis. *Blood*, p. blood.2018874214.
6. Dash, B., Schnöder, T., Kathner, C., Mohr, J., Weinert, S., Herzog, C., Godavarthy, P., **Zanetti, C.**, Perner, F., Braun-Dullaes, R., Hartleben, B., Huber, T., Walz, G., Naumann, M., Ellis, S., Vasioukhin, V., Kähne, T., Krause, D. and Heidel, F. (2018). Diverging impact of cell fate determinants Scrib and Lgl1 on adhesion and migration of hematopoietic stem cells. *Journal of Cancer Research and Clinical Oncology*, 144(10), pp.1933-1944.
7. Mohr, J., Dash, B., Schnoeder, T., Wolleschak, D., Herzog, C., Tubio Santamaria, N., Weinert, S., Godavarthy, S., **Zanetti, C.**, Naumann, M., Hartleben, B., Huber, T., Krause, D., Kähne, T., Bullinger, L. and Heidel, F., 2018. The cell fate determinant Scribble is required for maintenance of hematopoietic stem cell function. *Leukemia*, 32(5), pp.1211-1221.

authors contributed equally to the manuscript.